Russian Chemical Reviews **75** (6) 457 – 496 (2006) © 2006 Russian Academy of Sciences and Turpion Ltd

DOI 10.1070/RC2006v075n06ABEH003602

Molecular and crystal design of nonlinear optical organic materials

K Yu Suponitsky, T V Timofeeva, M Yu Antipin

Contents

I.	Introduction	457
II.	Methods for the assessment of molecular hyperpolarisabilities	458
III.	Characteristics of π-conjugated systems related to the efficiency of the second harmonic generation	464
IV.	Possible ways to improve thermal stability and optical transparency of NLO materials	476
V.	The design of NLO crystals	485
VI.	Conclusion	489

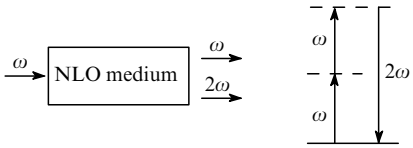
Abstract. The results of theoretical and experimental studies on the second-order molecular and crystal nonlinear optical susceptibilities of organic and several classes of organoelement compounds are summarised. Modern methods used in these studies are briefly characterised, their advantages and drawbacks are outlined as regards their application to the systematic search for efficient nonlinear optical materials. Recent achievements and the main challenges in the field are thoroughly discussed and an optimum algorithm of the design of such materials is proposed. The bibliography includes 479 references.

I. Introduction

Investigations into the nonlinear optical (NLO) materials is an actively developing field of the materials science.[1–10] These materials have to comply with specific requirements, such as manifestation of high quadratic nonlinear optical susceptibilities and thermal stability and transparency in the operational range of wavelengths. Inorganic materials that are most frequently implemented in various devices meet these requirements to a certain degree. However, as early as the 1970s it was realised [11–15] that organic compounds containing donor and acceptor (D/A) substituents linked through a π-electron system (the so-called D–π–A molecules) are capable of manifesting 1–2 orders of magnitude higher NLO efficiencies (NLO susceptibilities) due to the π-electrons weakly bound to the nuclear framework. This explains the great interest of researchers to the experimental elucidation of nonlinear optical susceptibilities of such compounds and the search for methods enabling prediction of the hyperpolarisabilities and structural simulations of highly efficient NLO molecules. Over the last two decades, the assortment of molecules under study has expanded substantially.[16–22] A considerable progress has been attained in the field of quantum-chemical calculations of the hyperpolarisabilities of molecules [23–27] thereby providing valuable insight into the optimum molecular structures and helping to establish the structure–property relationship. The effects of the nature of the π-conjugated system have been monitored using series of polyphenylenes, polyenes, polyynes, their diphenyl-substituted analogues and molecules with heterocyclic π-systems.[28–36] Various donor and acceptor substituents, in particular, NO_2, C(O)R, CN, OR, NR_2 as well as heterocyclic fragments and their combinations, have been studied in detail.[37–43]

Only one of numerous possible NLO effects, *viz*., the second harmonic generation (SHG), which is a special case of the sum frequency generation (SFG) is concerned in the present review. Incident photons with a frequency ω are absorbed by an NLO medium; the majority of photons are re-emitted at the same frequency but, for a small fraction of the incident radiation, the frequency of the generated photons is doubled (Scheme 1). This implies that the nonlinear optical effects can only be detected with powerful radiation sources, such as lasers.

Scheme 1



The dependence of the dipole moment (μ), which describes the perturbation of a system within the dipole approximation, on the external field strength (E) can be represented as a series [44, 45]

$$\mu_i = \mu_i^0 + \alpha_{ij}E_j + \beta_{ijk}E_jE_k + \gamma_{ijkl}E_jE_kE_l + \ldots, \quad (1)$$

where μ_i^0 is the ith component of the dipole moment of the unperturbed system; α_{ij} is the linear polarisability; β_{ijk} and γ_{ijkl} are nonlinear polarisabilities. The polarisabilities are frequency-dependent, which, strictly speaking, has to be reflected in their notation: for instance, $\beta_{ijk}(-\omega_1, -\omega_2, \omega_1, \omega_2)$, where ω_1 and ω_2 are incident radiation frequencies. The second harmonic generation is a particular case as a first-order nonlinear effect and thus it is described by the third term of the series (1), *i.e*., by the parameter $\beta(2\omega,\omega,\omega)$ [or $\beta(\omega)$], which is a third-rank tensor. Typically, the notation β refers to molecules, *e.g*., it is used in the studies of the second harmonic generation in solutions or gases or in theoretical calculations. In those cases, the proportionality coefficient is referred to as hyperpolarisability. In the case of crystal, the term

K Yu Suponitsky, M Yu Antipin A N Nesmeyanov Institute of Organoelement Compounds, Russian Academy of Sciences, ul. Vavilova 28, 119991 Moscow, Russian Federation. Fax (7-495) 135 50 85, tel. (7-495) 135 92 14, e-mail: kirshik@yahoo.com (K Yu Suponitsky), tel. (7-495) 135 92 15, e-mail: m_antipin@yahoo.com (M Yu Antipin)
T V Timofeeva Department of Chemistry, New Mexico Highlands University, 87701 Las Vegas, USA. Fax (1-505) 454 32 02, e-mail: t_timofeeva@yahoo.com

Received 24 August 2005
Uspekhi Khimii **75** (6) 515 – 556 (2006); translated by Ya V Zubavichus

second-order nonlineral optical susceptibility is used, which is denoted as $\chi^{(2)}$ or d. Static hyperpolarisabilities extrapolated to the zero frequency [referred to as β_0, $\beta(0,0,0)$ or $\beta(0)$] are often used for comparative analyses. It is related to the dynamical values by means of the following expression:[23]

$$\beta(\omega) = \beta(0)[1 + A\omega^2 + ...]. \quad (2)$$

The coefficient A depends exclusively on the nature of the molecule. The static hyperpolarisabilities are significantly easier to calculate and they are sufficient for the analysis of trends along various series of compounds, as will be demonstrated below. For the sake of easy comparison and interpretation, the molecular hyperpolarisabilities are usually represented as their vector components

$$\beta_{\text{vect}} = (\beta_x^2 + \beta_y^2 + \beta_z^2)^{1/2}, \quad (3)$$

where

$$\beta_i = \beta_{ixx} + \beta_{iyy} + \beta_{izz}\,.$$

Such representation is used due to the fact that β_{vect} can be determined experimentally from measurements of the hyperpolarisabilities of molecules. Sometimes, the hyperpolarisability is represented as the tensor norm

$$||\,\beta\,|| = \left(\sum_{ijk} \beta_{ijk}^2\right)^{1/2}. \quad (4)$$

In many cases, the tensor is degenerated into a vector due to a particular symmetry of the molecule. Thus, all even-order optical susceptibilities of any system with an inversion centre are strictly zero.

In order to compare and interpret the experimentally measured hyperpolarisabilities reported by different research groups, one has to critically assess them for several reasons. First, there are several independent representations of the NLO parameters related to modifications of the formulas (3) and (4), which is not always clearly specified in original papers.† Second, different research groups use different reference values of the same standard sample in the measurements. This problem has been specially addressed.[46] Nevertheless, even after detailed critical assessment, quantitative comparisons of results reported by different research groups is not recommended (see Section 6 in Ref. 46).

Following this guideline, below we compare only those results that were obtained by one research group within the same cycle of measurements. Such an approach made it possible to establish quantitative relationships between polarisabilities of different molecules and correlate their NLO activities with the molecular structure. The relationship between the hyperpolarisability of a molecule and its structure can be deduced from the quantum mechanical description of hyperpolarisability. The Hamiltonian of a system (*e.g.*, a molecule) in an external electric field can be represented as

$$\hat{H} = \hat{H}_0 + \hat{H}',$$

where $\hat{H}_0$ is the Hamiltonian of the unperturbed system and the term $\hat{H}'$ describes the effect of the field applied. If $\hat{H}'$ can be considered as a small perturbation, the hyperpolarisability (assuming only one excited state, which is referred to as the two-level model, and one-dimensional character of the tensor β, which is equivalent to the existence of one prevailing component, *e.g.*, β_{xxx}) can be written in a compact form as [3]

$$\beta_{xxx} = \frac{3\omega_{\text{ge}}^2 \Delta\mu_{ge}|\mu_{\text{ge}}|^2}{2\hbar^2(\omega_{\text{ge}}^2 - \omega^2)(\omega_{\text{ge}}^2 - 4\omega^2)}, \quad (5)$$

† In the present review, the notation β is adopted for the hyperpolarisability. By default, β without any additional indices, which was not explicitly commented, means vector component of hyperpolarisability [see Eqn (3)] in the static limit.

where ω_{ge} is the frequency of the transition from the ground (g) to the excited (e) state, μ_{ge} is the respective transition dipole moment and $\Delta\mu_{\text{ge}}$ is the difference between the dipole moments of the molecule in the ground and excited states. This formula clearly shows that β becomes larger with an increase in μ_{ge} and $\Delta\mu_{\text{ge}}$. This is achieved for molecules contaning donor and acceptor groups linked through a π-conjugated system. Mobile π-electrons in such molecules are readily redistributed upon perturbation with an electric field.

Importantly, as follows from the above relationship, NLO parameters of organic molecular crystals have a straightforward correlation with molecular hyperpolarisabilities. Since intermolecular interactions are significantly (2–3 orders of magnitude) weaker than the intramolecular ones,[47] the nonlinear susceptibility of a crystal can be represented as a sum of hyperpolarisabilities of the constituent molecules over the unit cell [48–50]

$$d_{IJK} = \frac{1}{V} f_I f_J f_K \sum_{n=1}^{Z} \left(\sum_{i=1}^{3} \sum_{j=1}^{3} \sum_{k=1}^{3} \cos\theta_{iI}^n \cos\theta_{jJ}^n \cos\theta_{kK}^n \beta_{ijk} \right). \quad (6)$$

Here, V is the unit cell volume; indices I, J and K refer to the crystallographic coordinate system; indices i, j and k define the components of β in the molecular coordinate system; the trigonometric terms $\cos\theta_{iI}^n$, $\cos\theta_{jJ}^n$ and $\cos\theta_{kK}^n$ define the transition matrix between these coordinate systems; f_I, f_J, f_K are the factors accounting the local field effects.

The experimental determination of the optical susceptibilities of crystals or polymers, which are of the greatest practical importance, is laborious (especially for single crystals), therefore, the design of NLO materials is based to a large extent on the knowledge and application of the relationship between the NLO susceptibilities of a crystal and hyperpolarisabilities of the constituent molecules.

The present review surveys the approaches to the design of NLO active materials at the molecular and crystal level. We limit ourselves to the consideration of organic and selected classes of organoelement compounds. Supplementary information on the use of organometallics in nonlinear optics can be found elsewhere.[51, 52]

II. Methods for the assessment of molecular hyperpolarisabilities

1. Experimental methods for measurement of molecular hyperpolarisabilities

One of the most popular method for the determination of molecular hyperpolarisabilities in solution or gas phase based on the measurements of the electrical field-induced second harmonic (EFISH) was developed in the early 1970s.[53–56] Prior to the measurement, molecules of the compound under study are oriented along a static electrical field. The third-order macroscopic optical susceptibility (Γ) obtained directly from the measurements relates to the respective microscopic value (γ) through the following expression

$$\Gamma = N\gamma f_0 f_\omega^2 f_{2\omega}\,,$$

where N is the number of molecules per unit volume, $\gamma = \gamma_{\text{e}} + \gamma_{\text{v}} + \gamma_{\text{r}}$ is the sum of electronic (γ_{e}), vibrational (γ_{v}) and orientational (γ_{r}) terms; $f_0, f_\omega, f_{2\omega}$ are the local field factors. The hyperpolarisability relates to the orientational term as

$$\gamma_{\text{r}} = \frac{\mu\beta_{\text{vect}}}{5kT}\,.$$

The orientational contribution can be separated using the temperature dependence $\gamma_{\text{r}}(T)$, and thus the scalar product of the dipole moment and the vector part of the hyperpolarisability $\mu\beta_{\text{vect}}$ can be determined. Often, the orientational term predominates, therefore other two terms can be neglected.[55] In order to retrieve the absolute value of β_{vect}, one should know the angle between the vectors μ and β_{vect} and the value of dipole moment.

The former can be estimated by means of quantum-chemical calculations, whereas the latter can be determined both theoretically and experimentally.

This means that the accuracy of the resultant value of β depends on the reliability of the quantum-chemical approximation applied and the accuracy of the determination of μ. Other tensor components β_{ijk} remain unknown and thus the formula (6) can only be applied to the calculation of the components of the NLO susceptibility tensor provided that the molecular hyperpolarisability is dominated by a single component (*e.g.*, β_{xxx}).

Yet another problem relates to the transition from the macroscopic (Γ) to the microscopic (γ) level of description, which requires an explicit allowance for the local field factors. In the case of weakly polar solute molecules and non-polar solvents, for which the intermolecular interactions can be neglected, the local field factors can be described within the Onsager model. However, the compounds that are of the greatest interest for nonlinear optics are polar and poorly soluble in non-polar solvents. Solute molecules in a polar solvent are additionally polarised by their solvate environment; furthermore, the formation of molecular associates, in particular, due to the H-bonding, is highly probable. Also there is a concentration dependence of the hyperpolarisability. Such effects have been studied in detail in the case of *p*-nitroaniline (*p*-NA, **1**). Measurements of the molecular hyperpolarisability were performed for solutions in polar methanol [57] and non-polar melt of *trans*-stilbene [58] and for a melt of *p*-NA itself.[57] The ratios obtained

$$\frac{\beta^{s}_{p\text{-NA}}}{\beta^{m}_{p\text{-NA}}} \approx \frac{\beta^{s}_{p\text{-NA}}}{\beta^{melt}_{p\text{-NA}}} = 0.33$$

(the superscripts s, m and melt denote the values for the solutions in stilbene and methanol and the melt, respectively) suggest a strong influence of the intermolecular interactions on the measured values. Both in the methanolic solution and the melt, *p*-nitroaniline molecules form H-bonded associates, which induce additional polarisation of the molecules thus giving rise to an increase in their hyperpolarisability. A similar relation has been obtained for *trans*-4-dimethylamino-4′-nitrostilbene (DANS, **2**) in *trans*-stilbene and acetone solutions [58, 59]

$$\frac{\beta^{s}_{DANS}}{\beta^{a}_{DANS}} = 0.3$$

(the superscript a and s correspond to the acetone and stilbene solutions, respectively).

The concentration dependences of β were studied for systems with both weak (*e.g.*, nitrobenzene – benzene or nitrobenzene – CCl_4) and strong intermolecular interactions prone to the formation of H-bonds (*e.g.*, water – methanol).[57] For polar and H-bonded systems, it was suggested to describe β with the following equation

$$\beta = \beta_0 + \beta^0_{dip}(1 - c) + \beta_{solv} f_s \,, \tag{7}$$

where β_0 is the hyperpolarisability of the isolated molecule, the second term quantifies the dipole – dipole interactions and the last term describes specific solute – solvent interactions; c and f_s are empirical parameters. This equation provides only a qualitative description of the real situation. For any specific case, additional measurements are required to estimate the two latter terms quantitatively, which becomes a separate problem.

Yet another experimental method exploits the phenomenon of incoherent scattering of the incident radiation by single molecules, the so-called Hyper Rayleigh Scattering (HRS), which was discovered in 1965.[60] For the measurements of the second harmonic generation, this method came in use only during the last decade owing to studies of *p*-NA, 4-methoxy- and 4-hydroxy-4′-nitrostilbenes by Clays and Persoons.[61, 62] The hyperpolarisabilities of these molecules measured using HRS were in agreement with the earlier EFISH results.

A clear advantage of HRS over EFISH is that [63] it does not require external static electrical fields for orienting the molecules, *i.e.*, for the induction of a non-centrosymmetric medium. This allows probing of molecules with the zero dipole moment (in particular, octupolar molecules and ions, which are described in more detail below). Furthermore, HRS can yield several components of the molecular hyperpolarisability tensor. Most typically, components β_{ZZZ} and β_{XZZ} in a laboratory coordinate system are determined, which relate to the molecular parameters as follows [64]

$$\langle \beta^2_{ZZZ} \rangle = \frac{1}{7}\sum_i \beta^2_{iii} + \frac{6}{35}\sum_{i\neq j} \beta_{iii}\beta_{ijj} + \frac{9}{35}\sum_{i\neq j} \beta^2_{ijj} + \frac{6}{35}\sum_{ijk} \beta_{ijj}\beta_{jkk} + \frac{12}{35}\beta^2_{ijk} \,, \tag{8}$$

$$\langle \beta^2_{XZZ} \rangle = \frac{1}{35}\sum_i \beta^2_{iii} - \frac{2}{105}\sum_{i\neq j} \beta_{iii}\beta_{ijj} + \frac{11}{105}\sum_{i\neq j} \beta^2_{ijj} - \frac{2}{105}\sum_{ijk} \beta_{ijj}\beta_{jkk} + \frac{8}{35}\beta^2_{ijk} \,. \tag{9}$$

Nevertheless, the principal of the aforementioned problems related to the use of EFISH are also typical of HRS, although to a lesser extent. First, even with HRS one cannot determine all the tensor component β_{ijk}. The second problem is due to the neglect of the solvation and association effects. For instance, the following ratios of hyperpolarisabilities were determined for acetonitrile and nitrobenzene in the gas (g) and liquid (l) phases [65]

$$\frac{\beta^{g}_{MeCN}}{\beta^{l}_{MeCN}} = 0.53, \quad \frac{\beta^{g}_{PhNO_2}}{\beta^{l}_{PhNO_2}} = 0.77 \,.$$

In the liquid phase, molecules stronger interact with each other and thus are stronger polarised as compared to the gas. More polar molecules are characterised by larger β, which is reflected in the ratios outlined above.

Huyskens *et al.*[66, 67] applied HRS to study the dependence of hyperpolarisability of *p*-NA and its *N*,*N*-dimethyl derivative on the solvent nature, in particular, polarity. They tested 50 different solvents and deduced the following formula representing the hyperpolarisability in a solution as a sum of the hyperpolarisability of an isolated molecule (gas-phase) β^g and corrections for the dipole – dipole interactions (the second term) and association (the third term)

$$\beta = \beta^g + \gamma_0 a\sqrt{\frac{\mu}{V}} + (1 - \gamma_0) b\sqrt{\mu} \,, \tag{10}$$

where γ_0 is the fraction of solute molecules not involved into H-bonding; a and b are empirical coefficients; μ is the dipole moment of the molecule in the gas phase; V is the solvent molar volume. Apparently, Eqn (10) is equivalent to Eqn (7), which was proposed to correct EFISH results for the solvation and association effects. Unfortunately, parametrisation of these equations for any particular compound is very demanding experimentally.

The problem of the interpretation of the solvation effects becomes especially important when the molecular hyperpolarisability has to be further used to estimate the NLO susceptibility of a crystal, in which the molecule is polarised by the crystal field evidently different from that experienced by the molecule in a solution or in a melt.

2. Theoretical approaches to the determination of the molecular hyperpolarisabilities

The major advantage of quantum-chemical methods for the determination of molecular hyperpolarisabilities is that [68 – 70] they enable calculation of all the tesnor components β_{ijk}. It has to be however noted that the problem of transferability of theoretical values for an isolated molecule to the molecule in a solid phase remains open and deserves a special consideration.

There are two basic approaches to the calculation of β. Within the first approach, the terms describing the interaction of a system

with an electromagnetic field are explicitly included into the Hamiltonian of the system. The second approach exploits the idea that the eigenfunctions of a molecule constitute a complete set and any state of the molecule perturbed by an electric field can be factorised in this basis.

In the first approach referred to as the Finite Field (FF) theory, the Hamiltonian of a system parturbed by an electrical field with a strength E is represented as

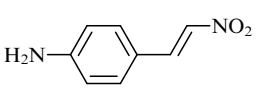
$$\hat{H} = \hat{H}_0 - \mathrm{e}E\hat{r}, \tag{11}$$

where $\hat{H}_0$ is the Hamiltonian of the unperturbed system and $\hat{r}$ is the dipole moment operator. The polarisability can be deduced as the derivative of the dipole moment $\mu(E)$ or energy $W(E)$ with respect to the field (E). For the first hyperpolarisability, the following expression can be written

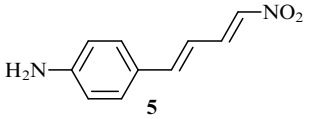
$$\beta_{ijk} = \frac{\partial^2 \mu_i(E)}{\partial E_j \partial E_k} = -\frac{\partial^3 W(E)}{\partial E_i \partial E_j \partial E_k}. \tag{12}$$

The differentiation can be performed either numerically or analytically. In the latter case, an acronym CPHF (Coupled Perturbed Hartree – Fock) is often used instead of FF.

This approach was further developed by Zyss [71–73] in a combination with the semiempirical approximation INDO/S. The hyperpolarisabilities were calculated as numerical derivatives of the dipole moment with respect to the electric field for a series of mono and disubstituted benzenes [**1**, *o*-NA (**3**), **4**, **5**] and compared to the available experimental data. A direct comparison of contributions made by σ- and π-electrons into the value of hyperpolarisability indicates that it is the π-electrons that are of predominant importance, which is fully in accord with earlier concepts. According to the values obtained for molecules **1**, **4** and **5**, β drastically increases with an increase in the conjugated chain length.



4



5

The theoretical values of β reported by Zyss [71–73] are underestimated by approximately one order of magnitude as compared to the experimental data, however, they correctly reproduce the experimental trends along the series of compounds studied (Table 1).

Kurtz *et al.* [75] utilised the MNDO approximation with the AM1 and PM3 parametrisation schemes and adopted the FF-based algorithm of the calculation of different-order polarisabilities for the MOPAC code. Matsuzawa and Dixon [76, 77] comprehensively tested this implementation by calculating hyperpolarisabilities of about 150 conjugated polar molecules with the PM3 parametrisation.

As shown in Fig. 1, a reasonably good agreement between the theoretical and experimental values was obtained, although the values for molecules with high hyperpolarisabilities were systematically underestimated by the calculation.

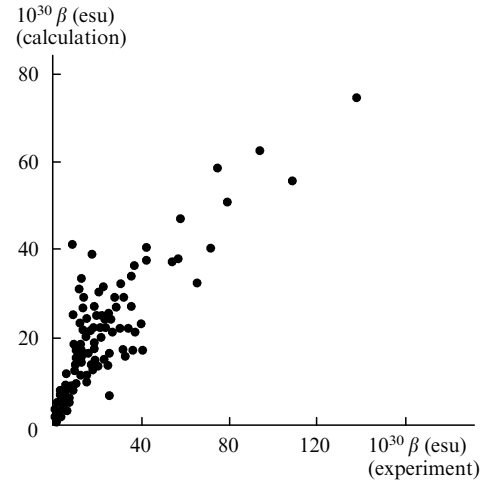
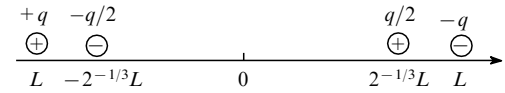


Figure 1. The correlation of calculated (FF/PM3 method) and experimentally determined (EFISH measurements) [78, 79] hyperpolarisabilities of D/A-substituted π-conjugated molecules.

Based on the FF theory, Cardelino *et al.*[80] suggested to simulate the perturbation field with a set of point charges.

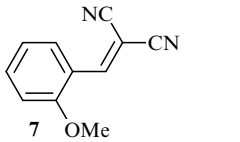


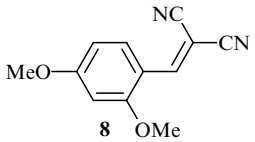
If the separation between the opposite charges $\pm q$ is sufficiently large ($L > 160$ Å), the probe molecule placed into the centre of the system experiences the influence of a constant electric field

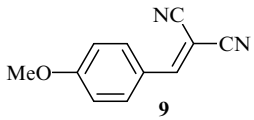
$$E = \frac{1}{4\pi\varepsilon_0}\left(2 - 2^{2/3}\right) qL^{-2}, \tag{13}$$

the field strength being varied from 0 to 7 V Å^{-1}.

The calculated values of β obtained for molecules **1**, **3**, *m*-NA (**6**) and **7**–**9** using this model [80–83] are in good agreement with the experimental ones (Table 2).







9

The Sum Over States (SOS) method is also widely applied to the theoretical evaluation of NLO susceptibilities of molecules.

Table 1. Calculated (FF/INDO, in the static limit) and experimental values of the molecular hyperpolarisabilities (10^{-30} esu) of D/A-substituted benzene derivatives.

Molecule	β(calc.)	β(exp.) [a]	Molecule	β(calc.)	β(exp.) [b]
3	0.2	1.9 – 10.2	**4**	12.9	146.6
1	3.4	6.4 – 46.9	**5**	50.6	433.2

[a] Hereinafter in this Section: a range of β values is given, if several experimental values were reported in the literature for the molecule;[46, 74] in the case of incident wavelength-dependent calculations, only the experimental data measured at the same wavelenth are given; in the case of calculations in the static limit (as in this case), the whole range of experimental values is given. [b] Results of EFISH measurements from Ref. 73.

Table 2. Calculated (modified FF/AM1 method, in the static limit) and experimental values of the molecular hyperpolarisabilities (10^{-30} esu) of D/A-substituted benzene derivatives.

Molecule	β(calc.)	β(exp.)	Molecule	β(calc.)	β(exp.) [a]
3	1.7	1.9 – 10.2	**7**	13.1	18.7
6	2.8	2.5 – 6.0	**8**	30.7	76.3
1	5.3	6.4 – 46.9	**9**	32.6	56.5

[a] EFISH measurements in 1,4-dioxane at an incident wavelength of $\lambda = 1064$ nm.[81]

According to this method, the hyperpolarisability can be represented as [84]

$$\beta(\omega)_{ijk} = -\frac{e^3}{8\hbar^2}\sum_n\sum_{n'}\left\{(r^j_{gn'}r^i_{n'n}r^k_{gn} + r^k_{gn'}r^i_{n'n}r^j_{gn}) \times \right. \quad (14)$$

$$\times\left[(\omega_{n'g}-\omega)^{-1}(\omega_{ng}+\omega)^{-1} + (\omega_{n'g}+\omega)^{-1}(\omega_{ng}-\omega)^{-1}\right] +$$

$$+\left(r_{gn'}r_{n'n}r_{gn}k + r^i_{gn'}r^k_{n'n}r^j_{gn}\right)\left[(\omega_{n'g}+2\omega)^{-1}(\omega_{ng}+\omega)^{-1} + \right.$$

$$\left.+\left(\omega_{n'g}-2\omega\right)^{-1}(\omega_{ng}-\omega)^{-1}\right] + \left(r^j_{gn'}r^k_{n'n}r^i_{gn} + r^k_{gn'}r^j_{n'n}r^i_{gn}\right) \times$$

$$\left.\times\left[(\omega_{n'g}-\omega)^{-1}(\omega_{ng}-2\omega)^{-1} + (\omega_{n'g}+\omega)^{-1}(\omega_{ng}+2\omega)^{-1}\right]\right\},$$

where the dipole moment operator r and the transition frequencies ω with subscripts correspond to transitions between the ground (g) and excited (n, n') states.

The dependence of the hyperpolarisability on ω is explicitly included in the Eqn (14), which is an advantage of this approach. However, an accurate calculation of β requires that the summation was performed over all excited states, which is associated with enormous computational costs. This approach is of low efficiency, especially as regards calculations for large and medium-sized molecules (*e.g.*, *p*-NA). The contributions of separate electron transitions into the total β value can be isolated and arranged in the descending order of their magnitudes. Then, the summation in the Eqn (14) can be aborted after reaching a preset accuracy level. Utilising of the SOS method makes it possible to analyse separate contributions thereby providing a valuable insight into the origin of the nonlinear susceptibility of a molecule, which is a prerequisite for establishing the structure–property relationship. Nevertheless, it should be kept in mind that the total contribution of neglected terms can prove significant impact despite the smallness of each separate term.

The SOS method within the CNDO/CI approximation was applied by Lalama *et al.*,[85] Morrell and Albrecht [86] for the evaluation of the hyperpolarisability of *p*-NA. The values of β (in esu) obtained in these two studies, 6.53×10^{-30} (Ref. 85) and 34.3×10^{-30} (Ref. 86) are significantly different due to the different parameter sets used, however, they both lie within the range of reported experimental values $(6.4-46.9)\times10^{-30}$ (Refs 57, 58, 74 and 87) measured in different solvents, at different incident wavelengths and using different reference values of d_{11} (for the quartz standard): 0.8×10^{-9} (Refs 57, 58) or 1.2×10^{-9} esu (Refs 74, 87).

The SOS method was further optimised by Morley and coworkers.[88–90] They parametrised the method for 22 π-conjugated molecules using the CNDO/CIS approximation. The formula (14) was modified by its transformation to a special coordinate system with the origin placed into the centre of gravity of the electron density distribution of the molecule in its ground state. The theoretical results for nitrobenzene (**10**), aniline (**11**), *p*-NA and molecules **12**–**15** obtained by this method reproduce the experimentally established trends, although the values themselves differ by a factor of 3–4 in some cases (Table 3). Here, it would be appropriate to mention the large scatter in the reported experimental data, which limits the reliability of the parametrisation. The method described above was implemented in the CNDOVSB software code.[89]

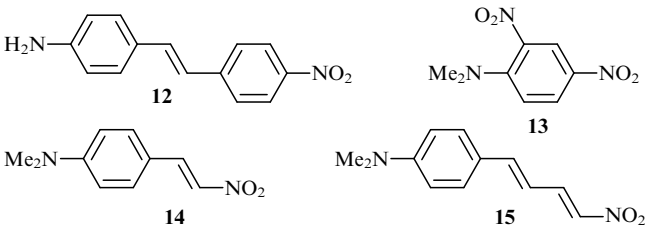


Table 3. Calculated (SOS method within the PPP and CNDO approximations) and experimental values of dynamic ($\hbar\omega = 1.17$ eV) hyperpolarisabilities (10^{-30} esu) of D/A-substituted benzene and stilbene derivatives.

Molecule	β_{PPP}	β_{CNDO}	β(experiment)
10	5.4	0.62	1.9–2.4
11	2.5	3.66	0.6–1.2
1[a]	35.9	12.18	9.6–46.9
12	300.0	69.15	225–295
13	39.1	9.25	21
14	179.3	126	180–260
15	687.9	355	470–790

[a] The experimental data for *p*-NA were measured at $\hbar\omega = 0.656$ eV; the photon energy values $\hbar\omega = 1.17$ and 0.656 eV correspond to the incident wavelengths of 1064 and 1907 nm, respectively.

Li, Marks and Ratner [91,92] combined the SOS method with the PPP/CIS approximation; some of their results are compared with the experimental data and CNDO-based theoretical estimates in Table 3. It is clearly seen that the calculated data agree qualitatively with the experimental ones. The PPP-based theoretical estimates agree with the experiment somewhat better than the CNDO-based ones, although the former approximation is by definition less accurate. Probably, the defficiency in the theory is compensated for by better parametrisation.

Verification of the adequacy of the SOS approach was carried out by Kanis *et al.*[39,93,94] for 203 polar organic molecules using the ZINDO code [95–98] (the SOS method coupled with the INDO approximation), the results obtained are shown in Fig. 2.

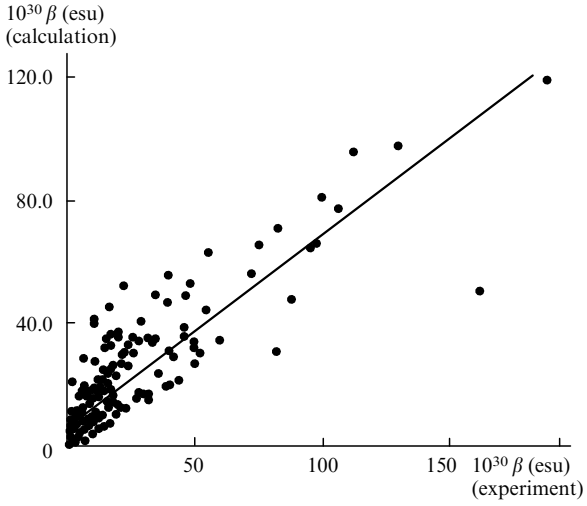


Figure 2. The correlation of calculated (SOS/INDO method) [95–95] and experimentally determined (EFISH measurements) [78,79] hyperpolarisabilities of D/A-substituted π-conjugated molecules.

Some common trends can be revealed from the comparison of theoretical (based on the FF and SOS approaches) and experimental results (see Figs 1 and 2). The agreement for lower values of β is better than for higher values (in the latter case, the calculated values are always smaller than the experimental ones). Taking into account that the reported experimental data refer to SHG measurements in solutions,[78,79] this discrepancy can be rationalised assuming the aforementioned solvation and association effects, which become important for easily polarisable molecules, *i.e.*, for molecules susceptible to the environmental effects. Apparently, the correlation between the theoretical and

experimental values is better described by a function $k\sqrt[y]{x}$ ($y > 1$) rather than a linear dependence.

The majority of calculations of the hyperpolarisabilities with *ab initio* quantum-chemical methods are based on the finite field (FF) formalism. For the calculation of the frequency dependent hyperpolarisabilities $\beta(2\omega,\omega,\omega)$, it is necessary to use the time-dependent Schrödinger equation. Such an approach employing the Hartree–Fock approximation was elaborated by Sekino and Bartlett [99] and tested on a number of small molecules. The calculated values were found to be $\sim 1.5-2$ times smaller than the respective experimental data. Karna and Dupuis [100,101] improved the computational algorithm and accomplished test calculations for molecules $CHHal_3$. The algorithm was implemented in the HONDO code.[101] Despite good agreement in polarisabilities $\alpha(\omega,\omega)$, the theoretical values of $\beta(2\omega,\omega,\omega)$ were several-fold smaller than the experimental ones. Most probably, this is due to the fact that the reported experimental values refer to measurements in solutions.

Further developments of the theoretical approaches to the determination of molecular hyperpolarisabilities are based on the account of the electron correlation. Sekino and Bartlett proposed [102] a multiplicative static correlation correction to $\beta(2\omega,\omega,\omega)$ calculated at the Hartree–Fock (HF) level. Within the ACES II software code developed by the authors, the correlated dynamical hyperpolarisability was obtained based on the value of $\beta(2\omega,\omega,\omega)$ calculated by the Hartree–Fock method and the values of $\beta(0)$ calculated both by the Hartree–Fock and by higher-level electron correlation methods {the perturbation (MP2) or Coupled Clusters theory [CCSD and CCSD(T)]} according to the formula

$$\beta_{cor}(2\omega,\omega,\omega) = \beta_{cor}(0)\,\frac{\beta_{HF}(2\omega,\omega,\omega)}{\beta_{HF}(0)}. \qquad (15)$$

Rice *et al.*[103] suggested to account the electron correlation in the calculations of the dynamic hyperpolarisabilities with an additive correction

$$\beta_{cor}(2\omega,\omega,\omega) = \beta_{cor}(0) + [\beta_{HF}(2\omega,\omega,\omega) - \beta_{HF}(0)]. \qquad (16)$$

Further, Rice and Handy,[104,105] Aiga and co-workers [106–109] elaborated a method for the calculation of the dynamic hyperpolarisabilities within the MP2 approximation with the simultaneous account of the electron correlation and frequency dependence. The validity of the additive scheme was verified [105] by comparing its results with the results of strict *ab initio* calculations of $\beta(2\omega,\omega,\omega)$ for formaldehyde and ammonia. The use of the additive correction underestimates the *ab initio* values for CH_2O and NH_3 by 4% and 13%, respectively, at the incident wavelength of a ruby laser. Hammond and Rice compared [110] the additive and multiplicative corrections in the case of HCl molecule by accounting the electron correlation with the CCSD(T) method. The frequency dependent values were calculated within the Hartree–Fock and MP2 methods. The latter approach yielded better (by 3%–8%) agreement with the experimental data and in this case, the additive correction performed slightly better (by 1%) than the multiplicative one. On the other hand, the multiplicative scheme appears preferable if the frequency dependence is taken into account by the Hartree–Fock method (the difference is 4%).

Yet another approach to the assessment of hyperpolarisability with account of the electron correlation was elaborated [111,112] based on the CCS, CC2, CCSD and CC3 methods. The following values of $\beta(2\omega,\omega,\omega)$ were obtained for hydrogen fluoride with the t-aug-cc-pVTZ basis set (in a.u. at $\omega = 0.0656$ a.u.):

Method	CCS	CC2	CCSD	CC3	Experiment [113] (gas phase)
$-\beta(2\omega,\omega,\omega)$	7.760	12.030	8.789	8.321	10.9 ± 0.95

It has to be mentioned that the hydrogen fluoride molecule represents a 'stumbling block' as regards the comparison of the theoretical and experimental results. Even after a vibrational correction (-1 a.u.) [114,115] is added, the theoretical estimation remains beyond the confidence interval of the experiment. Notwithstanding, the similar vibration-corrected calculations for a series of small molecules, including H_2O, CO, MeCN and HCl, give values of $\beta(2\omega,\omega,\omega)$ in quantitative agreement with the experiment (Table 4).[116–120]

High-level *ab initio* calculations make it possible to estimate $\beta(2\omega,\omega,\omega)$ to within 10%. It has to be stressed that the accurate

Table 4. The values of $\beta(2\omega,\omega,\omega)$ (a.u.) calculated with the MP2 and Coupled Clusters (CC) methods compared to the respective experimental values for small molecules.

Method	mHyPOL (see [a])	d-aug-cc-pVDZ	d-aug-cc-pVTZ	d-aug-cc-pVQZ	d-aug-cc-pV5Z	Ref.	Experiment	Ref.
CO molecule								
MP2	31.64	–	31.00	–	–	109	29.9 ± 3.2 [b]	119
CCSD	–	–	29.56	29.09	–	116		
CC3	–	–	31.91	–	–	116		
H_2O molecule								
MP2	-21.31	–	-19.89	–	–	109		
CCSD	–	–	-21.72	-21.98	–	116	-21.8 ± 0.9 [b]	119
CC3	–	–	-21.02	–	–	116		
NH_3 molecule								
MP2	-49.16	–	–	–	–	109	-48.4 ± 1.2 [b]	119
MeCN molecule								
MP2	–	31.5	–	–	–	117	26.3 ± 0.8 [c]	120
CCSD	–	29.3	–	–	–	117		
CCSD(T)	–	26.7	–	–	–	117		
HCl molecule								
CC3	–	–	–	–	4.57	118	4.9 ± 0.5 [b]	113

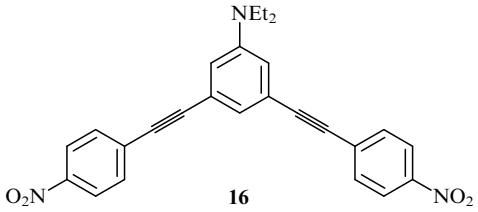
Note. The frequencies used in the calculations correspond to the experimental incident wavelengths (λ). [a] Modified [109] basis POL: (10s6p4d2f)/[5s3p3d2f] for the second-period elements, (6s4p2d)/[3s3p2d] for the hydrogen atoms. [b] Gas phase, $\lambda = 694.3$ nm. [c] Gas phase, $\lambda = 514.5$ nm; the value is multiplied by 3/5.

reproduction of experimental data is the only reasonable criterion for the adequacy of the theoretical method applied. However, the experimental measurements are dependent on the selection of the reference values. Unfortunately, no unambiguous criteria for the correct selection of such standard values have been proposed so far.[23, 65, 121, 122] Furthermore, the application of highly accurate calculations is restricted to the size of molecules under study. It is evident that the molecules considered above, composed of two–six atoms, are exclusively of theoretical interest.

Thus, two major directions of modern theoretical investigations into the NLO properties of molecules can be distinguished. The first direction implies the development of high-level *ab initio* methods and their verification by comparing the calculation results with the accurate experimental data from gas-phase measurements. Such calculations should use sufficiently broad basis sets that include polarisation and diffusion functions,[123] take into account the electron correlation and vibrational corrections,[124, 125] which can amount up to several per cent of the total value[126] (this correction is typically neglected in lower-level calculations).

The second direction consists of the use of less accurate but faster methods for the calculation of hyperpolarisabilities enabling studies of larger molecules for the prediction of trends in their NLO properties and selection of promising systems for the experimental study. For instance, Beck and Grummt analysed[127] 200 different conjugated polar molecules using the FF and SOS methods with semiempirical approximations (AM1, PM3, CNDO/S). They concluded that the semiempirical methods adequately reproduce the experimentally observed trends, and the discrepancies between the theoretical and experimental values are due to the lack of treatment (or insufficient model treatment) of the environmental effects rather than mere theory deficiencies.

The density functional theory (DFT) is widely employed for the evaluation of NLO properties of molecules, in particular, hyperpolarisabilities, since it provides the most efficient means (in terms of computational costs) to account the electron correlation.[128] Nevertheless, the reliability and validity of DFT-derived results remain disputable. Some authors criticise[129–132] theoretical hyperpolarisabilities calulated using very well known functionals, such as SVWN, BLYP and B3LYP.[128, 133] Meanwhile, other research groups (see, for instance, Refs 134–138) advocate the validity of the DFT calculations. Tables 5–9 compare theoretical hyperpolarisabilities of small molecules, benzene diyne derivative **16**, triazines **17**–**19**, NH_2/NO_2-substituted π-conjugated molecules (compounds **1**, **12**, **20**, **21**), D/A-substituted benzenes (**22a**–**d**) and stilbenes (**23a**–**d**) calculated within the density functional theory with the respective experimental values.

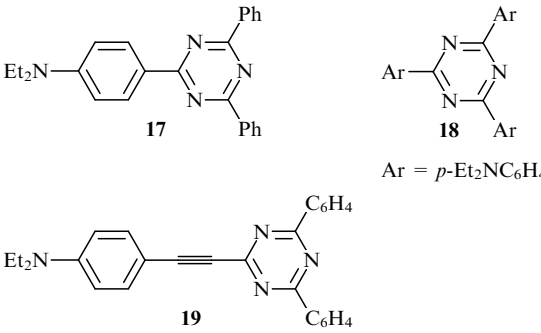


16

Table 5. Calculated[129] (DFT) and experimental[119] (gas phase, λ = 694.3 nm) values of $\beta(2\omega,\omega,\omega)$ (a.u.) for small molecules.

Molecule	SVWN/TZ2P + diff	BLYP/TZ2P + diff	LB94/TZ2P + diff	Experiment
NH_3	−109	−138	−46.0	−48.4 ± 1.2
CO	36.6	37.8	23.4	29.9 ± 3.2
H_2O	−34.4	−37.3	−20.3	−21.8 ± 0.9
HF	−10.7	−11.2	−7.68	−10.9 ± 0.95[a]

Note. The basis TZ2P was augmented with diffuse functions; the frequencies used in the calculations correspond to the experimental incident wavelengths (λ). [a] Data from Ref. 113.



D = MeO (**a**), HO (**b**), Me (**c**), HC(O) (**d**).

The application of DFT gives rise to a problem of an inexact asymptotic behaviour of the majority of functionals at distances far from nuclei (*i.e.*, in the region of vacant molecular orbitals): they decrease exponentially rather than as $\sim 1/r$. The functionals with improved asymptotic behaviour [*e.g.*, LB94, HCTH(AC) or BP86-GRAC] often perform better in terms of agreement with the experimental data and accurate *ab initio* quantum mechanical calculations (see Tables 5, 6).

However, an HCTH(AC)-based calculation incorrectly predicts the hyperpolarisability of acetonitrile, whereas the use of the B97-1 functional yields more accurate estimates. An incorrect ratio of the hyperpolarisabilities of molecules **17** and **18** was obtained in a theoretical study of triazine derivatives with the

Table 6. Theoretical values of $\beta(0,0,0)$ (a.u.) for small molecules according to DFT and strict calculations based om the Coupled Clusters method.

Molecule	LDA[a]	BLYP[a]	B3LYP[a]	B97-1[a]	HCTH (AC)[a]	BP86-GRAC[b]	BLYP[c]	CCSD(T)[d]
NH_3	−55.66	−58.59	−41.03	−38.93	−33.30	−37.87	−87.09	−34.3
H_2O	−24.79	−24.40	−19.19	−18.65	−18.31	−18.2	−28.19	−18.0
H_2S	−14.73	−10.48	−7.15	−7.37	−10.22	–	–	−7.7
CO	29.46	29.30	26.86	26.33	22.60	21.9	32.89	23.5
HF	−8.86	−8.73	−7.42	−7.21	−7.35	−7.2	−8.85	−7.3
MeCN	36.97	38.53	31.73	27.77	87.3	–	–	24.2[e]

[a] Data from Ref. 130; The basis set POL was augmented with d-functions for the hydrogen atoms and s- and p-functions for heavier atoms. [b] Data from Ref. 132; the basis sets 7s5p4d for H, 9s7p5d4f for C, N, O and 11s7p5d4f for F. [c] Data from Ref. 135; the basis set DNP + FIP. [d] Data from Ref. 102; the same basis as in Ref. 130. [e] Data from Ref. 120; the basis [4 + 1s3 + 1p2 + 1d/3 + 1s2 + 1p] + (2s2p1d1f/2s).

Table 7. Theoretical dynamic hyperpolarisabilities (10^{-30} esu, λ = 1064 nm) calculated within the LB94/DZP(fc) approximation for molecules **16**–**19** [137] compared to results of the HRS measurements in 1,4-dioxane at λ = 1064 nm.[139,140]

Molecule	β(calc.)	β(exp.)	Molecule	β(calc.)	β(exp.)
16	31	43	**18**	313	383
17	323	259	**19**	1211	447

Table 8. The values of β(0,0,0) (a.u.) for NH_2/NO_2-substituted π-conjugated molecules calculated using the DFT and MP2 methods.[131]

Molecule	SVWN/ 6-31G	BLYP/ 6-31G	B3LYP/ 6-31G	LB94/LDA/ TZ2P	MP2/ 6-31G
1	1650	1656	1698	1903	1931
12	29 298	28 349	20 153	36 695	10 110
20	47 090	47 140	54 710	52 040	62 660
21	682 000	677 000	611 000	784 000	184 000

LB94 functional (see Table 7). The hybrid functionals B3LYP and B97-1 perform somewhat better than LDA and BLYP (see Table 6).

Table 8 summarises computational results for a number of molecules with extended π-conjugated bridges. According to the tabulated data, the values predicted by DFT (in particular, in the case of the LB94 functional with improved asymptotic behaviour) are significantly larger than those predicted by MP2. Based on this conclusion, Champagne *et al.*[131] warned against the use of DFT for the evaluation of hyperpolarisabilities. However, we should point out that the hyperpolarisabilities increase by factors of 12 and 5 on going from molecule **1** to **12**, as estimated with B3LYP and MP2, respectively. Meanwhile, according to the experimental measurements, the ratio of hyperpolarisabilities of D/A-substituted stilbenes and benzenes varies in the range from 6 to 10, depending on substituents and experimental conditions (see Table 9). This means that the increase in β with an increase in the conjugation chain length is somewhat underestimated by MP2 and overestimated by B3LYP in the above caclualtions by Champagne *et al.*[131] It is also of note that β of *p*-NA has been accurately determined experimentally in the gas phase (1787 ± 73 a.u., EFISH, λ = 1064 nm) [65] and it is unclear, why Champagne *et al.*[131] did not compare their theoretical results with this experimental value. From Table 8, it is apparent that the B3LYP-based estimate is closer to the experimental value than that of MP2.

As has been mentioned above, the B3LYP functional perfoms slightly better than the non-hybrid ones and, in this particular case, also proves superior to LB94 (which estimates the increase in hyperpolarisability on going from **1** to **12** to be 19-fold). Unfortunately, the lack of experimental data for **21** prevents the respective analysis of the increase in hyperpolarisability on going from **20** to **21**. We suggest that the use of DFT gives rise to the overestimation of hyperpolarisabilities in the case of extended easily polarisable π-systems, such as polyenes. At the same time, the π-systems containing aromatic rings are less polarisable and can be adequately described within DFT.

Table 9. The values of static and dynamic hyperpolarisabilities (10^{-30} esu, λ = 1907 nm) of D/A-substituted benzene and stilbene derivatives calculated by the LDA/POL [136] method compared to the respective experimental values.[78]

Molecule	β(0,0,0)	$\beta(2\omega,\omega,\omega)$	Experiment [a]
22a	6.74	8.18	15.3
22b	4.91	5.85	9.0
22c	3.56	4.24	6.3
22d	0.32	0.52	1.8
23a	96	153	84
23b	79	123	51
23c	63	95	45
23d	17	27	18

[a] EFISH measurements in 1,4-dioxane at λ = 1907 nm.

Regardless of the aforementioned drawbacks, the majority of functionals correctly reproduce the experimental trends in β (see Tables 5–8). It thus follows that the B3LYP and, especially, B97-1 functionals are slightly superioir to others.

It is important to keep in mind the major purpose of the use of various computational methods. Most often, in the search for promising materials for NLO applications it is reasonable to monitor relative changes in hyperpolarisabilities along a specific series of compounds. Apparently, DFT provides the optimum efficiency for this task.

III. Characteristics of π-conjugated systems related to the efficiency of the second harmonic generation

1. Qualitative criteria of hyperpolarisability. Hyperpolarisability as a function of the conjugated chain length

The condition that an NLO active molecule should contain strong donor and acceptor substituents linked by an easily polarisable π-bridge can be considered as a basic prerequisite in the search for NLO compounds. The optimum combination of the π-system and D/A-substituents provides the maximum NLO efficiency.

Marder *et al.*[141–145] proposed a convenient criterion for the description of NLO active molecules, which characterises the degree of delocalisation of the electron density over the π-system as a function of the nature (weak/strong) of D/A-substituents, *viz.*, Bond Length Alternation (BLA), calculated as a mean difference between the lengths of formally ordinary and double bonds. This difference can be determined from either experimental data on the molecular structure or quantum-chemical calculations. A series of substituted polyenes was analysed in order to verify the applicability of the criterion.



The distribution of bond lengths in the polyenes shifts either towards the non-polar form (a non-polar solvent, weak D/A-substituents) or towards the zwitter-ionic form (a polar solvent, strong D/A-substituents).

The BLA criterion was used [141] to monitor the effects of the strength of D/A-substituents on the degree of the electron delocalisation over the polyene π-chain. The criterion makes it possible to arrange any D/A-substitutents in a common scale of their relative strengths and depict the molecular hyperpolarisability as a function of the substituent strength.

Within the two-level model, the static hyperpolarisability can be represented as

$$\beta = \frac{3}{2}(\mu_e - \mu_g)\frac{\mu_{ge}^2}{E_{ge}^2}, \qquad (17)$$

where $(\mu_e - \mu_g)$ is the difference between the dipole moments of the molecule in the ground and excited states, μ_{ge} is the transition dipole moment and E_{ge} is the corresponding energy [this is a static analogue of the formula (5)]. Terms in the right part of Eqn (17) are related to the ground state wavefunction (Fig. 3), which in turn correlates with BLA according to the definition of the criterion.[141,142]

Hyperpolarisabilities of molecules with identical substituents (*viz.*, NMe_2 and CHO) as a function of BLA and another similar criterion, Bond Order Alternation (BOA), were analysed theoret-

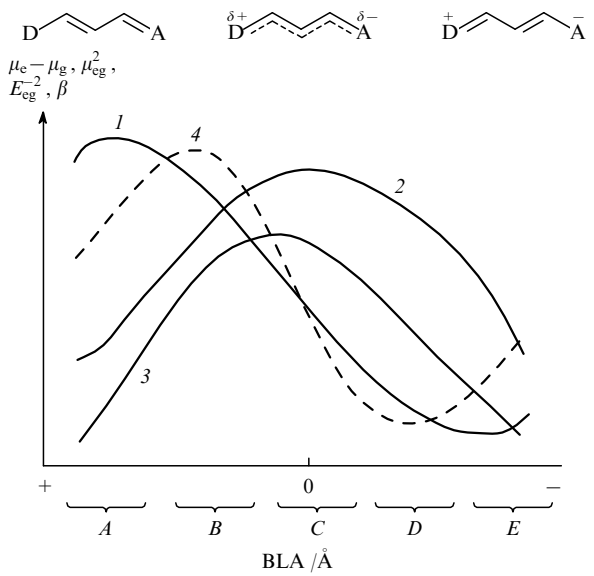
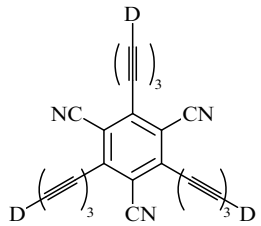


Figure 3. Dependences of $(\mu_e-\mu_g)$ (*1*), μ_{eg}^2 (2), E_{eg}^{-2} (3) and β (*4*) on the ground-state wavefunction of a polyene system represented by the BLA parameter.
It is commonly adopted that BLA > 0 for molecules in the neutral form and BLA < 0 for zwitter-ions. *A* – *E* are arbitrarily selectred regions.

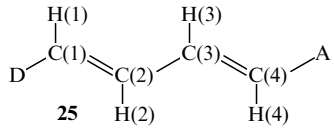
ically using the SOS/INDO/CISD and FF/AM1 methods.[144–146] Solvent effect were simulated by applying an electric field. The dependence β *vs.* BOA fully consistent with the curve *4* in Fig. 3 was obtained. The function β *vs.* BLA was also analysed [147] for the case of octupolar molecules (see below).



24

The values of β for molecules **24** with the donor substituent (D) varied over the series H, Me, OH, OMe, NH_2 and NMe_2 were estimated within the CPHF/6-31G approximation. The resultant values of β increase with an increase in the donor strength of the substitient along the above series, but it does not reach the maxium probably remaining in the region *A* (see Fig. 3).

Yet another criterion, BACS (Bridge Atomic Charge Sum), which characterises the effects of substituents and/or environment on the degree of conjugation over the π-chain linking donor and acceptor groups in molecules of the type **25**, was suggested.[148–150] It is defined as the sum of charges on the atoms constituting the chain.

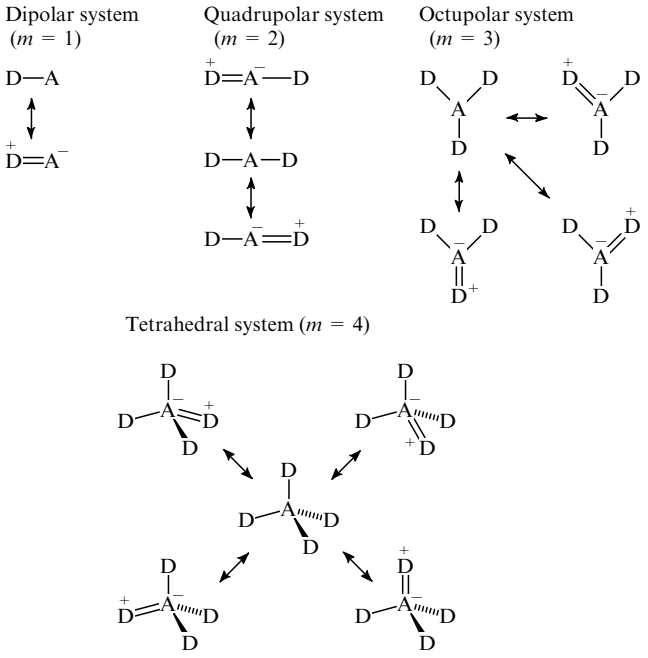


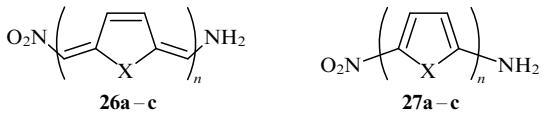
25

$$BACS = q_{C_i} + q_{H_j}$$

Solvent effects were also simulated by adjusting the external electric field strength. D/A-substituted polyenes and five-membered heterocycles (**26a**–**c**, **27a**–**c**) were selected as model systems. The optical characteristics were calculated within the FF/AM1 approximation. The linearity between BACS and BLA criteria was demonstrated for the case of polyenes,[148] which implies that BACS also correlates with the ground state wavefunction. It was established [149, 150] that the dependences β *vs.* BACS for the substituted heterocycles studied are similar to those for polyenes. Thus, it may be concluded that the curve *4* in Fig. 3 describes the general trend in hyperpolarisability of any π-conjugated system on going from its neutral to the zwitter-ionic form.

Scheme 2





26a–**c** **27a**–**c**

X = NH (**a**), O (**b**), S (**c**).

Yet another prameter utilised to represent the ground state wavefunction within the VB-*m*CT model is worth mentioning. A molecule can be represented as a combination of its valence-bond structure (VB) that characterises of the neutral form and *m* charge-transfer (CT) states corresponding to different zwitter-ionic forms (Scheme 2).

The ground-state wavefunction (ψ_g) can be written in the basis of VB (φ_{VB}) and CT (φ_{CT}) functions as

$$\psi_g = \varphi_{VB}\sqrt{1-ml} + \sqrt{l}\sum_{j=1}^{m}\varphi_{CT\,j}\,, \qquad (18)$$

where *m* is the number of zwitter-ionic states, *l* is the parameter quantifying the degree of mixing between the neutral and the zwitter-ionic forms. The latter parameter was selected by some researchers [151–156] as a criterion for the evaluation of β, whereas another criterion, MIX, was preferred in a series of works [157–160] for linear molecules. MIX relates to *l* in a simple way

$$MIX = 2l - 1.$$

The linearity between *l* and MIX, on the one side and BLA, on the other was demonstrated for linear,[151, 157–160] quadrupolar,[152] octupolar [153–155] and tetrahedral molecules.[156] Furthermore, Laage *et al.*[161] applied the MIX criterion to the description of hyperpolarisabilities of charged D/A-substituted polyenes.

It has to be noted that the criteria considered above, despite their convenience, have specific limitations and are only of a qualitative character. For instance, the use of BLA for molecules containing heteroatoms is hardly justifed. The BACS criterion is more suitable for the comparative analyses of results obtained for different π-conjugated chains but it has to be kept in mind that the values of atomic charges depend on the computational method

and basis sets selected.[162] Probably, the criteria *l* or MIX are more versatile, however, their determination requires special calculations, whereas molecular geometry parameters and atomic charges are listed in default outputs of all major quantum-chemical codes. The common feature of all the criteria considered above is that they correlate with the ground state wavefunction, which primarily defines the efficiency of the second harmonic generation. All the above-mentioned criteria can only be used for the visualisation of the wavefunction.

As has been shown both theoretically (*e.g.*, see Ref. 163) and experimentally,[78, 79] an elongation of the conjugation chain gives rise to a significant increase in the molecular hyperpolarisability. Zhu and Jiang [150] estimated the increase in β with an increase in the number of units (n) in the conjugation chain. Comparative data for molecules with polyheterocyclic chains are shown in Fig. 4. The quinonoid-type polyheterocylces **26a**–**c** reveal high NLO activity, whereas that in the case of polyheterocycles **27a**–**c** is significantly lower and the activity increases more slowly with the chain elongation. According to the computation, β increases in the series pyrrole < furan < thiophene, but this empirical observation was not explained.

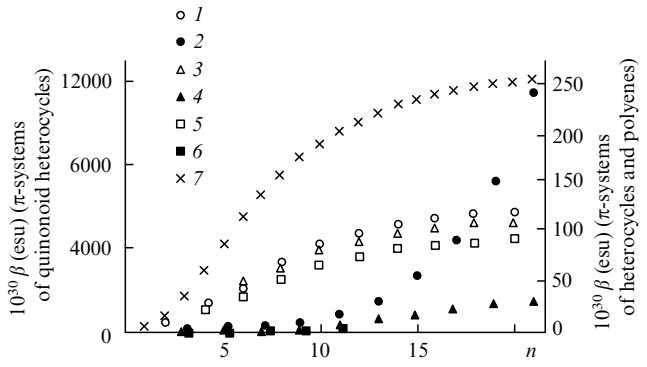


Figure 4. Hyperpolarisability as a function of the number of conjugated chain units for NH_2/NO_2-substituted polyheterocycles (*1*–6) and polyenes (*7*);
(*1*) polythiophene (**27c**), (*2*) quinonoid analogue of polythiophene (**26c**), (*3*) polyfuran (**27b**), (*4*) quinonoid analogue of polyfuran (**26b**), (*5*) polypyrrol (**27a**), (*6*) quinonoid analogue of polypyrrol (**26a**), (*7*) polyenes.

Similar results were obtained by Morley,[164] who applied the software code CNDOVSB to calculate the polarisabilities of NMe_2/NO_2-substituted polyheterocycles. The same series of ascending β (pyrrole < furan < thiophene) was obtained. Morley speculated [164] that such a sequence is due to the combined effect of the degree of charge transfer and energy gap between the ground and excited states.

Investigation into the dependence of hyperpolarisabilities of NMe_2/NO_2-substituted polyenes, polyynes and polyphenylenes on the conjugation chain length under assumption of planarity of the molecules using the SOS/CNDO/CI method (Fig. 5), for molecules with sufficiently long π-chains ($n > 7$), showed that β increases in the series polyphenylenes < polyynes < polyenes. Furthermore, in the case of polyphenylenes, the increase β stops for $n > 8$.[165–168]

Champagne, Jacqemin *et al.*[169–174] investigated a number of molecules containing polymethinimine (PMI) π-chains. Since the fragment CH=N can be simultaneously regarded as a chain unit and a D/A-pair, they analysed [169, 170] molecules H–(CH=N)$_n$–H, *i.e.*, molecules without supplementary substituents. Under assumption of the planar *trans*-structure of the chain, the values of the hyperpolarisability were estimated for n varied from 1 to 20 and the hyperpolarisability increment per CH=N unit in an infinite chain was determined

$$\Delta\beta = \beta(n) - \beta(n-1).$$

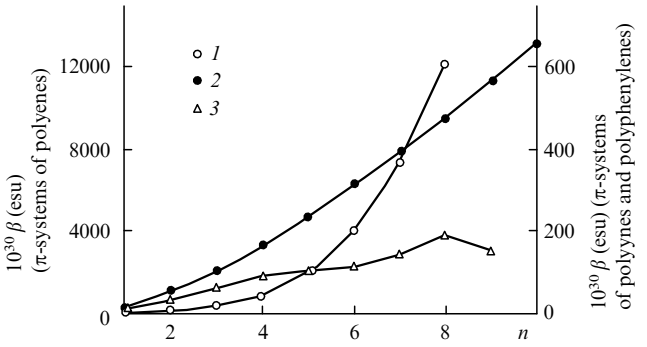


Figure 5. Hyperpolarisability as a function of the number of conjugated chain units for NMe_2/NO_2-substituted oligomers;
(*1*) polyenes, (*2*) polyynes, (*3*) polyphenylenes.

If the lengths of formally ordinary and double carbon–nitrogen bonds are kept fixed,[170] the absolute values of hyperpolarisability significantly diminish with an increase in BLA, in agreement with the general dependence β(BLA) (see Fig. 3). Moreover, the increment of $|\beta|$ increase with a chain elongation also decreases

BLA /Å	0.100	0.126	0.150	0.190	0.220
$\Delta\beta_{zzz}(\infty)$ (a.u.)	-2753 ± 129	-1461 ± 51	-869 ± 28	-434 ± 7	-293 ± 2

The authors explained this by a decrease in the degree of the electron density delocalisation. In another study of the same system,[171] the bond lengths were allowed to vary in the geometry optimisation procedure and the BLA values were adjusted by allowance for the solvent effects. As expected, BLA somewhat decreased with chain elongation: from 0.132 Å to 0.095 Å and from 0.137 Å to 0.092 Å on going from $n = 2$ to 18 for an isolated molelcule and acetonitrile solution, respectively.

The ratio β/M, where M is the molecular mass, was suggested as a convenient criterion to compare unsubstituted PMI (4.2 in units of 10^{-30} esu) with other types of compounds.[172] For instance, $\beta/M = 0.76$, 0.16 and 0.10 for D/A-polyenes,[175] *p*-NA [176] and 3-methyl-*p*-NA,[177] respectively.

PMI and polyenes with identical D/A-substituents were directly compared in a theoreticl study within the CPHF/6-31G approximation [173, 174] (Table 10, Fig. 6). The authors considered [173] the effects of different D/A-substituents and their mutual arrangement (which is especially important for PMI) at a constant length of the PMI and polyene chains ($n = 4$).

Table 10. The values of β_{zzz} for D/A-substituted polymethinimines and polyenes.

Molecule	β_{zzz} (a.u.)	Molecule	β_{zzz} (a.u.)
O_2N–(CH=N)$_4$–NH_2	7598.2	F–(CH=N)$_4$–OH	1038.0
H_2N–(CH=N)$_4$–NO_2	−3446.3	HO–(CH=N)$_4$–F	198.8
O_2N–(CH=N)$_4$–OH	5650.9	O_2N–(CH=CH)$_4$–NH_2	8330.3
HO–(CH=N)$_4$–O_2N	−2501.0	O_2N–(CH=CH)$_4$–OH	6526.3
F–(CH=N)$_4$–NH_2	1495.5	F–(CH=CH)$_4$–NH_2	1109.9
H_2N–(CH=N)$_4$–F	−456.6	F–(CH=CH)$_4$–OH	707.5

According to the data listed in Table 10, the PMI chain provides higher optical efficiencies with weakly polarising substituents (OH/F, NH_2/F). However, the situation is reversed upon the introduction of strong D/A-groups (*i.e.*, OH/NO_2 or NH_2/NO_2). The authors explained this by a combined action of three factors: the degree of the electron density delocalsation and the asymmetry in the electron density distribution relative to the unsubstituted polyene either intrinsic (due to the alternating

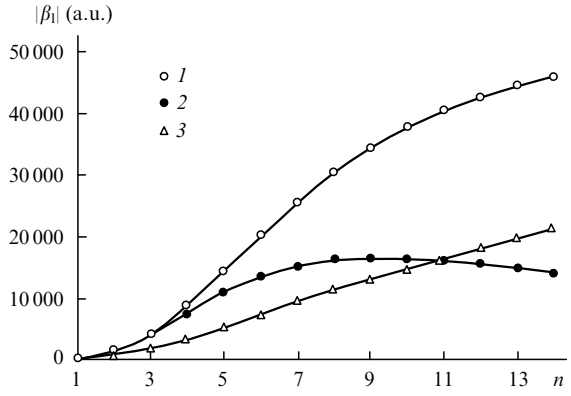
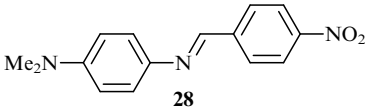


Figure 6. Component of hyperpolarisability parallel to the conjugated chain (β_l) as a function of its length for H_2N–(CH=CH)$_n$–NO_2 (*1*), O_2N–(CH=N)$_n$–NH_2 (*2*) and H_2N–(CH=N)$_n$–NO_2 (*3*).
Calculation within the CPHF/6-31G approximation.

$N^{\delta-}$=$C^{\delta+}$ fragments) or extrinsic (induced by D/A-substituents). The higher NLO efficiency of polyenes in the case of strong D/A-substituents (NH_2/NO_2) can be explained by the higher degree of the π-electron delocalisation in polyenes with respect to PMI, which dominates over the asymmetry contribution. The situation is reversed in the case of weak D/A-pairs: the asymmetry effect prevails. The best result upon PMI substitution can be achived by attaching donor groups from the side of nitrogen atoms (see Table 10), since the asymmetry effects of the D/A-groups and CH=N fragments are oppositely directed in this case. A study of changes in hyperpolarisability of NO_2/NH_2-substituted PMI and polyenes with chain elongation [174] (see Fig. 6) indicated that the attachment of donor groups from the side of nitrogen atoms enhanced the polarisability only for short and medium-length PMI chains ($n < 11$), which is in agreement with the data presented in Table 10. The opposite effect was observed for long PMI chains: the absolute value of β continued to increase for H_2N–(CH=N)$_n$–NO_2, whereas it started to decrease for O_2N–(CH=N)$_n$–NH_2.

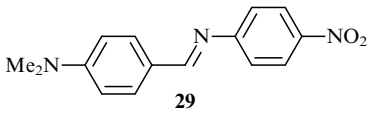
These results can be rationalised within the concept of auxiliary D/A-substituents. The terminal nitrogen atom in a PMI chain carries a partial negative charge; the attachment of a donor group to it increases its donor ability, and thus this acts as an auxiliary donor. The partially positively charged terminal carbon atom behaves similarly with respect to acceptor groups attached. In such a situation, the asymmetry induced by the D/A-pair is opposite to the intrinsic asymmetry due to the CH=N fragments. For relatively short PMI chains ($n < 4$), the D/A-pair asymmetry prevails. Upon an increase in the chain length, the induced asymmetry becomes weaker and thus the intrinsic asymmetry due to the CH=N fragments starts to dominate, which gives rise to a decrease in the hyperpolarisability at $n > 10$; the effect of substitution vanishes for $n \to \infty$. If D/A-substituents are attached to the opposite terminal atoms, both asymmetry effects act in the same direction. However, the terminal $N^{\delta-}$ and $C^{\delta+}$ atoms of the PMI chain deactivate the acceptor and donor properties of the substituents attached, which gives rise to β lower than that of analogous D/A-polyenes. This concept is also supported by results obtained for molecules **28**–**37** (Table 11).[4, 178–182]



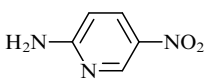
28

Table 11. Calculated values of static hyperpolarisabilities (10^{-30} esu) for molecules **28**–**37**.

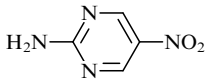
Molecule	β	Calculation method	Ref.
28	28.0	FF/PM3	178–180
29	36.8	FF/PM3	178–180
30	33.9	SOS/PPP/CI	4
31	25.6	SOS/PPP/CI	4
32	46.7	SOS/PPP/CI	4
33	47.6	SOS/PPP/CI	4
34	4.87	CPHF/6-31G	181, 182
35	3.94	CPHF/6-31G	181, 182
36	6.35	CPHF/6-31G	181, 182
37	4.26	CPHF/6-31G	181, 182



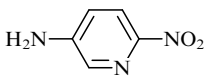
29



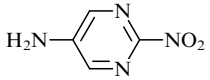
30



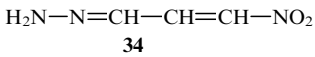
31



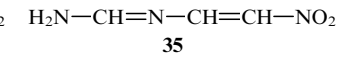
32



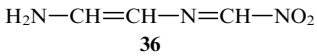
33



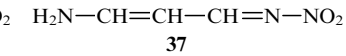
34



35



36



37

The bridging nitrogen atom in molecule **28** acts as a weak acceptor, and the central CH group acts as a donor. This deactivates the terminal D/A-substituents. In contrast, the central fragments in molecule **29** enhance the strength of D/A-substituents, which gives rise to an increase in the hyperpolarisability.[178–180] The heterocyclic nitrogen atoms in molecules **30**–**33** withdraw the electron density thus increasing the partial positive charge on the adjacent carbon atoms.[4] This attenuates the donor properties of molecules **30** and **31** but enhances the acceptor properties of molecules **32** and **33**. An analogous situation is observed in molecules **34**–**37**.[181, 182]

Jacqemin *et al.*[183–186] published the first estimates (calculated with the CPHF/6-31G method) of the hyperpolarisabilities of molecules $(X-Y)_n$, where X, Y = B, P, Si, N, C characterised by the *trans*-cisoid structure [except for the $(B{=}N)_n$ molecule, which is linear]. In particular, they estimated the values of β/M (Table 12). It is apparent that the PMI systems considered above manifest significantly higher NLO activities.

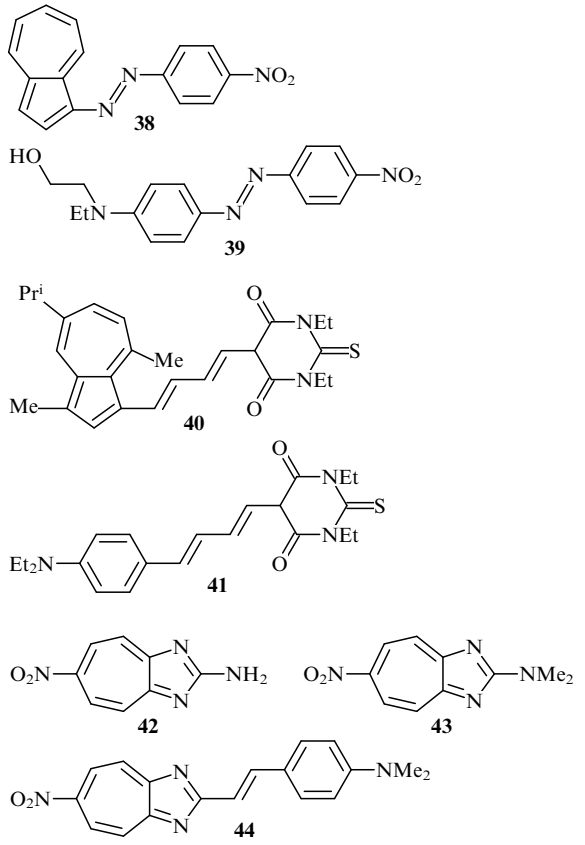
Table 12. Calculated values of β/M (10^{-30} esu) for $(X-Y)_n$ oligomers.

Molecule	β/M	Ref.	Molecule	β/M	Ref.
$(B=N)_n$	~0	183	$(SiH=PH_2)_n$	0.33	184
$(BH=NH)_n$	0.03	186	$(BH=PH)_n$	0.95	185
$(BH_2-NH_2)_n$	0.01	186	$(BH_2=PH_2)_n$	0.02	185
$(N=PH_2)_n$	0.03	184	$(CH=NH)_n$	4.2	172
$(CH=PH_2)_n$	0.06	184			

2. Molecules with heteroatoms

Fragments containing heteroatoms, in particular, heterocyclic π-systems, are widely used in the design of NLO-active compounds as both π-bridges and the D/A groups.[187–190]

The NLO properties of azulene-containing molecules, their heteroanalogues and related reference compounds (**38**–**44**) have been studied.[191–193]



The azulene bicyclic system can be used as either a donor or an aceptor or as a unit of a π-bridge. The donor properties of azulene were estimated based on the EFISH measurements in dioxane (λ = 1907 nm)[191] and SOS-based calculations (INDO, λ = 1907 nm).[192] Its behavior as a π-bridge was considered theoretically using the FF method (AM1 in the static limit).[193] The donor properties of azulene are comparable to those of RR′N groups (R, R′ = Alk or Ar, see molecules **38**–**41**), which are among the strongest π-donors. Diazaazulene derivatives **42**–**44** manifest higher hyperpolarisabilities than DANS (Table 13), which indicates the higher NLO activity of azulene-containing molecules. Probably, this is due to the lower energy barrier to the electron delocalisation and enhanced donor and acceptor ability of the substituents attached to the five- and seven-membered rings of azulene, respectively.

Table 13. Calculated hyperpolarisabilities of azulene-containing molecules, their hetero analogues and reference compounds.

Molecule	$10^{30}\beta_0$ (esu)	$10^{48}\mu\beta_0$ (esu)
38	50	–
39	48	–
40	–	1323
41	–	1400
42	20	–
43	36	–
44	106	–
2	43	–

The spectral properties of unsubstituted five-membered heterocycles C_4H_4X (X = O, S, Se and Te) were studied theoretically using *ab initio* calculations at different levels.[194–196] The hyperpolarisability increases in the following series: thiophene < furan < selenophene < tellurophene. It is of interest that the results of theoretical studies of the D/A molecules with π-systems built up of such heterocycles (see above) manifest the reversed trend, *viz*., thiophene > furan. As it will be discussed in more detail below, both thiopene and furan can act as a π-bridge of choice depending on the specific structure of the D–π–A molecule. It is of note that the sequence of ascending β for unsubstituted heterocycles partly correlates with the aromaticity series: thiophene > selenophene > tellurophene > furan.[197] The correlation is violated by the position of furan. However, the aromaticity of furan is still a subject of debate: it is estimated to be in the range from 20% to 60% of the benzene value, depending on the theoretical method utilised.[198]

For unsubstituted fused heterocycles, β increases[199] and the aromaticity decreases[200] on going from benzothiazole to benzoxazole.

Most probably, the following trend is observed: the less aromatic unsubstituted heterocycle is characterised by larger β due to the lower energy barrier to the electron density redistribution.

Jen and co-workers[201–205] analysed the effects of thiophene for benzene substitution in π-conjugated chain on the spectral properties.

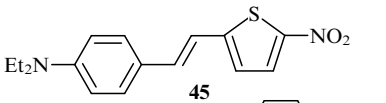
According to the results obtained (Table 14, molecules **2**, **45**–**49**), the substitution for the phenylene fragment from the donor side is more efficient, since the electron-rich thiophene fragment acts as an auxiliary donor in this case. If the bridge is built up of two thiophene fragments, the value of β increases further, since only a readily polarisable conjugated system appears between the D/A groups. The introduction of strong π-acceptors, such as a tricyanoethylene substituent, gives rise to an even further increase in the hyperpolarisability. On the other hand, it has to be

Table 14. Spectral properties [$10^{48}\mu\beta_0$ (esu); λ_{max}/nm] of heterocyclic molecules.

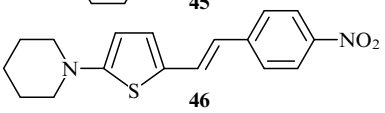
Molecule	$\mu\beta$	λ_{max} (see [a])	Ref.	Conditions
2	580	424	201, 205	1,4-dioxane, EFISH measurements at λ = 1907 nm
45	600	478	201, 205	the same
46	660	460	201, 205	"
47	1040	516	201, 205	"
48	6200	640	201, 205	"
49	6900	718	201, 205	"
50	51	480	206	CH_2Cl_2, EFISH measurements at λ = 1579 nm extrapolated to $\lambda = \infty$ using the two-level model
51	104	579	206	the same
52	1.8	282	207	1,4-dioxane, EFISH measurements at λ = 1064 nm extrapolated to $\lambda = \infty$ using the two-level model
53	7.1	312	207	the same
54	8.0	338	207	"
55	8.2	310	207	"
56	119		208, 209	1,4-dioxane, EFISH measurements at λ = 1064 nm
57	502		208, 209	the same
58	769		208, 209	"
59	314		208, 209	"
60	395		208, 209	"
61	1364		208, 209	"

[a] Hereinafter, λ_{max} is the absorption maximum in the UV spectrum.

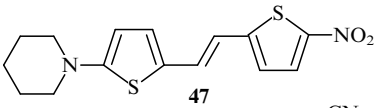
noted that the increase in β is accompanied by a narrowing of the region of the optical transparency of these compounds.



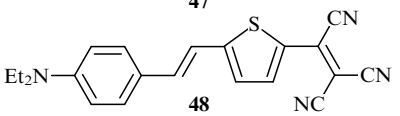
45



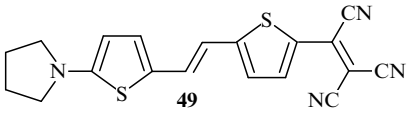
46



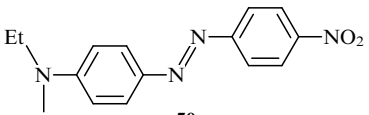
47



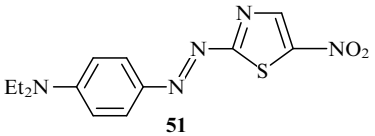
48



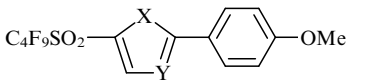
49



50

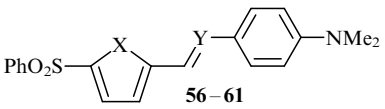


51



52 – 55

Y = N: X = NMe (**52**), O (**53**), S (**54**);
X = CH=CH, Y = CH (**55**).



56 – 61

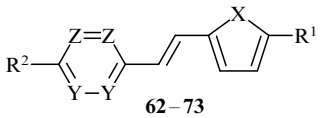
Y = N: X = NMe (**56**), O (**57**), S (**58**);
Y = CH: X = NMe (**59**), O (**60**), S (**61**).

Dirk *et al.*[206] proposed to use thiazole as a structural unit of π-bridges. The substitution of this five-membered heterocycle for the benzene ring doubles β (see Table 14, molecules **50** and **51**). The authors explained this increase by the lower energy barrier to the electron delocalisation in the case of thiazole. Meanwhile, molecule **51** is less optically transparent.

The hyperpolarisabilities of biaryls **52 – 54** increase[207] in the series **52** (imidazole) < **53** (oxazole) < **54** (thiazole), although they remain lower than β of their biphenyl analogue **55**. Similar trends in β on going from π-systems containing nitrogen heterocycles to oxygen and further to sulfur heterocycles were obtained for molecules **56 – 58** and **59 – 61**.[208, 209]

It is evident that the aforementioned trends can be explained only by a combined account of the effects of the energy barrier to the electron delocalisation and the π-electron density excessiveness or deficiency (relative to that in benzene) in these heterocyclic systems.

A detailed theoretical background for the results considered above was given[210–212] taking heteroanalogues of D/A-substituted stilbenes as model molecules. Breitung *et al.*[212] also analysed five-membered heterocyclic compounds containing two heteroatoms, for which the non-equivalence of positions 2 and 5 in the heterocycles has to be addressed. Albert *et al.*[210] considered a series of molecules **62 – 73**. Their spectral properties were assessed using the SOS/INDO method ($\hbar\omega$ = 0.1 eV) for molecular geometries optimised at the AM1 level (Table 15).



62 – 73

$R^1 = NH_2$, $R^2 = NO_2$, Y = Z = CH: X = S (**62**), O (**63**), NH (**64**);
$R^1 = NH_2$, $R^2 = NO_2$, Y = N, Z = CH: X = S (**65**), O (**66**), NH (**67**);
$R^1 = NO_2$, $R^2 = NH_2$, Y = Z = CH: X = S (**68**), O (**69**), NH (**70**);
$R^1 = NO_2$, $R^2 = NH_2$, Y = N, Z = CH: X = S (**71**), O (**72**), NH (**73**).

Table 15. Spectral characteristics of heterocyclic analogues of NH_2/NO_2-substituted stilbenes.[210]

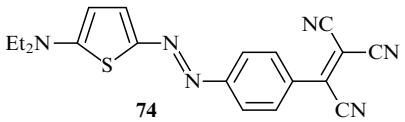
Molecule	$10^{30}\beta_{vect}$ (esu)	λ_{max} /nm	Molecule	$10^{30}\beta_{vect}$ (esu)	λ_{max} /nm
62	43.9	402	**68**	45.0	424
63	46.6	410	**69**	37.5	424
64	55.7	418	**70**	33.5	417
65	53.8	423	**71**	36.1	419
66	53.2	425	**72**	27.7	414
67	62.5	430	**73**	24.4	409

Note. For molecule **12**, λ_{max} = 363 nm, $\beta_{vec} = 31.7 \times 10^{-30}$ esu.

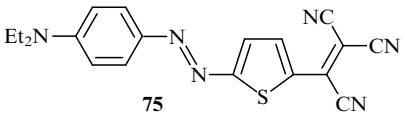
According to the data summarised in the left part of Table 15, the heterocyclic substitution for one of the benzene rings at the donor side increases the hyperpolarisability, which is in accordance with the lower aromaticity of the heterocycles. However, the energy of aromatic stabilisation decreases in the series benzene > thiophene > pyrrole > furan,[213, 214] whereas the hyperpolarisability increases in the series **12** (benzene) < **62** (thiophene) < **63** (furan) < **64** (pyrrole). The latter series conforms to the sequence of ascending π-electron excessiveness.[215]

Therefore, heterocycles act as auxiliary donors; apparently, this factor prevails over the aromatic stabilisation effects. Moreover, both factors act in the same direction. Upon replacement of carbon atoms in the benzene ring from the acceptor side by the nitrogen atoms (molecules **65 – 67**), β further increases. The resultant π-electron-deficient ring enhances the effect of the NO_2 group and, moreover, provides a lower delocalisation barrier. If nitrogen atoms are introduced at the position Z (no such compounds are mentioned in Table 15), the hyperpolarisability increases even further. Meanwhile, if the five-membered heterocycle is located at the acceptor side (right part of Table 15), the order of ascending β is reversed, i.e., **68** > **69** > **70**, which corresponds to the decrease in the π-electron excessiveness and does not correlate with the changes in the energy barrier to the aromatic delocalisation. Still, all three molecules **68 – 70** manifest higher NLO activity than molecule **12**, which is due to the lower aromatic delocalisation barrier therein with respect to benzene. In this case, the effects of the π-electron density excessiveness are of low importance. It seems strange that the hyperpolarisability of molecule **68** is larger than that of **62**. This violates the concept of auxiliary D/A-substituents and is not supported by other theoretical[211] and experimental[201–205] estimates.

Moylan *et al.*[216] analysed β as a function of the thiophene location in the π-chain using compounds **74** ($10^{30}\beta = 686 \pm 21$ esu; λ_{max} = 708 nm) and **75** ($10^{30}\beta = 867 \pm 35$ esu; λ_{max} = 719 nm) as examples.



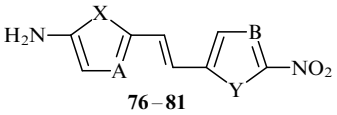
74



75

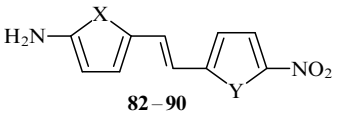
According to the EFISH measurements (at $\lambda = 1907$ nm in chloroform), higher NLO activity is observed for molecule **75**, which contains the thiophene fragment substituted with an acceptor group, despite molecule **74** is more polar, *i.e.*, it possesses a higher dipole moment. This discrepancy can be explained [216] based on the β(BLA) dependence (see Fig. 3) assuming that both molecules are located in the region *B*. This implies that an increase in the polarity of the π-system, for instance, induced by a stronger D/A group or by a change in the thiophene position, gives rise to a decrease in β. Thus the authors concluded that the concept of auxiliary D/A groups is not versatile. Nevertheless, it remains unclear, why the authors [216] did not study molecules with weaker substituents. Following the authors' logic, such molecules should fall into the region *A* (see Fig. 3), such that the thiophene location from the side of the donor should appear preferable. This is supported by the experimental data [201–205] for weaker D/A groups. In our opinion, the results by Moylan *et al.*,[216] once again corroborate the above statement that the optimum combination of D/A groups and a π-system in a D–π–A molecule is required for the efficient manifestation of the NLO properties. According to the dependences shown in Fig. 3, the majority of NLO active molecules studied fall into the region *A* where all the aforementioned concepts are valid. Meanwhile, for molecules in the region *B*, all these regularities (not only the concept of auxiliary D/A groups) are violated thus giving rise to a decrease in β.

The hyperpolarisabilities of a series of analogues of NH_2/NO_2-substituted stilbene derivatives [211] are listed in Table 16. The calculations were accomplished using different methods, but all qualitative trends were fully consistent.



76–81

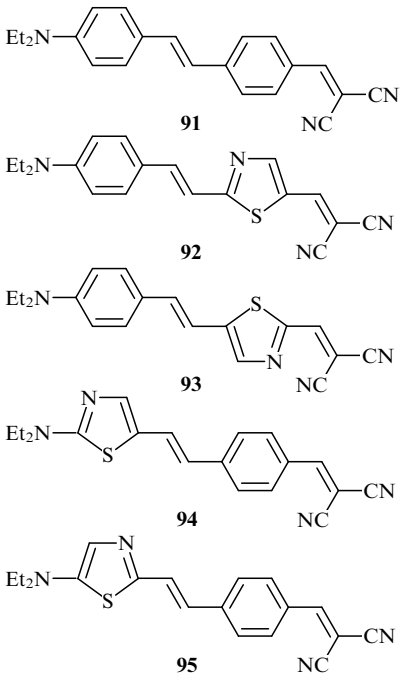
X = NH, A = CH, B = N: Y = S (**76**), O (**77**), NH (**78**);
Y = NH, A = N, B = CH: X = S (**79**), O (**80**), NH (**81**).



82–90

X = S: Y = S (**82**), O (**83**), NH (**84**); X = O: Y = S (**85**), O (**86**), NH (**87**); X = NH: Y = S (**88**), O (**89**), NH (**90**).

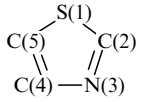
These results support the above-mentiobed regularities regarding the replacement of the benzene ring by heterocyclic fragments. The hyperpolarisability increases in the following series **82** < **85** < **88**, **83** < **86** < **89**, **84** < **87** < **90** and decreases in the series **82** > **83** > **84**, **85** > **86** > **87**, **88** > **89** > **90**. In the case of five-membered rings with two heteroatoms, β manifests the following trends: **76** > **77** > **78**, **79** < **80** < **81**. It is of interest that the hyperpolarisability increases in the series **79** < **80** < **70** < **84** < **81** < **87** < **90**. The electron density deficiency decreases in the series thiazole > oxazole > imidazole.[215] Some authors [217] consider imidazole already as a weakly electron-rich fragment. Apparently, this is supported by the presented set of molecules where the imidazole ring adjacent to a donor group (**81**) results in higher NLO activity than benzene (**70**) and thiophene (**84**) rings. It is also important to stress that the charges on the carbon atoms in positions 2 and 5 of azoles are different. In molecule **81**, the donor is attached to the carbon atom in position 5, which has a lower positive charge than that in position 2, which is more favourable. Unfortunately, no examples with the reversed situation were considered.[211] Such a study has been carried out by McMahon and co-workers,[212] who considered D/A-substituted stilbene analogues with one Ph ring replaced by thiazole using the SOS method ($\lambda = 1907$ nm).



91 **92** **93** **94** **95**

Molecule	**91**	**92**	**93**	**94**	**95**
$10^{30}\beta$ (esu)	36	54	118	42	57

Therefore, the difference in the π-density at the carbon atoms in positions 2 and 5 differently affects the hyperpolarisabilities of molecules.



$q_{C(2)} = +0.135$
$q_{C(5)} = +0.077$

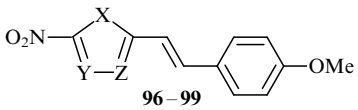
The maximum value of β is achieved upon the introduction of a π-electron deficient thiazole ring from the side of an acceptor in a way that the latter is bound to the more positive carbon atom at position 2. This was also rationalised by the contribution made by the heterocycle into the total dipole moment of the molecule directed from the acceptor to the donor. The dipole moment vector in the heterocycle is directed approximately from the nitrogen atom to the sulfur atom and thus, in the case of molecule **93**, it makes a certain positive contribution to the total dipole moment. A similar situation is observed in molecule **95**, but the heterocycle, being π-electron deficient, behaves as a 'counteracting' donor.

Table 16. Calculated values of β_0 (CPHF/4-31G) for NH_2/NO_2-substituted stilbenes and their heterocyclic analogues under the assumption of their planarity.[211]

Molecule	$10^{30}\beta_0$ (esu)	Molecule	$10^{30}\beta_0$ (esu)
9	26.0	**82**	32.9
64	45.2	**83**	29.0
70	21.6	**84**	23.0
76	50.8	**85**	36.9
77	45.3	**86**	32.1
78	37.3	**87**	27.5
79	18.0	**88**	47.1
80	20.2	**89**	40.8
81	26.3	**90**	35.0

It is interesting to note that the replacement of one of the benzene rings by the thiazole fragment both from the donor and acceptor sides gives rise to an increase in the hyperpolarisability of the D/A-substituted stilbene analogue, *i.e.*, the aromaticity effects prevail. For molecules **76** and **79** (see Table 16), where the thiazole fragment substitutes one of the pyrrole rings in molecule **90**, the hyperpolarisability decreases in a different series, *viz.*, **76** > **90** > **79**, which means that the π-electron deficiency of the thiazole ring becomes the dominant factor. Two reasons can be suggested to explain this apparent discrepancy: first, molecules **76** and **79** contain pyrrole as the second aromatic ring involved into the π-system (rather than benzene in molecules **92**–**95**), and second, different D/A pairs were used. This changes the balance between the aromaticity and the π-electron deficiency effects.

Results similar to those discussed above [212] were obtained by Jug *et al.*[218] for imidazole and oxazole analogues of D/A-substituted stilbenes **96**–**99** (CPHF-based calculations within the VWN/TZVP-FIP approximation).



96–**99**

X = NH, Y = CH, Z = N (**96**); X = NH, Y = N, Z = CH (**97**); X = O, Y = CH, Z = N (**98**); X = O, Y = N, Z = CH (**99**).

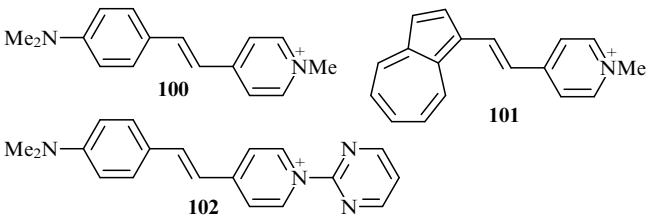
The following values of β_0 were obtained:

Molecule	**96**	**97**	**98**	**99**
$10^{30}\beta_0$ (esu)	77	78	84	99

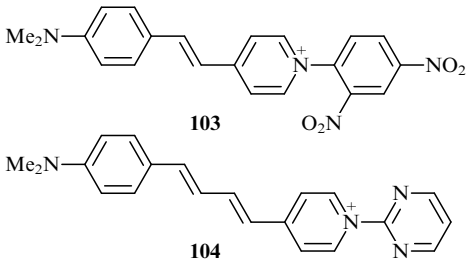
The examples discussed above, despite the existence of specific discrepancies, demonstrate the general approach to the design of efficient NLO molecules based on the concept of auxiliary electron donors (acceptors) and fragments with low energy barriers to the electron delocalisation. Notwithstanding, the prediction of a net balance of particular factors on the hyperpolarisability remains a challenging task. In addition, the effects of aromaticity delocalisation barrier and electron deficiency/excessiveness can vary, depending on the computational method or experimental conditions. However, regardless of the method applied, the results can always be rationalised based on the interplay of three factors, *viz.*, the energy barrier to the delocalisation (aromaticity), the π-electron density deficiency/excessiveness and the charge distribution within the heterocycle (*i.e.*, the orientation of the dipole moment of the ring).

It is of note that the hyperpolarisability can be used as a criterion of the combined influence of the π-electron density deficiency/excessiveness and aromatic stabilisation.

Over the recent years, considerable efforts have been put forth to study the NLO properties of organic cations due to the fact that the probability of the crystallisation in non-centrosymmetric space groups for salts is higher than for neutral molecules. This implies that the molecular design step should include an analysis of ions. The hyperpolarisability of a series of cations **100**–**104** was measured by means of HRS in MeCN (with PF_6^- as a counterion).[219–222]



100 **101** **102**



103 **104**

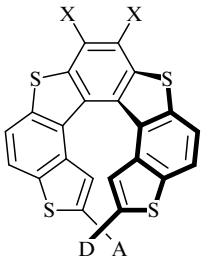
The cations reveal the same trends in the spectral properties as analogous D–π–A molecules.

Cation	**100**	**101**	**102**	**103**	**104**
λ_{max} /nm	470	477	553	537	579
$10^{30}\beta_0$ (esu)	110	108	130	130	227

The aryl substitution for an alkyl group at the N^+ atom and the elongation of the conjugation chain gives rise to an increase in β and narrowing of the optical transparency range. The cations manifest rather high hyperpolarisabilities. However, an important question arises: what a system is actually probed in these cases. The acceptor ability of the pyridinium cation should depend on the strength of its interaction with a counteranion,[223] which in turn depends on the experimental conditions, such as the nature of the solvent and of substituents at the N^+ atom and solution concentration. The exact structure of a cation–anion complex can be unambiguously determined in the crystalline state (which has indeed been done for a number of samples), whereas it is impossible for solutions. Thus it remains unclear, whether the regualities revealed reflect changes in the structure of the cation itself or they are due to the counterion effects. Yet another important problem has also to be addressed: how one can utilise the results of measurements in solution to predict the NLO susceptibility of a crystal, which can feature a totally different mutual orientation of the cation and anion? However, taking into account that the basic trends obtained are very similar to those for neutral D–π–A molecules (β increases with an increase in the acceptor strength and the length of the conjugation chain), it might be assumed that the counterion-induced effects are insignificant and the experimental results can well be interpreted in the same way as for the neutral molecules. Quantum-chemical calculations could help to clarify this problem, but no theoretical studies of this kind were carried out.[219–222]

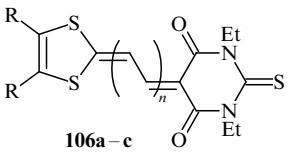
According to the literature data, vinylene (sometimes, acetylene) and thiophene (or other heterocyclic) fragments are combined in the vast majority of molecules considered as promising NLO materials. In addition, phenylene fragments are also often used as structural blocks of π-bridges. Examples of diverse NLO active molecules are discussed below and their spectral properties are summarised in Table 17.

The molecules considered incorporate heterocyclic fragments (**105**–**108**), phosphorus-containing groups (**109**, **110**), branched π-chains (**111**, **112**) and azo-groups (**109**, **113**). Unfortunately, the results obtained for them cannot be directly compared; however, the general trend of an increase in β with an increase in the conjugation chain length, strength of D/A substituents, λ_{max} and a decrease in the aromaticity degree are evident. Table 17 also indicates that the molecules transparent in the visible region (λ_{max} < 400 nm) typically manifest rather low values of β (*e.g.*, **106a**, **108a**,**b**). Criteria for the selection of specific combinations of fragments should include, in addition to achieving the maximum possible hyperpolarisabilities, high optical transparency, thermal stability and synthetic accessibility. An elongation of a π-bridge typically diminishes the thermal stability and narrows the optical transparency range. The introduction of strong D/A substituents (NR_2, NO_2, CN) induces a batochromic shift of the absorption band. In overall, the design of D–π–A molecules by combining different D/A groups and building blocks of π-bridges is aimed at



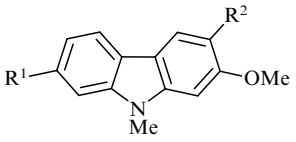
A = NO_2, X = H: D = NH_2 (**a**), OH (**b**), Cl (**c**); A = H, D = H: X = NO_2 (**d**), NH_2 (**e**); A = NO_2, X = NH_2: D = NO_2 (**f**); A = NH_2, X = NO_2: D = NH_2 (**g**).

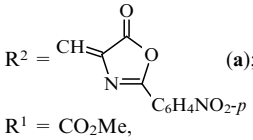
105a–g



n = 0, R = H (**a**); n = 1, R = Me (**b**); n = 2, R = Me (**c**).

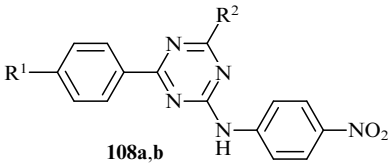
106a–c



R^1 = $OC_{11}H_{23}$-n, R^2 =  (**a**);

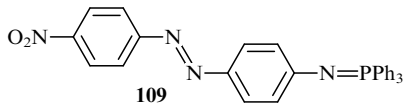
R^1 = CO_2Me, R^2 = $C(CN)=C(CN)_2$ (**b**).

107a,b

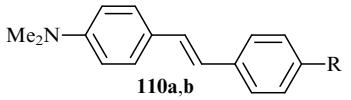


R^1 = NMe_2, R^2 = CN (**a**); R^1 = Me, R^2 = Cl (**b**).

108a,b

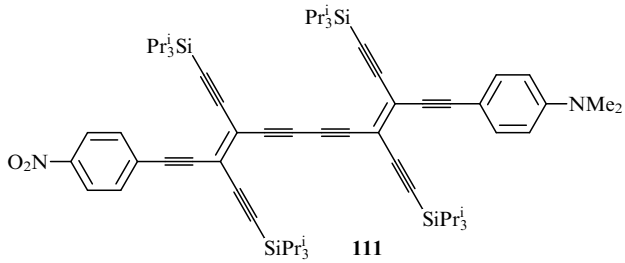


109

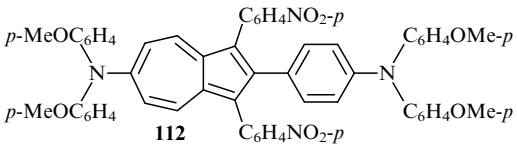


R = P(O)(OPh)$_2$ (**a**), P(O)(OH)$_2$ (**b**).

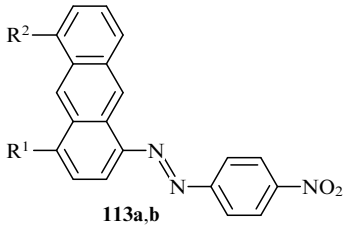
110a,b



111



112



R^1 = MeNH, R^2 = H (**a**); R^1 = H, R^2 = MeNH (**b**).

113a,b

Table 17. Optical characteristics of NLO-active molecules belonging to various classes of organic compounds.

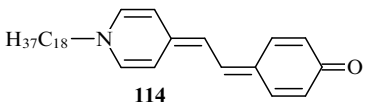
Molecule	β (see [a])	$\mu\beta$ (see [b])	λ_{max} /nm	Method of calculation or measurement	Ref.
105a	27.6	–	–	CPDFT/B3LYP/6-311G,	224
105b	22.9	–	–	calculation in the static limit	224
105c	22.1	–	–		224
105d	63.7	–	–	TDHF/AM1	225, 226
105e	35.8	–	–	TDHF/AM1	225, 226
105f	127.5	–	–	TDHF/AM1	225, 226
105g	107.3	–	–		225, 226
106a	–	–12	403	EFISH	227, 228
106b	–	100	558	(CH_2Cl_2; λ = 1907 nm)	227, 228
106c	–	1100	642		227, 228
107a	–	550	502	EFISH	229, 230
107b	–	280	475	($CHCl_3$; λ = 1907 nm)	229, 230
108a	45.8	–	319.6	β: calculation FF/AM1 in	231, 232
108b	19.3	–	306.2	the static limit;	231, 232
				λ_{max}: calculation ZINDO/S	
109	–	1100	490	EFISH (DMF; λ = 1579 nm)	233
110a	94	–	–	CPDFT/VWN/TZVP-FIP,	234
110b	111	–	–	calculation in the static limit	234
111	400	–	481	EFISH ($CHCl_3$;	235
	–	–	–	λ = 1907 nm)	
112	32	–	458	HRS ($CHCl_3$; λ = 1500 nm)	236
113a	81.6	–	538	calculation by the	237
113b	56.5	–	553	CNDOVSB code	237
				(λ = 1907 nm)	

[a] In 10^{-30} esu; [b] in 10^{-48} esu.

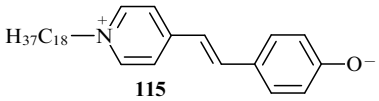
achieving a desired level of the thermal stability and optical transparency while keeping sufficiently high values of β.

3. Zwitter-ionic molecules

One of the approaches to the design of NLO active molecules implies the use of aromatic D/A groups either directly attached to each other or linked through a short π-bridge.[238] Among this class of compounds, merocyanine dyes are studied most intensely. The ground state of merocyanines can be represented as a superposition of the non-polar quinonoid form (*e.g.*, **114**) and the zwitter-ionic form (*e.g.*, **115**) that makes a significant contribution.



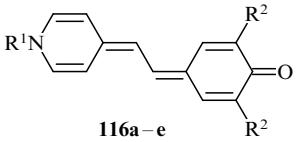
114



115

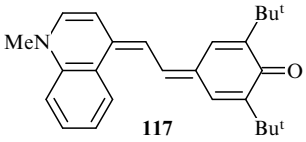
Merocyanines exhibit negative solvatochromism and are exceptionally sensitive to the nature of the solvent.

The first study of the NLO properties of merocyanine was accomplished by Levine *et al.*[239] The absorption maximum was observed at λ_{max} of 605 nm and 440 nm in pyridine and water, respectively. According to the EFISH measurements in pyridine and methanol (which is close to water in terms of polarity), β is negative in both solvents but its absolute value is larger in methanol (-51×10^{-30} esu *vs.* -34×10^{-30} esu). Similar results were obtained for dyes **116**–**118**; their experimentally measured spectral characteristics are compiled in Tables 18 and 19.

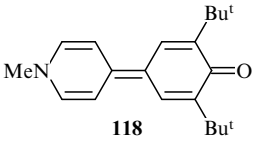


116a – e

R^2 = H: R^1 $(CH_2)_2OH$ (**a**), Me (**b**), iso-$C_{10}H_{21}$ (**c**); R^2 = Bu^t: R^1 = Me (**d**), iso-$C_{10}H_{21}$ (**e**).

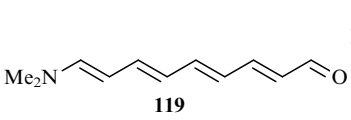


117

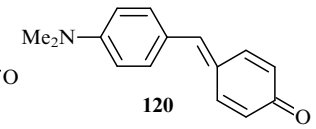


118

A comprehensive theoretical study of merocyanines was performed by Albert *et al.*[247] (SOS/INDO, $\hbar\omega = 0.65$ eV). In particular, they reported functions β *vs.* ground state wavefunction for molecules **116b**, **119**, **120** (Fig. 7).



119



120

Molecule **119** contains no aromatic groups; both the neutral and zwitter-ionic forms of **120** are stabilised by one aromatic ring, whereas in the zwitter-ionic form of **116b**, both six-membered rings are aromatic. The curves obtained have generally the same shape as function β(BLA) depicted in Fig. 3. In the case of molecule **116b**, this dependence differs drastically from those for **120** and **119** because of the aromatic stabilisation of the zwitter-ionic form. This form makes a dominant contribution to the ground state of the molecule already in weakly polar solvents, and an increase in the solvent polarity gives rise to an increase in $|\beta|$.

Table 18. The values of λ_{max} (nm) for merocyanines **116**.[240–244]

Solvent	**116a**	**116b**	**116c**	**116d**	**116e**
Dioxane	–	614	619	626	626
$CHCl_3$	–	620	620	633	634
Pyridine	–	605	600	630	632
Acetone	586	585	599	619	620
DMF	584	582	–	–	–
DMSO	–	572	579	617	618
MeCN	571	571	–	–	–
Ethanol	–	514	521	616	617
Formamide	–	494	502	578	581
Methanol	488	483	491	582	601
Water	448	442	447	527	526

Table 19. Experimental values of $\mu\beta$ (10^{-48} esu) for merocyanines **116d**, **117** and **118** from EFISH measurements at 1907 nm.[245, 246]

Solvent	**116d**	**117**	**118**
Dioxane	–	−45	–
THF	−300	–	–
$CHCl_3$	−325	−275	−325 (524)
CH_2Cl_2	−425	–	–
Acetone	−600	−460	−600 (512)
DMF	−525	–	–
DMSO	−1000	−970	–
MeCN	−700	–	−700 (503)
Ethanol	−110	–	–
Methanol	−900	−1000	−900 (482)

Note. The values of λ_{max} (nm) are given in parentheses.

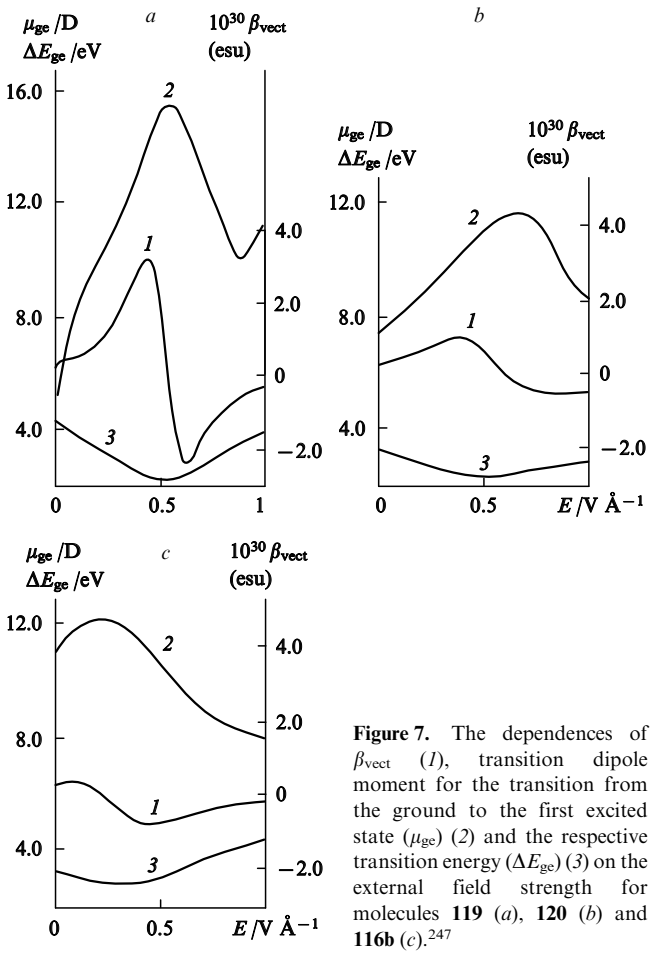
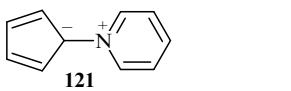
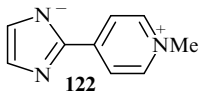


Figure 7. The dependences of β_{vect} (*1*), transition dipole moment for the transition from the ground to the first excited state (μ_{ge}) (*2*) and the respective transition energy (ΔE_{ge}) (*3*) on the external field strength for molecules **119** (*a*), **120** (*b*) and **116b** (*c*).[247]

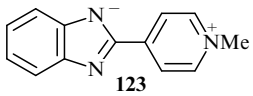
The spectral properties of heterocyclic zwitter-ionic molecules **121 – 129** were the subject of both theoretical (CNDOVSB, $\hbar\omega = 0.95$ and 0 eV; SOS/INDO/S, $\hbar\omega = 0.65$ and 0 eV; CPHF/6-31G) and experimental investigations.[248–250]



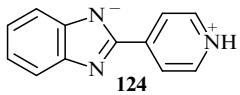
121



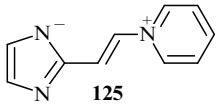
122



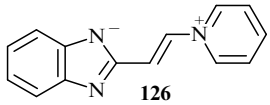
123



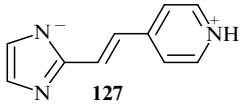
124



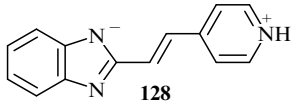
125



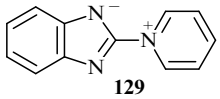
126



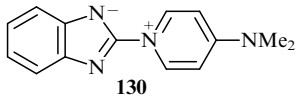
127



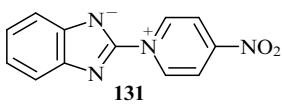
128



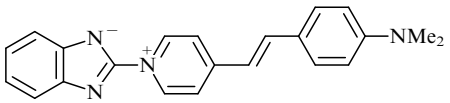
129



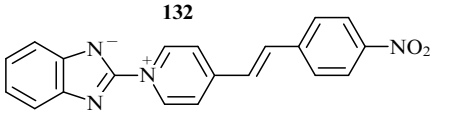
130



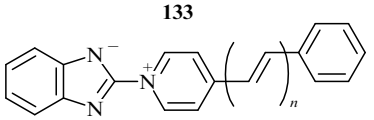
131



132



133



134 – 136

n = 1 (**134**), 2 (**135**), 3 (**136**).

There is qualitative agreement between the results obtained by different methods. According to calculations at the CPHF/6-31G level presented in Table 20, the NLO activities of molecules **121 – 129** are 3 – 5 times higher than those of the well-known NLO molecules **1** and **2**. This difference was explained by a larger change in the dipole moment ($\Delta\mu$) upon the transition into the excited state. And this effect is achieved for relatively small molecules, whereas an increase in $\Delta\mu$ for normal D – π – A systems can only be achieved by an elongation of a π-conjugated chain.

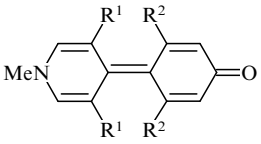
Table 20. Spectral properties and dipole moments of heterocyclic zwitterionic molecules in the ground (μ_g) and excited (μ_e) states.

Molecule	$10^{30}\beta_0$ (esu)	Molecule	$10^{30}\beta_0$ (esu)	λ_{max} /nm	μ_g	μ_e
121	−55.8	**129**	−33	281	10.3	−5.9
122	−32.6	**130**	−16	252	14.8	0.1
123	−93.9	**131**	−132	358	3.5	−15.9
124	−67.5	**132**	−25	307	17.5	9.1
125	−161.5	**133**	−100	316	5.9	−14.0
126	−244.7	**134**	−46	302	13.4	−2.7
127	−9.3	**135**	28	310	14.3	0.8
128	−78.5	**136**	11	316	14.9	5.0

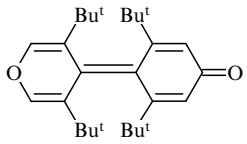
Abe *et al.*[250] carried out an experimental (measurements of HRS) and theoretical investigation into the behaviour of molecule **124** in solvents of different polarities. The experimental measurements indicated that the hyperpolarisability slightly decreases in more polar solvents. The theoretical values were calculated using the CPHF/6-31G method and the solvent effects were taken into account within the Onsager model by varying the dielectric permittivity (ε) from 1 to 90. It was found that the hyperpolarisability decreases from the maximum value of $|\beta| = 33 \times 10^{30}$ esu at $\varepsilon = 2$ to nearly zero with an increase in ε up to 90. It is of note that the opposite results were obtained for merocyanines, as discussed above. Probably, this difference is due to the fact that the isolated molecule **124** in the ground state falls into the region close to the minimum of $\beta(\varepsilon)$ (see Fig. 7), *i.e.*, the contribution of the zwitter-ionic form is significantly larger than that for merocyanines and thus $|\beta|$ decreases with an increase in the solvent polarity.

Abe *et al.*[251] analysed (within the CPHF/6-31G approximation) the spectral properties of molecules **130 – 136** taking molecule **129** as a reference. An extended conjugated chain was introduced from the side of an acceptor group rather than between the D/A substituents. In addition, some molecules with non-aromatic D/A groups were considered (see Table 20).[251] Upon introduction of additional π-substituents into the pyridinium fragment, the hyperpolarisability first increases but then starts to decrease after a certain threshold length of the conjugation chain (*cf.* molecules **129** and **134 – 136**). This phenomenon was explained by competing effects of $\Delta\mu$ and $\lambda_{max} \sim 1/E_{ge}$. The value of $\Delta\mu$ remains virtually constant on going from **129** to **134**, whereas the transition energy E_{ge} decreases, which results in an increase in β. Upon further elongation of the π-chain, E_{ge} changes insignificantly, whereas $\Delta\mu$ decreases resulting in a respective decrease in β. Upon introduction of an additional donor group, β decreases (molecules **130** and **132**), since both $\Delta\mu$ and λ_{max} decrease. In contrast, the introduction of an acceptor group (molecules **131** and **133**) leads to the opposite effect due to an increase in $\Delta\mu$ and λ_{max}.

Interesting results were reported by Albert *et al.*[252, 253] for a series of merocyanine dyes and their analogues (molecules **137 – 140**).

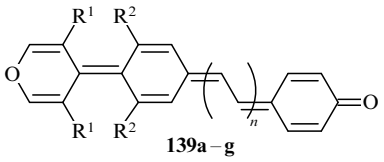


137a – e

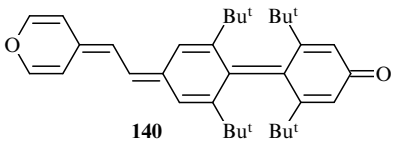


138

$R^1 = R^2 = H$ (**a**); $R^1 = H$, $R^2 = Me$ (**b**);
$R^1 = R^2 = Me$ (**c**); $R^1 = Me$, $R^2 = Bu^t$ (**d**);
$R^1 = R^2 = Bu^t$ (**e**).



139a – g



140

Using the Hückel method within the two-level model [see Eqn (17)], they demonstrated that an increase in the torsion angle θ at the central double bond from 0° to 90° gives rise to an increase in the difference between the dipole moments of the molecule in the ground and excited states as well as in the transition dipole moment and to a decrease in the transition energy ($E_{ge} = 0$ at $\theta = 90°$). This combination of factors should lead to the existence of a maximum value of β at $\theta = 70 – 89°$. Figure 8 compares the function $\beta(\theta)$ for unsubstituted molecule **137a** with freely variable θ with the hyperpolarisabilities of molecules **137a – e** in which the respective torsion angles are determined by steric repulsion of substituents. Both the dependences have similar behaviour. The maximum value of β is in the range of 70 – 80° and significantly exceeds that for the planar structure.

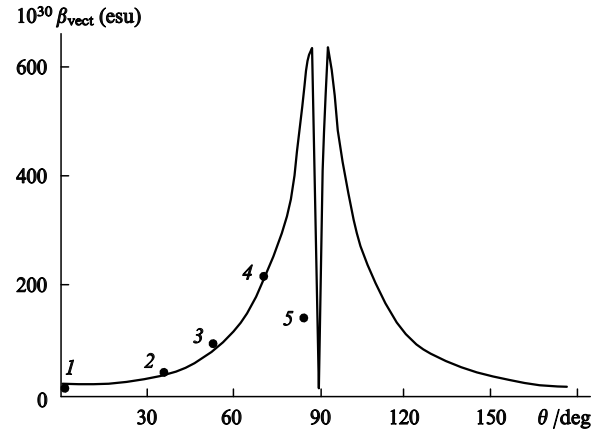
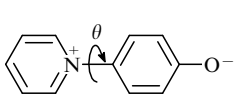
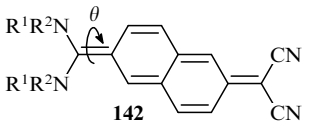


Figure 8. Hyperpolarisability of molecule **137a** (solid line) (SOS/INDO, $\hbar\omega = 0.1$ eV, AM1 optimisation) as a function of an angle between the six-membered rings (θ) and the hyperpolarisabilities of molecules **137a – e** (small circles marked as *1 – 5*, respectively).

Calculations for molecules **141** and **142** with the FF/AM1 method yielded similar results.[254,255] Here, the maximum value of β is reached at θ of 60–80°.



141



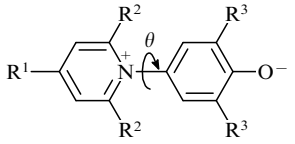
142

Albert *et al.*[253] also analysed the effects of the elongation of a π-conjugated chain (*cf.* molecules **139** and **140**) on β. The chain fragments were introduced in such a way as to retain the steric effects of substituent resulting in the non-planar structure. Selected results are shown in Table 21. Variation of the torsion angle in molecule **139** by introducting various substituents gives rise to the same type dependence as that for molecule **137** discussed above. It is worth mentioning that the molecule **139e** with the conjugation chain elongated from the side of the acceptor group is characterised by higher β as compared to molecule **140** (the elongation from the donor side), which is probably due to the more efficient stabilisation of the zwitter-ionic (benzenoid) form. A decrease in β with an elongation of the conjugation chain in the series of molecules **139e–g** was explained in a similar way. Unfortunately, trends in β upon chain elongation in **140** were not considered by the authors;[253] however, based on the results discussed above, it might be assumed that β should decrease with an increase in the length of the conjugation chain owing to smaller contribution of the zwitter-ionic form to the ground state of the molecule.

Table 21. Spectral characteristics of molecules **138**–**140**.[253]

Molecule	R^1	R^2	n	λ_{max} /nm	$10^{30}\beta$ (esu)
138	–	–	–	1206.8	352.8
139a	H	H	1	535.6	34.0
139b	Me	H	1	579.2	1.7
139c	Me	Me	1	643.4	189.8
139d	Bu^t	Me	1	805.3	391.7
139e	Bu^t	Bu^t	1	1204.5	2398.6
139f	Bu^t	Bu^t	2	1093.4	1749.0
139g	Bu^t	Bu^t	3	971.0	754.5
140	–	–	–	991.6	1119.4

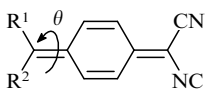
The effects of deviation from planarity for quinonoid molecules were also considered by other research groups.[256,257] Bartkowiak *et al.*[256] analysed the hyperpolarisabilities of molecules **143a**,**b** as a function of their conformations using the SOS and FF methods within the AM1 approximation and found that the maximum β is reached at angles θ between the six-membered rings of 60° and 75° for **143a** and **143b**, respectively



143a,**b**

$R^1 = R^2 = R^3 =$ Ph (**a**);
$R^1 =$ Ph, $R^2 = R^3 =$ H (**b**).

According to the results of X-ray crystallographic studies,[258–260] the angle θ lies in the range of 55–70° for molecules similar to **143** containing phenyl substituents in the *ortho*-positions of the pyridine ring (R^2 = Ph), which is close to the optimum value for the manifestation of the NLO properties. Gangopadhyay *et al.*[257] selected 7-R^1-7′-R^2-8,8′-dicyanoquinodimethane as a reference molecule.



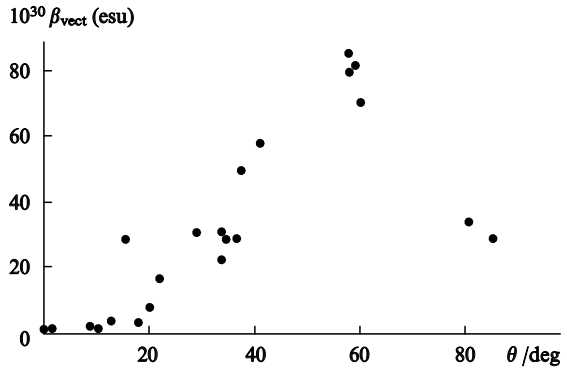


Figure 9. A graphical representation of hyperpolarisabilities (FF/AM1) of various 7-R^1-7′-R^2-8,8′-dicyanoquinodimethane derivatives.

They constructed 22 molecules with the torsion angle varying from 0° to 86° by introducing donor groups with different steric volumes (Fig. 9). Assuming that the strengths of donor groups differed insignificantly, it was concluded that the maximum of β reached at $\theta \sim 60°$ suggests the preferred non-planar conformation.

It is of note that in the majority of ordinary D–π–A molecules, the deviation from planarity results in a decrease in the hyperpolarisability due to a break of the π-conjugation chain.[261–264]

Ravi and Radhakrishnan[265] proposed to describe the balance between the quinonoid and zwitter-ionic forms of a molecule with a criterion QBC (Quinonoid-Benzenoid Character) defined as

$$QBC = 1 - 6\sum_{1}^{3}|1.400 - r_i|,$$

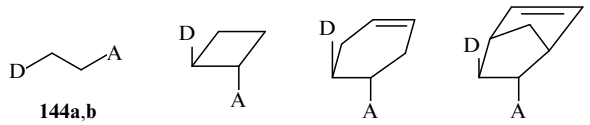
where 1.400 Å is taken as the standard value of the bond length in benzene; r_1, r_2, r_3 are the bond lengths in the six-membered quinonoid ring. The value of QBC can be varied by adjusting the electric field strength. 7,7′-Diamino-8,8′-dicyanoquinodimethane was ued as a reference molecule. The calculations were carried out using the SOS/AM1/CISD method. Table 22 summarises the values of hyperpolarisabilities, energies of transitions to the excited states and QBC. It is seen that the absorption maximum appears in the visible region at the QBC corresponding to the maximum value of β; upon further increase in QBC, β decreases only to 50% of its maximum value, whereas the absorption band shifts to the UV range. It has to be pointed out that the actual values of QBC for quinonoid molecules investigated by X-ray crystallography[266–269] lie in the range 0.75–0.82, which corresponds to the range of optical transparency.

Table 22. The values of the QBC parameter, hyperpolarisability (10^{-30} esu) and energies of transitions into the first and second excited states for 7,7′-diamino-8,8′-dicyanoquinodimethane.

QBC	β_{vect}	Transition energy /eV	QBC	β_{vect}	Transition energy /eV
0.088	−9.7	2.83 (0.006)	0.358	−75.4	2.65 (0.390)
		3.42 (1.130)			3.72 (0.471)
0.118	−18.5	2.80 (0.044)	0.436	−86.5	2.67 (0.457)
		3.39 (1.065)			3.75 (0.032)
0.190	−35.4	2.77 (0.195)	0.592	−94.0	2.87 (0.583)
		3.44 (0.841)			3.71 (0.050)
0.232	−46.2	2.71 (0.264)	0.730	−67.4	3.17 (0.571)
		3.50 (0.718)			3.75 (0.000)
0.286	−58.6	2.66 (0.326)	0.790	−47.7	3.37 (0.479)
		3.59 (0.599)			3.78 (0.000)

Note. Transition oscillator strengths are given in parentheses.

Rao and Bhanuprakash studied [270] molecules **144**–**147** with D/A groups linked by a σ-bridge, CH_2-CH_2 using the FF/AM1 method.



144a,**b** **145a**,**b** **146a**,**b** **147a**,**b**

D = *p*-$NH_2C_6H_4$, A = *p*-$NO_2C_6H_4$ (**a**);
D = *p*-$C_6H_4O^-$, A = $C_5H_5N^+$ (**b**).

The following values of hyperpolarisability were found

Molecule	**144a**	**145a**	**146a**	**147a**	**144b**	**145b**	**146b**	**147b**
$10^{30}\beta$ (esu)	6.3	6.3	6.1	4.2	−625.0	−437.3	−683.5	−301.8

Molecules **144a**–**147a** contain traditional D/A substituents, whereas molecules **144b**–**147b** are of the zwitter-ionic character. The calculated values of β indicate substantial weakening of interactions between the NH_2 and NO_2 groups in molecules **144a**–**147a** since σ-fragments break the conjugation. In contrast, in the case of zwitter-ionic molecules **144b**–**147b**, the σ-bridge stabilises the zwitter-ionic form, which gives rise to an increase in β, *i.e.*, the introduction of a σ-bridge is formally equivalent to a rotation of the phenyl rings (see Fig. 9).

Changes in the hyperpolarisability due to the replacement of a benzene ring by a heterocycle were considered.[271–273] In contrast to non-quinonoid D–π–A molecules, whose hyperpolarisabilities increase owing to the lower energy barrier to the electron delocalisation in heterocycles with respect to benzene, the opposite trend is manifested by quinonoid molecules. This can be explained in the same way: the higher the energy barrier to the electron delocalisation, the higher the stability of the zwitter-ionic form.

IV. Possible ways to improve thermal stability and optical transparency of NLO materials

The possibility of the use of organic compounds for the second harmonic generation is determined by a number of parameters and, as has been mentioned above, it often happens that an enhancement of one parameter deteriorates others. Therefore, the molecular design of NLO materials has to include simultaneous optimisation of several key molecular characteristics. For instance, most tables in the previous section listed data on the optical transparency of molecules (λ_{max}) in addition to the values of their hyperpolarisabilities. The results discussed above indicate that the function $\beta(\lambda_{max})$ increases with an increase in the strength of D/A substituents or the length of the π-system or with the introduction of less aromatic fragments in place of more aromatic ones. Several studies were related to investigations within different classes of compounds, such as imidazoles,[274] tolans,[275] pyrazoles,[276] thiazoles,[207] coumarins.[277] The dependences

$$\beta = k\log\lambda_{max} + a$$

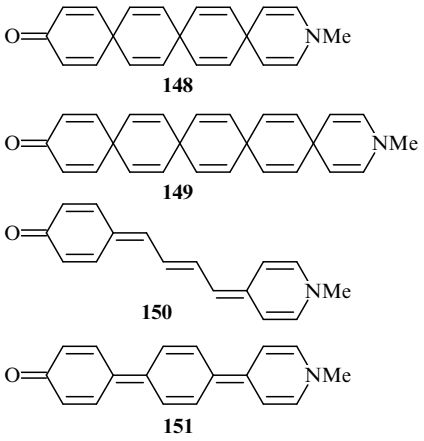
obtained are nearly linear with the coefficient k varyng from 5 to 8. A number of approaches to the search for optimal combinations of the desired properties have been proposed.

1. Linear molecules with one-dimensional hyperpolarisability

Polyene systems are among the most efficient NLO-active π-systems. Unfortunately, they are characterised by rather low thermal and chemical stabilities (moreover, these characteristics are getting worse with an increase in the length of the π-system [278]) and absorbtion maxima in the visible range. Several attempts to improve these characteristics have been undertaken. Thus it was suggested [279] to use spyro-conjugated chains (molecules **148** and **149**). Their comparison with polyene and quinonoid polyphenylene-type molecules **150** and **151** showed (Table 23) that the hyperpolarisabilities of spyro-systems are lower by an order of magnitude while the range of their optical transparency is significantly wider.

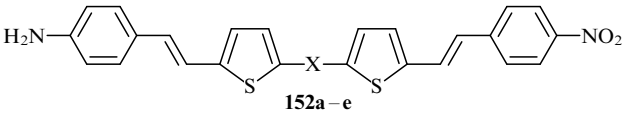
Table 23. Calculated spectral characteristics (SOS/INDO/CI) of spyro-conjugated, polyene and polyphenylene D/A molecules with geometries optimised using the AM1 method and experimental optical characteristics of molecules with σ-fragments (HRS measurements in $CHCl_3$ at λ = 1064 nm extrapolated to the zero frequency).

Molecule	$10^{30}\beta_0$ (esu)	λ_{max} /nm	Molecule	$10^{30}\beta_0$ (esu)	λ_{max} /nm
148	1.7	398	**152a**	69.2	405
149	2.9	430	**152b**	69.8	395
150	17.6	594	**152c**	86.4	407
151	16.6	668	**152d**	80.0	406
			152e	174.4	500



148 **149** **150** **151**

Jerome and co-workers [280, 281] proposed to brake the conjugation chains of conjugated molecules by introducting σ-fragments in order to broaden the range of their optical transparency (see Table 23). The values of hyperpolarisability were both calculated and measured, and qualitative agreement of theoretical and experimental results was observed.

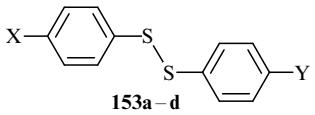


152a–**e**

X = CMe_2 (**a**), $SiMe_2$ (**b**), $(SiMe_2)_2$ (**c**), S (**d**), CH=CH (**e**).

It should be taken into account that the experimental NLO efficiency of molecule **152e** can be strongly overestimated since its absorption maximum is very close to the second harmonic. According to the results obtained, the introduction of a central σ-fragment gives rise to a significant hypsochromic shift of the absorption band but the hyperpolarisability decreases severalfold. The spectral parameters of molecules **152a**,**b** are close to each other, whereas molecule **152d** manifests a slighlty higher hyperpolarisability and its absorption band is shifted to the visible range, which suggests weak involvement of the sulfur lone-pair electrons into the delocalised π-system. It is noteworthy that the value of β for molecule **152c** is larger than those for molecules **152a**,**b**,**d**. This can be explained by the involvement of both σ- and σ–π delocalisation mechanisms in polysilanes.[282–284]

Sudharsanam *et al.*[285] utilised the S–S fragment for the break of conjugation chains in a series of molecules **153**. The hyperpolarisabilities of these molecules were measured by HRS method at λ = 1064 nm in $CHCl_3$ using a value of 17×10^{-30} esu for **1** as a reference.



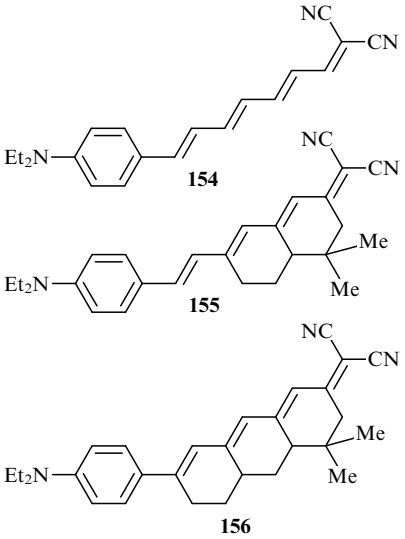
153a–d

X = Me_2N: Y = CHO (**a**), NO_2 (**b**); Y = NO_2: X = H_2N (**c**), Cl (**d**).

Molecule	**153a**	**153b**	**153c**	**153d**
$10^{30}\beta$ (esu)	36	102	98	44
λ_{max} /nm	304	319	321	317

The data obtained show that the introduction of stronger D/A groups affects β to a larger extent than λ_{max}. The values of λ_{max} remain sufficiently low, so that the molecules remain optically transparent in the whole visible spectral range. The authors adopted value 55.4×10^{-30} esu as a reference for **2** for a comparative analysis of the hyperpolarisabilities, however, this value was determined under different conditions and is strongly underestimated. For instance, according to measurements performed under the same conditions,[286] the value of β for **2** is almost 9 times larger than for **1**, *i.e.*, it would be more appropriate to use the value of $\sim 150 \times 10^{-30}$ esu for the sake of comparison. Thus the hyperpolarisability of **2** is $\sim$1.5 times larger than that for its disulfide analogue, while molecule **2** is less optically transparent (λ_{max} = 427 nm in $CHCl_3$).

The use of sterically stabilised polyenes **154**–**156** was suggested[287–289] as a way to improve the thermal stabilities of D–π–A systems with polyene π-bridges.



154

155

156

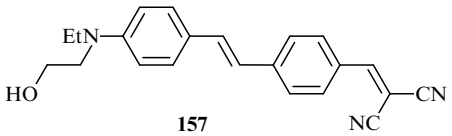
The absorption spectra were measured in 1,4-dioxane, the polarisabilities were determined using EFISH measurements in chloroform (λ = 1907 nm); the decomposition temperatures (T_d) of molecules **154**–**156** were 170, 317 and 343 °C, respectively, as estimated by differential scanning calorimetry (DSC).

The following values of spectral parameters were obtained for the sterically stabilised π-conjugated molecules:

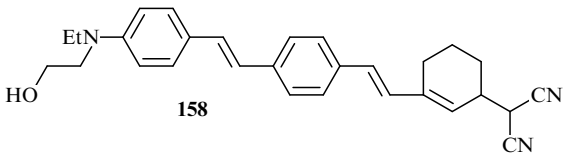
Molecule	**154**	**155**	**156**
$10^{30}\beta$ (esu)	453	378	–
λ_{max} /nm	563	538	518

The above data clearly demonstrate that the introduction of cyclohexene fragments simultaneously brings about some increase in the optical transparency and a significant increase in the thermal stability. As expected, this occurs at the cost of a decrease in β, since λ_{max} also decreases.

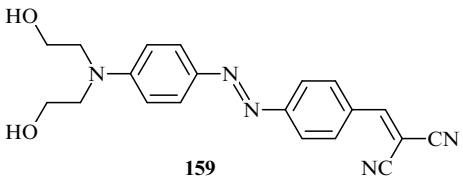
Luo, Hua *et al.*[290,291] investigated sterically stabilised π-conjugated molecules **157**–**160**. Their absorption spectra were measured in chloroform and the hyperpolarisabilities were determined using HRS measurements in methanol (λ = 1064 nm).



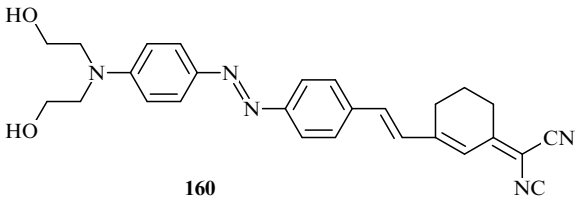
157



158



159

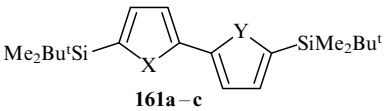


160

Molecule	**157**	**158**	**159**	**160**
$10^{30}\beta$ (esu)	1393	1564	1086	2890
λ_{max} /nm	493	474	508	490

Despite the molecules stabilised with a cyclohexene fragment contain longer π-chains, they are characterised by slightly shorter absorption wavelengths and higher β.

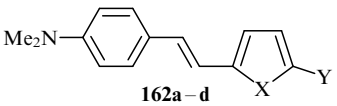
It was shown[292,293] that the thermal stabilities of molecules **161** increase upon transition from thiophenes to their analogues containing thiophene 1,1-dioxide moiety (λ_{max} were determined for $CHCl_3$ solutions).[293]



161a–c

X = Y = S (**a**); X = SO_2, Y = S (**b**); X = Y = SO_2 (**c**).

Molecule	**161a**	**161b**	**161c**
λ_{max} /nm	326	390	406
M.p. /°C	118	137	226

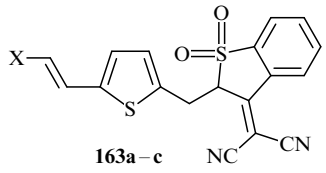


162a–d

Y = NO_2: X = S (**a**), SO_2 (**b**); Y = HC=$C(CN)_2$: X = S (**c**) , SO_2 (**d**).

Molecule	**162a**	**162b**	**162c**	**162d**
$10^{30}\beta$ (esu)	61.4	116.1	84.7	175.7

This also leads to an increase in the hyperpolarisability, as evidenced by the theoretical calculations (FF/AM1 in the static limit)[292] for molecules **162**, due to the loss of aromaticity in the five-membered heterocycles. The latter factor, on the other hand, narrows the optical transparency range of these molecules. Likely, the acceptor properties of the SO_2 group are also partly responsible for the increase in β. This suggestion is supported by rather high hyperpolarisabilities of molecules **163** (measurements in CH_2Cl_2 at λ = 1907 nm extrapolated to the zero frequency).[294]

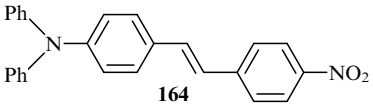


163a–c

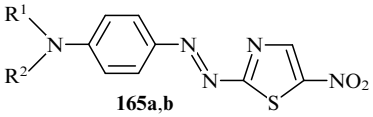
X = Me_2N– (**a**), Ph_2N– (**b**), Ph_2N– (**c**).

Molecule	**163a**	**163b**	**163c**
$10^{30}\beta$ (esu)	3070	2320	4880
λ_{max} /nm	704	660	738

The use of amino or alkylamino groups as donors is preferable for achieving high values of β, however, these compounds are less thermally stable than, for instance, their alkoxy analogues.[295,296] With this regard, Moylan *et al.*[297–299] and other researchers (see Refs 300–302) proposed to use a diarylamino group and showed that its introduction significantly increases thermal stability without narrowing of the optical transparency range (Table 24).

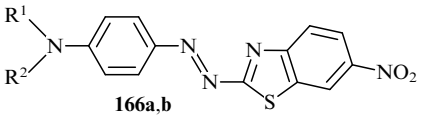


164



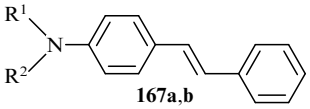
165a,b

R^1 = Et, R^2 = $(CH_2)_6OH$ (**a**); R^1 = R^2 = Ph (**b**).



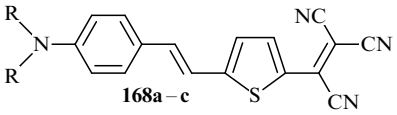
166a,b

R^1 = Et, R^2 = $(CH_2)_6OH$ (**a**); R^1 = R^2 = Ph (**b**).



167a,b

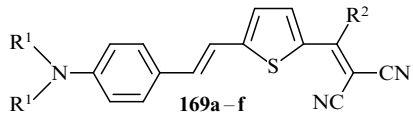
R^1 = H, R^2 = Ph (**a**); R^1 = R^2 = Ph (**b**).



168a–c

R = Et (**a**), Ph (**b**), *p*-$MeOC_6H_4$ (**c**).

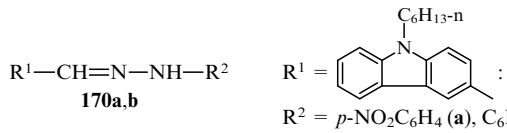
The use of tetra- or pentafluorophenyl groups (molecules **169–171**) as acceptors instead of π-acceptor groups results in broadening of the optical transparency range and an increase in the thermal stability[303–305] (Table 25, molecules **169a**,**c**,**e**, **170a** and **169b**,**d**,**f**, **170b**). The data from Table 25 also indicate that it is difficult to unambiguously predict the trend in β upon transition



169a–f

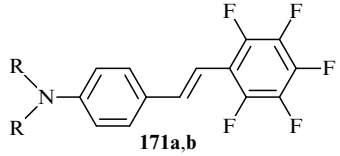
R^1 = Bu: R^2 = CN (**a**), $CF_3C_6F_4$ (**b**);
R^1 = Ph: R^2 = CN (**c**), $CF_3C_6F_4$ (**d**).

R^1 = Me_2N– : R^2 = *p*-$NO_2C_6H_4$ (**e**), C_6F_5 (**f**).



170a,b

R^2 = *p*-$NO_2C_6H_4$ (**a**), C_6F_5 (**b**).



171a,b

R = Me (**a**), Ph (**b**).

Table 24. Optical and thermal characteristics of D/A-substituted stilbenes and their analogues.

Molecule	$10^{30}\beta_0$ (esu)	λ_{max} /nm	T_d /°C	Comments	Ref.
2	42.1	438	290	measurement of optical characteristics in $CHCl_3$; β from EFISH measurements (λ = 1907 nm) extrapolated to the zero frequency using the two-level model; T_d from DSC measurements	297–299
164	37.3	436	358	the same	297–299
165a	52.2	582	213	"	297–299
165b	68.2	582	295	"	297–299
166a	60.1	548	259	"	297–299
166b	71.8	550	356	"	297–299
167a	17.7	417	288	measurement of λ_{max} in hexane; β calculated by the FF/AM1 method in the static limit; T_d from TGA measurements	300
167b	20.0	411	313	the same	300
168a	6700[a]	640	240	measurement of optical characteristics in dioxane; $\mu\beta$ (10^{-48} esu) from EFISH measurements (λ = 1907 nm); T_d from TGA measurements	301
168b	3510[a]	601	315	the same	301
168c	–	683	295	λ_{max} measured in $CHCl_3$; T_d from TGA measurements	302

[a] The value of $\mu\beta$ is given.

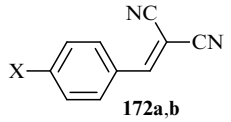
from the nitrophenyl to the pentafluorophenyl acceptors (molecules **169e**,**f** and **170a**,**b**). The result depends on the structure of the π-system and the donor type, in addition to the mere strength of the acceptor group to be replaced. It is also evident that the use of NPh_2 groups instead of $NAlk_2$ leads to a significant increase in the thermal stability (molecules **169a–d**, **171a**,**b**).

Table 25. Decomposition temperatures (according to DSC measurements), absorption band maxima and hyperpolarisabilities of molecules **169–171**.

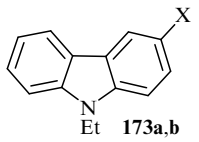
Molecule	$10^{30}\beta_0$ (esu)	λ_{max} /nm	T_d /°C	Comments
169a	–	640	240	measurement of λ_{max} in dioxane
169b	–	591	310	the same
169c	–	601	315	"
169d	–	553	340	"
169e	95	431	–	β_0: HRS measurement in methanol at λ = 1064 nm; λ_{max} measured in methanol
169f	84	344	–	the same
170a	46	423	–	"
170b	62	331	–	"
171a	100[a]	341	177	$10^{48}\mu\beta$ (esu), EFISH measurements in $CHCl_3$ at λ = 1907 nm; λ_{max} measured in CH_2Cl_2
171b	110[a]	379	> 300	the same

[a] The value of $\mu\beta$ is given.

An original approach to increase thermal stability of potential NLO molecules was suggested by Nesterov *et al.*[306, 307] They used D–π–A— D′ molecules in which the amino groups liable to the formation of H-bonds were introduced as auxiliary donors D′. Although the melting point of a compound does not correlate directly with crystal lattice energy, nor with the presence of H-bonds in the structure, the literature data (see, for instance, Refs 308–311) indicate that crystals of similar molecules differing from each other only by the presence/absence of H-bonding sites possess higher melting points provided that the crystal structure involves H-bonds. In particular, crystals built up of H-bonded molecules **172a**–**174a** melt at significantly higher temperatures than crystals built up of molecules **172b**–**174b**, which do not form H-bonds.

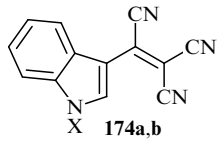


172a,**b**

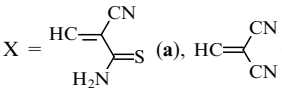


173a,**b**

X = HO (**a**), MeO (**b**).



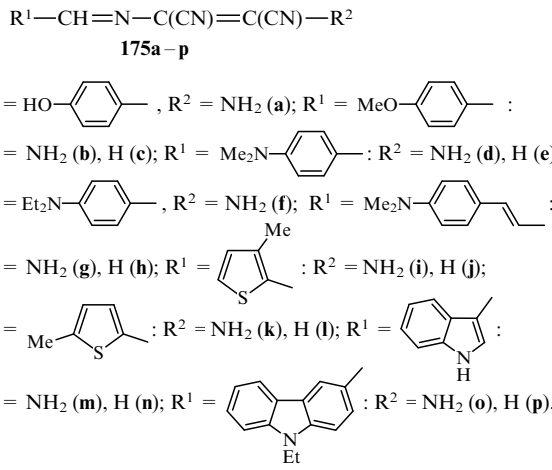
174a,**b**

X =  (**a**), (**b**).

X = H (**a**), $CH_2-CH=CH_2$ (**b**).

Molecule	**172a**	**172b**	**173a**	**173b**	**174a**	**174b**
M.p. /°C	188	114	216	157	275	145

Table 26 summarises the results of theoretical calculations of dipole moments and hyperpolarisabilities (FF/AM1 in the static limit) and experimental characterisation (measurements of λ_{max} in THF) [306, 307] for imines **175** and their D–π–A–H analogues.



175a–**p**

R^1 = HO–C$_6$H$_4$–, R^2 = NH_2 (**a**); R^1 = MeO–C$_6$H$_4$–:

R^2 = NH_2 (**b**), H (**c**); R^1 = Me_2N–C$_6$H$_4$–: R^2 = NH_2 (**d**), H (**e**);

R^1 = Et_2N–C$_6$H$_4$–, R^2 = NH_2 (**f**); R^1 = Me_2N–C$_6$H$_4$–CH=CH–:

R^2 = NH_2 (**g**), H (**h**); R^1 = : R^2 = NH_2 (**i**), H (**j**);

R^1 = : R^2 = NH_2 (**k**), H (**l**); R^1 = :

R^2 = NH_2 (**m**), H (**n**); R^1 = : R^2 = NH_2 (**o**), H (**p**).

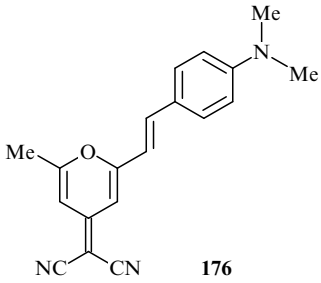
It is evident that the substitution of the amino group for a hydrogen atom results in a decrease in the hyperpolarisability, this is also accompanied by a decrease in the dipole moment. The latter factor as well as the availability of active sites prone to H-bonding increase the probability of crystallisation of these compounds in a non-centrosymmetric space group. Indeed, five out of nine compounds studied crystallise in such groups.

2. Molecules with two- and three-dimensional hyperpolarisability

In the case of molecules possessing two- and three-dimensional hyperpolarisabilities, non-diagonal components of the tensor β becomes significant making an additional contribution to the value of β.[312, 313] In particular, for 1,3-dinitro-4,6-diaminobenzene, the diagonal component β_{zzz} is an order of magnitude smaller than β_{zxx}.[314] The so-called V- or X-shaped molecules **176**–**182** were a subject of a series of studies.[315–319] By comparing characteristics of molecules **176** and **179** with those of molecules **177**, **178** and **180** one may conclude that the attachment of a second donor group, at least, doubles β and enhances the thermal stability but somewhat narrows the range of the optical transparency (Table 27). In contrast, a comparison of characteristics of molecules **181** and **182** indicates that the introduction of a second acceptor group broadens the range of optical transparency in addition to increase in β and T_d.

Table 26. Melting points, spectral characteristics and crystallographic data for imines **175** and their D–π–A–H analogues.

Molecule **175**	μ /D	$10^{51}\beta_0$ /C m^3 V^{-2}	λ_{max} /nm	M.p. /°C	Space group
a	4.5	54	375	209–210	$Pca2_1$
b	5.1	64	374	220–221	$Pna2_1$
c	6.0	81	–	–	
d	6.2	87	414	222–223	$P2_1/c$
e	6.5	109	–	–	
f	7.4	140	430	211–212	$C2/c$
g	6.8	189	442	210–211	$Pca2_1$
h	8.1	242	–	–	
i	5.3	34	384	207–208	$P2_1/c$
j	5.7	46	–	–	
k	5.8	41	387	219–220	$P2_1$
l	6.0	55	–	–	
m	6.8	71	379	217–218	$Pna2_1$
n	8.0	83	–	–	
o	7.3	99	395	213–214	$P2_1/c$
p	8.2	128	–	–	



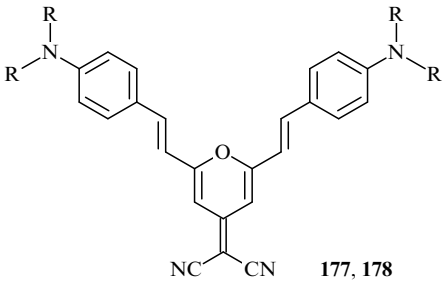
176

Table 27. Spectral characteristics and decomposition temperatures of molecules **176**–**182**.

Molecule	$10^{30}\beta_0$ (esu)	λ_{max} /nm	T_d /°C
176	88.8 ± 6.6	468	332
177	175 ± 3	486	404
178	197 ± 2	496	348
179	1043 [a]	541	301
180	5920 [a]	564	315
181	34.8	401	335
182	50.9	384	377

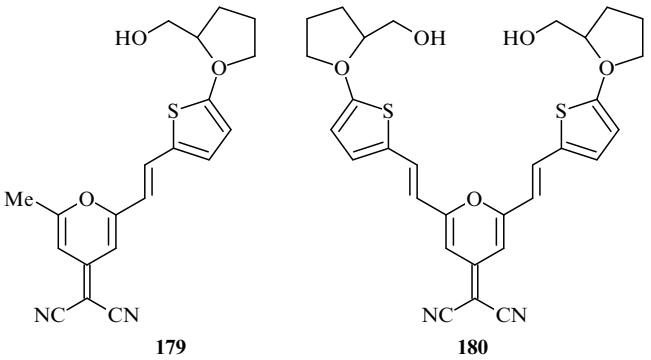
Note. The values of β and $\mu\beta$ for molecules **176**–**180** were measured using EFISH at λ = 1907 nm in chloroform, for molecules **181**, **182**, these values were calculated theoretically (FF/AM1 in the static limit), T_d were determined from DSC and TGA measurements for molecules **176**–**178** and **179**–**182**, respectively.

[a] The value of $10^{48}\mu\beta$ (esu) is given.

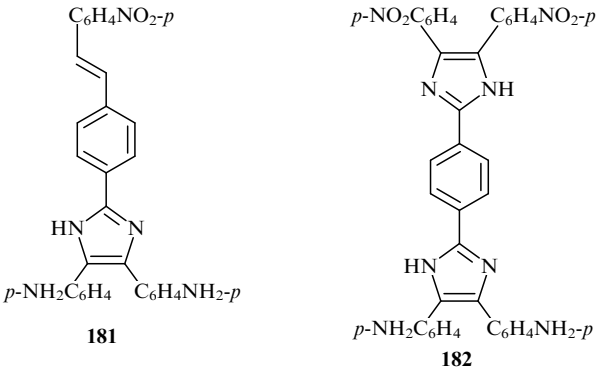


177, **178**

R = Ph (**177**), Bu (**178**).

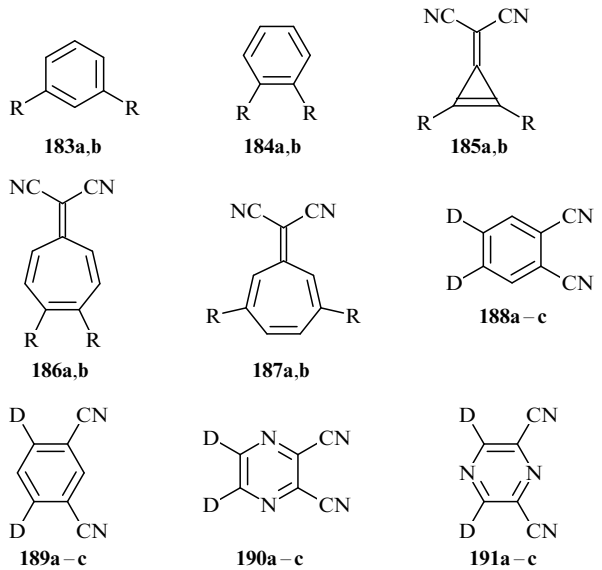


179 **180**



181 **182**

A detailed theoretical investigation into the trends in hyperpolarisability of X-shaped molecules **183**–**191** was performed by Yang and Champagne [320] for a series of small π-conjugated systems.



183a,**b** **184a**,**b** **185a**,**b**

186a,**b** **187a**,**b** **188a**–**c**

189a–**c** **190a**–**c** **191a**–**c**

R = NH_2 (**a**), OH (**b**); D = NH_2 (**a**), OMe (**b**), Br (**c**).

Table 28. Calculated hyperpolarisabilities (in 10^{-30} esu) of X-shaped molecules **183**–**191**.

Molecule	β_{xxz}	β_{yyz}	β_{zzz}	β_{tot}	φ /deg	Molecule	β
183a	310	42	35	386	121	**188a**	6.8
183b	218	−63	−38	−320	116	**188b**	3.4
184a	110	56	362	528	56	**188c**	3.0
184b	−99	−97	−307	−503	60	**189a**	3.5
185a	374	−19	−54	301	60	**189b**	1.9
185b	282	10	107	399	61	**189c**	1.8
186a	696	−152	2302	2846	27	**190a**	5.2
186b	566	5	2181	2752	24	**190b**	3.2
187a	1277	−76	−671	530	76	**190c**	1.9
187b	725	−25	579	1279	77	**191a**	2.1
						191b	1.2
						191c	1.6

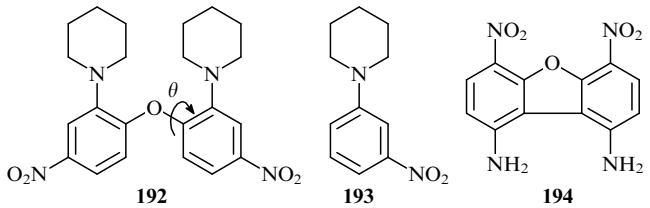
Note. The FF/MP2/6-31 + G* [320] and FF/AM1 [321] methods were used for molecules **183a**–**187b** and **188a**–**191c**, respectively.

The results of this work are compiled in Table 28. Provided that the coordinate system is selected so as the axis Y is perpendicular to the molecular plane, the components β_{xxz}, β_{yyz} and β_{zzz} make the dominant contributions to the total hyperpolarisability β_{tot}. The optimisation of the hyperpolarisability

$$\beta_{tot} = \beta_{xxz} + \beta_{yyz} + \beta_{zzz}$$

for such molecules requires a consistent selection of D/A-substituents and the angle φ between the directions of the charge transfer. In particular, the absolute value of β increases on going from molecules **183** to **184** due to a change in φ. A comparison of characteristics of molecules **185b** and **187b** with those of **185a** and **187a**, respectively, indicates that an increase in the strength of a D group (*i.e.*, the use of the amino instead of the hydroxy group) gives rise to a decrease in β, whereas the reversed trend is observed for molecules **186a** and **186b**. It is also worth noting that the relative significance of contributions β_{xxz} and β_{zzz} changes on going from molecule **186** to **187**. A study of didonor/diacceptor-substituted six-membered rings [321] (see Table 28) gave similar results. Molecules with donor groups occupying adjacent positions possess higher values of β.

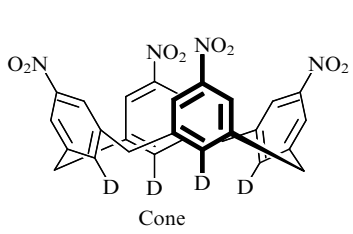
Sudharsanam *et al.*[322] considered molecules **192** and **193** (FF/AM1 in the static limit). Molecule **192** possesses a severalfold higher NLO activity and a broader range of optical transparency. However, it is non-planar. Meanwhile, β should prominently increase if $\theta \to 0$.[323] Analysis of molecule **194** with the strictly planar structure revealed a rather high β (SOS/INDO/CIS, λ = 1064 nm).



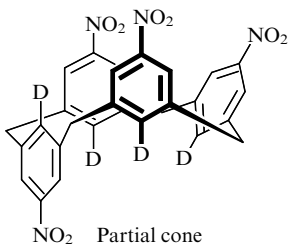
192 **193** **194**

Molecule	**192**	**193**	**194**
$10^{30}\beta$ (esu)	8.9	2.9	472
λ_{max} /nm	377	393	–

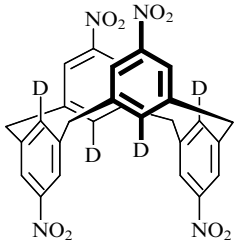
Calix[4]arenes, like V-shaped systems discussed above, also incorporate several D/A pairs in one molecule. These molecules were a subject of several investigations.[324–326] They can adopt the following conformations:



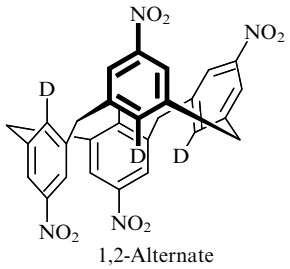
Cone



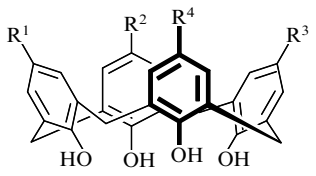
Partial cone



1,3-Alternate

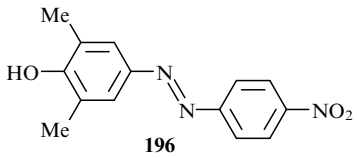


1,2-Alternate



195a–d

$R^1 = R^2 = R^3 = R^4 = p\text{-}NO_2C_6H_4-N=N$ (**a**); R^1 = H, $R^2 = R^3 = R^4 = p\text{-}NO_2C_6H_4-N=N$ (**b**); $R^1 = R^2$ = H, $R^3 = R^4 = p\text{-}NO_2C_6H_4-N=N$ (**c**); $R^1 = R^2 = R^3$ = H, $R^4 = p\text{-}NO_2C_6H_4-N=N$ (**d**).



196

Molecule	**195a**	**195b**	**195c**	**195d**	**196**
$10^{30}\beta$ (esu)	296.6	275.2	302.6	233.1	186.7
λ_{max} /nm	374	378	382	378	387

Interestingly, the absorption band maximum remains constant for all the conformers,[324] which implies that this parameter is weakly affected by the mutual orientation of the D/A-phenyl fragments. In contrast, the value of hyperpolarisability strongly depends on the conformation, which is evidenced by the experimental and theoretical data presented in Table 29.

According to the calculations, 1,2- and 1,3-alternates are characterised by values of β close to zero, which is in agreement with the zero hyperpolarisability experimentally found for the 1,3-conformer. This is due to the complete mutual cancellation of the NLO activity of different D/A-phenyl fragments. The ratio of activities cone/partial cone depends on the inclination angle of the phenyl rings. Brouyere *et al.*[326] additionally compared the hyperpolarisability of NO_2/OH-substituted calix[4]arene in the cone conformation with those of *o*,*o*′-dimethyl-*p*-nitrophenol and its dimer built up of two parallel molecules. As can be judged from Table 29, additive schemes are applicable to the evaluation of β neither for the dimer nor for calix[4]arene (with a correction for the non-parallel arrangement of the rings), which clearly implies interaction between the π-systems. Further arguments in favour of the substantial influence of the intermolecular π–π interactions on the spectral properties were presented by other authors.[327–329]

Similar conclusions were derived[330,331] for NO_2/OH-substituted calix[4]arenes **195a–d** in the cone conformation.

The experimental values (HRS, THF, λ = 1064 nm) for tetrahydroxycalix[4]arene successively substituted with *p*-nitrophenylazo groups (molecules **195**) were compared with that of the monomeric analogue **196**. The value of λ_{max} for calix[4]arenes is virtually independent of the number of acceptor groups and is slightly smaller than that of the monomer, whereas β is larger. The observed variations in β are probably due to different mutual orientations of the fragments in the calix[4]arene molecule, which is determined by the steric interaction of the substituents.

It is important that the absorption band is blue-shifted and β is increased on going from the monomer to calix[4]arenes (*i.e.*, tetramers). It should be noted that it is possible to achieve a significantly higher NLO activity by sequential coupling of monomers, however at the cost of narrowing of the optical transparency range.

Paracyclophane derivatives **199–201** represent yet another example of molecules possessing non-standard conjugated systems (to be compared with reference molecules **197** and **198**).[332–334]

Table 29. Calculated and experimental values of β (10^{-30} esu) and λ (nm) for D/A-calix[4]arenes in different conformations.

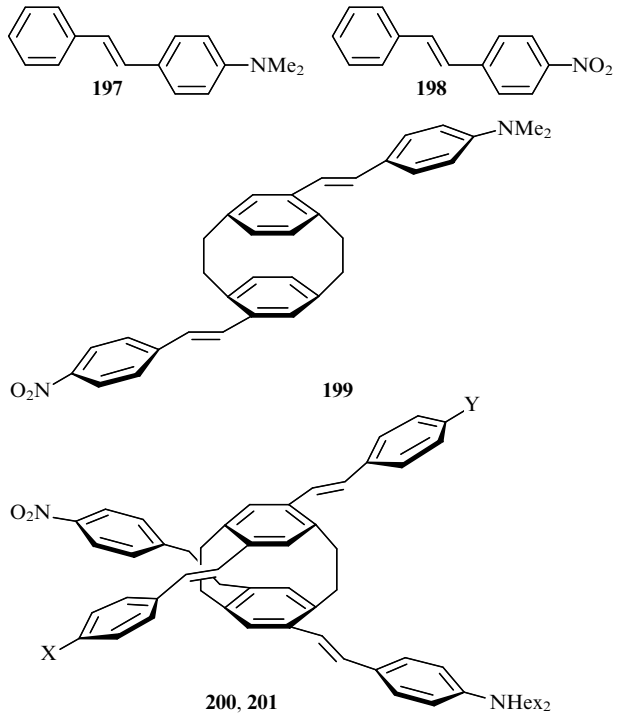
Conformation	Donor	β_{EFISH} (calculation)	β_{HRS} (calculation)	β_{EFISH} (experiment)	β_{HRS} (experiment)	λ_{max} (calculation)	λ_{max} (experiment)
Cone	OH	22.9	23.8	–	–	290	–
Partial cone	OH	12.5	12.8	–	–	290	–
1,2-Alternate	OH	6.3	7.1	–	–	290	–
1,3-Alternate	OH	0.1	0.3	–	–	290	–
Cone	OMe	22.1	24.4	30.0	27.0	290	291
Partial cone	OMe	11.8	13.8	27.0	–	290	291
1,2-Alternate	OMe	1.0	1.1	–	–	290	–
1,3-Alternate	OMe	0.8	0.8	0	0	290	291
Monomer [a]	OMe	12.5	13.1	12.0	–	301	302
Dimer [a]	OMe	18.3	18.3	–	–	284	–

Note. The calculated values of β were obtained[326] using the SOS method within the INDO/CIS approximation;

$$\beta_{EFISH}\,(\text{calculation}) = \beta_{zzz} + \frac{1}{3}(\beta_{zxx} + \beta_{zyy} + \beta_{xzx} + \beta_{yzy} + \beta_{xxz} + \beta_{yyz});\ \beta_{HRS}\,(\text{calculation}) = \sqrt{\frac{35}{6}}\langle\beta^2_{HRS}\rangle,\ \text{where}\ \langle\beta^2_{HRS}\rangle = \langle\beta^2_{ZZZ}\rangle + \langle\beta^2_{XZZ}\rangle,$$

see Eqns (8), (9); experimental measurements were performed in $CHCl_3$ at λ = 1064 nm.[324,325]

[a] Data for *o*,*o*′-dimethyl-*p*-nitrophenol.



X = $NHex_2$, Y = NO_2 (**200**); X = NO_2, Y = $NHex_2$ (**201**); Hex = n-C_6H_{13}.

The experimental data in Table 30 unambiguously confirm the through-space electron density transfer between the two phenyl rings. The hyperpolarisability of molecule **199** estimated within the additive scheme as a sum of values for molecules **197** and **198** appears three times smaller than the experimental value. Molecule **199** manifests relatively high β and remains optically transparent in virtually entire visible range. On the other hand, the additive model applied to molecules **200** and **201** describes the vector part of the hyperpolarisability tensor ($\beta_{j=1}$) relatively well but fails to estimate the septor component ($\beta_{j=3}$), which makes the predominant contribution. It is of note that the charge transfer in substituted paracyclophanes was also confirmed by the topological analysis of the electron density distribution based on high-precision X-ray diffraction studies.[335] The introduction of an OH group (which is a strong donor) into one of the benzene rings of the paracyclophane molecule gives rise to the emergence of a critical point (3, −1) between carbon atoms of different benzene rings,[335] which is indicative of a chemical interaction according to the Bader theory.‡ Meanwhile, the correspondent critical points are observed neither in unsubstituted paracyclophane nor in its quinonoid analogue, which means that in these cases, no direct through-space charge transfer is involved.[336, 337]

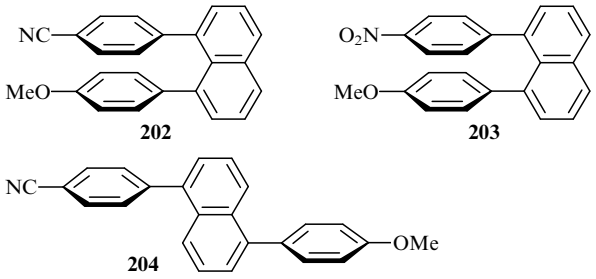
Table 30. Spectral characteristics [$10^{30}\beta$ (esu)] of monosubstituted stilbenes and D/A-substituted paracyclophanes.

Molecule	β	λ_{max} /nm	Molecule	$\lvert\beta_{j=1}\rvert$	$\lvert\beta_{j=3}\rvert$	$\lvert\beta^{ad}_{j=1}\rvert$	$\lvert\beta^{ad}_{j=3}\rvert$
197	9	320	**200**	190	430	170	620
198	9	345	**201**	260	580	290	0
199	60	378					

Note. All measurements were performed in chloroform; the results of EFISH measurements extrapolated to the zero frequency are given for molecules **197**–**199**; the measurements were performed at λ = 1907 nm for **197** and **198** and at λ = 1064 nm for **199**;[332] HRS results measured at λ = 1320 nm are given for molecules **200** and **201**.[333, 334]

‡ R Bader *Atoms in Molecules: A Quantum Theory* (Oxford: Clarendon Press, 1990)

Bahl *et al.*[338] reported experimentally measured spectral characteristics (HRS in $CHCl_3$, λ = 1064 nm) of naphthalene derivatives **202**–**204**.



Molecule	**202**	**203**	**204**
$10^{30}\beta$ (esu)	26	32	18
λ_{max} /nm	298	308	312

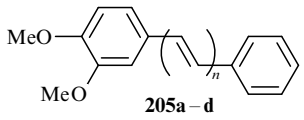
Probably, the reason for the larger value of β in the case of molecule **202** as compared to molecule **204** is again the direct through-space interaction. According to X-ray crystallographic results,[338] the phenyl rings in molecule **203** are nearly parallel to each other and rotated by 62.6° relative to the central naphthalene fragment. The absorption bands of molecules **202** and **203** are blue-shifted with respect to that of molecule **204** and their hyperpolarisabilities are 1.5–2 times larger. Therefore, it may be conlcuded that the involvement of the direct through-space electron density transfer increases β but does not result in narrowing of the optical transparency range.

Octupolar molecules that are characterised by a three-fold symmetry axis and zero dipole moments represent yet another promising class of molecules for the design of NLO materials. Some representatives of this class were considered by Zyss and Ledoux.[339, 340] The vector part of the tensor β is zero for octupolar molecules, whereas the septor part remains significant[341] thus determining the macroscopic spectral properties of the compound. Due to the absence of dipole–dipole interactions, octupolar molecules crystallise in non-centrosymmetric space groups with higher probability than other classes of molecules, which is one of their major advantages.[342, 343]

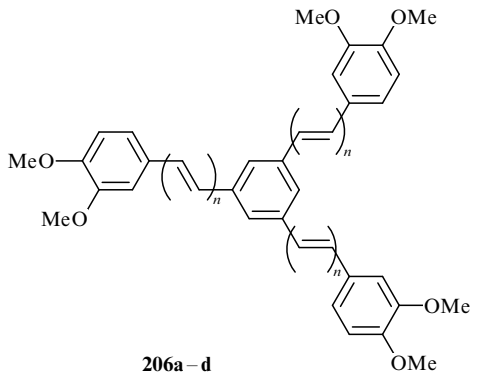
Under the assumption of non-interacting substituents (*i.e.*, provided that the effects of D/A pairs are additive), the hyperpolarisability increases by a factor of 1.5 on going from a dipolar to the respective octupolar molecule (featuring the same substituents and π-bridge).[344]

Bredas *et al.*[345] perfomed a comparative analysis of the spectral characteristics of *p*-NA and triaminotrinitrobenzene (TATB). The hyperpolarisabilities β estimated as norms of the respective tensors [Eqn (4), FF/AM1] were equal to 12.1 and 22.2×10^{-30} esu, and absorption band maxima were located at 4.6 eV and 5.3 eV for *p*-NA and TATB, respectively,[344] which means that TATB is characterised by a broader optical transparency range.

Andraud *et al.*[346] compared the spectral characteristics of dipolar and octupolar systems for a series of molecules **205a**–**d** and **206a**–**d**.



205a–**d**



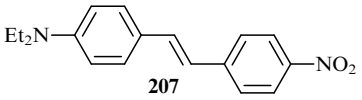
206a–d

n = 1 (**a**), 2 (**b**), 3 (**c**), 4 (**d**).

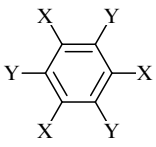
Molecule	**205a**	**205b**	**205c**	**205d**	**206a**	**206b**	**206c**	**206d**
$10^{30}\beta$ (esu)	18.5	29.0	40.4	52.0	27.4	44.4	58.6	72.0
λ_{max} /nm	391	426	455	480	396	434	458	484

The results obtained [SOS/INDO/S, β estimated according to the Eqn (4)] reveal some general trends also typical of one-dimensional polar molecules. In particular, β and λ_{max} increase with an elongation of the conjugation chain. A systematic comparison of molecules **205a–d** and **206a–d** indicated that octupolar molecules are characterised by higher NLO activities and small batochromic shifts of the absorption bands.

Spectral and thermal properties of octupolar molecules were also studied by Cho *et al.*[347–351] The experimental HRS data extrapolated to the zero frequency within the three-level model are presented in Table 31 together with the results of thermogravimetric analysis (TGA). Additionally, the spectral characteristics of dipolar molecules **207** and octupolar molecules **208a–i** were compared.[347]



207



208a–i

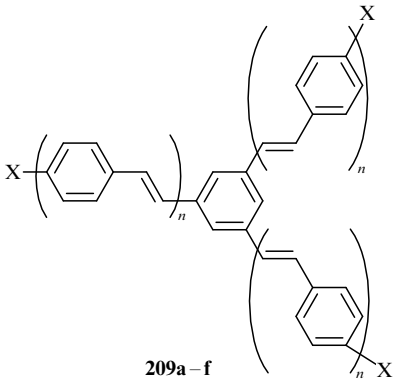
X = NO_2: Y = *p*-$Et_2NC_6H_4-CH=CH$ (**a**);
X = OMe: Y = *p*-$O_2NC_6H_4-CH=CH$ (**b**),
p-$[(NC)_2CH]C_6H_4-CH=CH$ (**c**);
X = CN: Y = $NMe_2-CH=CH$ (**d**),
p-$Et_2NC_6H_4-CH=CH$ (**e**),
p-$Ph_2NC_6H_4-CH=CH$ (**f**),
p-$Bu_2N-(C_6H_4-CH=CH)_2$ (**g**),
p-$Hex_2N-(C_6H_4-CH=CH)_2$ (**h**),
p-$Et_2NC_6H_4-N=N-C_6H_4-CH=CH$-*p* (**i**).

The hyperpolarisabilities β of octupolar molecules **208** are larger than those of their dipolar counterpart **207**. Furthermore, the octupolar molecules manifest broader optical transparency ranges. As expected, the hyperpolarisability increases and the optical transparency range becomes narrower with an elongation of the conjugation chain (*cf.* molecules **208d**,**e** and **g**) and the introduction of stronger acceptors (*cf.* **208b** and **c**). It is of note that the introduction of the phenyl fragments in place of the Et groups at the nitrogen atom (*cf.* **208e** and **f**) gives rise both to a significant increase in β and a hypsochromic shift in the absorption band. The replacement of a CH=CH fragment (**208h**) by N=N (**208i**) results in a decrease in β due to a decrease in the degree of conjugation of the π-bridge. It seems unusual that the hyperpolarisabilities of molecules **208g** and **208h** differing only in the alkyl substituents differ as much as by a factor of 3. In the experimental measurements, solvents with similar polarities were used and, as has been mentioned above, the measured values were extrapolated to the zero frequency. Most probably, this discrepancy reflects the inadequacy of the three-level model to the extrapolation of the experimental data measured at different incident wavelengths. An analysis of the literature data shows that the use of two- and three-level models for the extrapolation of hyperpolarisability values can indeed yield incorrect results.[352]

Table 31. Spectral and thermal characteristics of molecules **207** and **208**.

Molecule	$10^{30}\beta$ (esu)	λ_{max} /nm	T_d /°C	Experimental conditions	
				λ /nm	solvent
207	43	450	–	1560	$CHCl_3$
208a	63	428	278	1560	$CHCl_3$
208b	11	370	305	1560	$CHCl_3$
208c	35	415	354	1560	$CHCl_3$
208d	25	389	340	1560	$CHCl_3$
208e	65	493	390	1560	$CHCl_3$
208f	124	488	422	1560	$CHCl_3$
208g	116	499	340	1560	$CHCl_3$
208h	348	480	–	1064	THF
208i	246	485	–	1064	THF

A similar dependence of β on the structure of dipolar and octupolar molecules was obtained for a series of compounds **209** and **210**. Molecules with long conjugation chains (*e.g.*, **209e**,**f**) manifest larger β and λ_{max} (Table 32). A comparison of hyperpolarisabilities of molecules **209a** and **209b** confirms the validity of the concept of auxiliary D/A groups. The introduction of a donor into the electron-rich thiophene ring is energetically more favourable than the introduction of an acceptor. Molecules **210a–d** contain σ-fragments, such as CH_2 and CH_2-CH_2, providing high optical transparencies of these compounds (λ_{max} < 300 nm), and the introduction of the CH_2-CH_2 fragment proves more efficient. The introduction of an acceptor sulfo group instead of a donor amino group (*cf.* molecules **209c,e** and **209d,f**) both increases β and broadens the optical transparency range. According to the results[358] devoted to the design of 1,3,5-substituted benzene derivatives with acceptor groups at the terminal positions of π-conjugated substituents, these molecules are optically transparent in a broader range. For instance, λ_{max} is equal to 317 nm ($\beta = 39 \pm 5 \times 10^{-30}$ esu) for 1,3,5-(*p*-$CF_3C_6H_4C\equiv C)_3$-2,4,6-$(MeO)_3C_6$, according to the HRS measurements in $CHCl_3$ at λ = 800 nm.

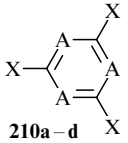


209a–f

X = Me_2N-(S)-$CH=CH-C_6H_4$-*p* (**a**), n = 0;

X = O_2N-(S)-$CH=CH-C_6H_4$-*p* (**b**), Hex_2N (**c**), SO_2Me (**d**), n = 1;

X = Hex_2N (**e**), SO_2Me (**f**), n = 2.



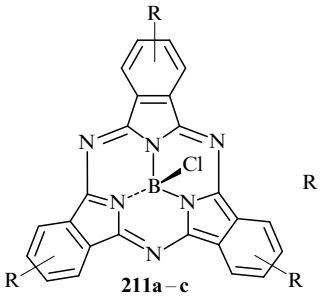
210a–d

X = *p*-$Me_2NC_6H_4CH_2$: A = CH (**a**), N (**b**);
X = *p*-$Me_2NC_6H_4(CH_2)_2$: A = CH (**c**), N (**d**).

Table 32. Spectral characteristics of octupolar NLO-active molecules.

Molecule	$10^{30}\beta$ (esu)	λ_{max} /nm	Method of calculation or measurement	Ref.
209a	79	392	the SOS method in the	353
209b	29	437	INDO/CISD approximation at $\lambda = \infty$	
209c	29	387	HRS measurements	354
209d	30	342	(in $CHCl_3$):	355
209e	150	407	λ = 1060 nm for **209c**,**d**;	356
209f	250	377	λ = 1340 nm for **209e**,**f**	
210a	12.1	269	FF/AM1 calculation in	357
210b	16.1	267	the static limit	
210c	17.4	268		
210d	23.4	267		

Subphthalocyanines can also be classified as systems with a significant contribution of non-diagonal components of the tensor β and an approximate C_3 point symmetry.[359] Unsubstituted and D/A-substituted subphthalocyanines **211** were the subject of studies by Zyss and co-workers.[360–362]



211a–c

R = H (**a**), NO_2 (**b**), SC_8H_{17}-n (**c**).

The experimental results summarised in Table 33 (HRS measurements in $CHCl_3$) were obtained with different incident wavelengths, which complicates their comparative analysis. In particular, a large value of β reported in Ref. 361 was explained later [362] by the impossibility of accurate registration of the second harmonic intensity due to a contribution of fluorescence at the same wavelength. The changes in β measured at λ = 1064 nm along the series **211a–c** are also difficult to rationalise. The introduction of substituents should, in principle, increase the hyperpolarisability, however the experimental data contradict to the expectation. Probably, the proximity of λ_{max} to the second harmonic wavelength (532 nm) results in its resonant enhancement, which prevents correct comparison. Notwithstanding, the above results are sufficient to conclude that the introduction of acceptor substituents in the phenyl groups is preferable.

Table 33. Spectral characteristics [$10^{30}\beta$ (esu)] of subphthalocyanines.[357, 359, 360]

Molecule **211**	λ_{max} /nm	β (λ = 1064 nm)	β (λ = 1340 nm)	β (λ = 1460 nm)
a	565	92	296	–
b	586	–	2000	144.3
c	584	–	–	76.5

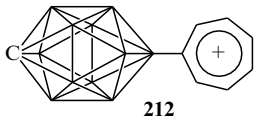
3. *closo*-Carboranes

closo-Carboranes possess a great potential in the design of NLO materials due to their thermal and chemical stability.[363–366] Experimental and theoretical investigations into the NLO properties of carboranes were started only in the early 1990s.[367, 368] According to the first experimental measurements, the hyperpolarisability of 12-vertex *ortho*-carboranes substituted with nitrophenyl and aminophenyl at the carbon atoms groups were comparable to that of *p*-NA. A few years later, Abe *et al*.[369] calculated the spectral properties of a borane-carborane system ($[B_{12}H_{11}-C_2B_{10}H_{11}]^{2-}$) and obtained somewhat smaller but still comparable with *p*-NA values of hyperpolarisability (Table 34). It is important to note that the absorption bands of all polyhedral systems studied so far lies in the UV range (λ_{max} = 260–271 nm).

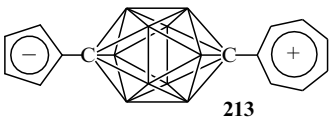
Table 34. Calculated optical characteristics of $[B_{12}H_{11}-C_2B_{10}H_{11}]^{2-}$ isomers compared to those of *p*-NA.

Compound	$10^{30}\beta$ (esu) (HF/6-31G**)	λ_{max} /nm (CIS/6-31G**)
$[B_{12}H_{11}$-*o*-$C_2B_{10}H_{11}]^{2-}$	3.4	271
$[B_{12}H_{11}$-*m*-$C_2B_{10}H_{11}]^{2-}$	3.6	265
$[B_{12}H_{11}$-*p*-$C_2B_{10}H_{11}]^{2-}$	3.6	260
p-NA	6.2	374

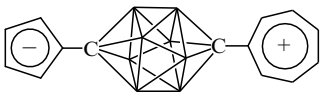
Some representative results of more recent studies,[370–372] including HRS measurements in chloroform at λ = 1064 nm for molecule **212** and SOS/AM1 calculations ($\hbar\omega$ = 0.5 eV) for molecules **213** and **214** are given below.



212



213



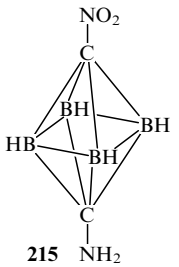
214

Molecule	**212**	**213**	**214**
$10^{30}\beta$ (esu)	236 ± 50	682	503
λ_{max} /nm	340	–	–

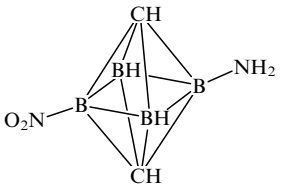
The NLO properties of NH_2/NO_2-substituted 6- and 10-vertex carboranes were systematically investigated in a series of theoretical works by Suponitsky and Timofeeva.[373–375] In particular, the following values of hyperpolarisabilities were obtained [CPDFT/6-31 + G*, in the static limit, β_{vect} (a.u.) calculated by the formula (3)]:

Molecule	**215**	**216**	**217**	**218**	**219**	**220**	**1**
β_{vect}	683	1154	808	403	3675	677	1745

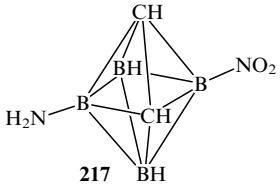
The value of β for *p*-NA estimated within the same approximation is also given for the sake of comparison.



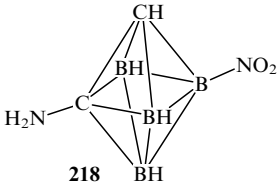
215



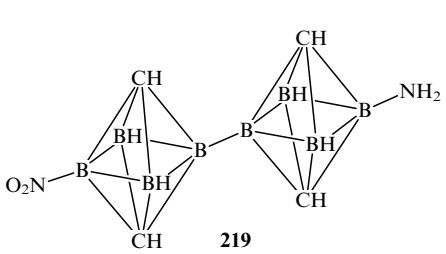
216



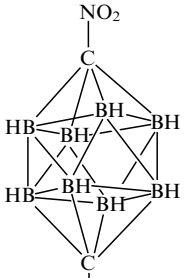
217



218



219



220

These results show again that the hyperpolarisabilities of carboranes and *p*-NA are comparable. This suggests the conjugation between substituents and the carborane cage and three-dimensional delocalisation of electrons over the carborane core. This suggestion is supported by the results of the topological analysis of the electron density distribution function in carborane derivatives (based on the experimental high-precision X-ray diffraction data) [376] and by mandatory utilisation of the resonance structures for the description of chemical bonding in carboranes within the concept of three-centre bonds.[377] Furthermore, according to calculations of magnetic properties [378] and an analysis of chemical properties,[379] carboranes can be regarded as aromatic systems. A significant increase in β upon introduction of another carborane cage into the conjugation chain (molecules **216** and **219**) gives an additional argument in favour of the analogy between the two- and three-dimensional aromaticity. It can seem strange that molecule **220** is characterised by smaller hyperpolarisability than molecule **215**, despite the presence of a longer conjugated bridge. The probable reason for this is the higher degree of aromaticity of 10-vertex carboranes as compared to 6-vertex ones.[380]

The above data clearly show that the use of carboranes as building blocks of conjugation bridges gives rise to relatively high values of hyperpolarisability with a simultaneous broadening of the optical transparency range. Taking into account the high thermal stability of carboranes, they should be recognised as a very promising class of compounds for applications in nonlinear optics.

V. The design of NLO crystals

The search for crystalline materials with high nonlinear optical susceptibilities d_{ijk} includes two principal steps. In the first step, most promising compounds are selected based on the information regarding their molecular spectral properties. In the second step, d_{ijk} has to be estimated, which can be done with a number of theoretical [381] and experimental [3, 382] methods.

1. Experimental methods for the determination of the NLO susceptibilities of crystals

The NLO susceptibility of a crystal can be measured both for single crystals and polycrystalline powders. In the former technique, the interference pattern (also referred to as the Maker fringes) produced by the second harmonic radiation transmitted through a single crystal is registered and the intensities in its maxima are compared to a standard reference.[383–385] This method enables independent determination of all components of the susceptibility tensor. For the determination of specific components d_{ijk}, polished parallel-sided plate crystals are used, which were carefully cut along the respective crystallographic directions.

Generally, the incident wave with a frequency ω and the secondary wave with a frequency 2ω propagating in a crystal are characterised by different phase velocities, so that the interaction area is small and thus the measured intensity of the second harmonic is low. Nevertheless, in the majority of organic crystals, there are specific crystallographic directions, the so-called synchronism directions,[3] along which the phase velocities are identical and thus the second harmonic intensity is amplified proportional to the squared distance traveled by the secondary wave in the crystal. This makes it possible to significantly improve the accuracy of the measurements. However only the effective susceptibility coefficient (d_{ef}) can be determined in this way, whereas every single component of the susceptibility tensor become inaccessible. However, it is the effective susceptibility that is of greatest practical importance. Provided that the refractive index of the material and all the tensor components d_{ijk} are known, the synchronism directions can be approximately found and the value of d_{ef} can be assessed.

A method for the determination of the NLO susceptibility in polycrystalline powders is based [386–388] on the registration of intensity of the second harmonic transmitted through a cell filled with a powder under study and its comparison with a reference signal. Such measurements are significantly simpler since they do not require time-consuming manipulations with optical-quality single crystals, *i.e.*, their growth, cutting and polishing.

A detailed description of both experimental methods can be found elsewhere.[3, 382] Here, we only mention their major advantages and drawbacks as regards their application to the design of NLO materials.

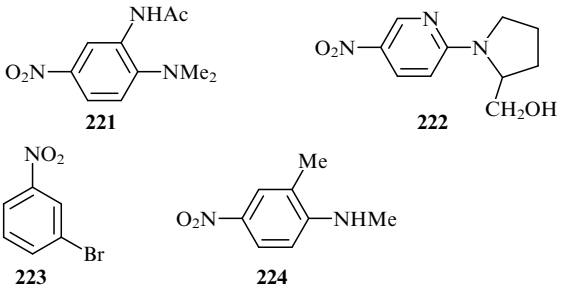
It is evident that the Maker fringe method provides comprehensive information on the NLO properties of a material. Its main disadvantage consists of the necessity to grow and process relatively large optical-quality crystals (with a volume of up to ~ 1 cm^3), which is very demanding. Therefore, this method is not applicable to the systematic search for the NLO materials. The powder method is by far simpler; it makes it possible to find out whether a crystal possesses synchronism directions and assess its potential in a rather straightforward way. The drawbacks of this method include the relatively low accuracy (50% at most) and the lack of information on single components of the susceptibility tensor.

It has to be noted that the experimental determination of the NLO susceptibility of a crystal does not generally require the detailed knowledge of its crystal structure. In particular, only space group is required for the interpretation of the Maker fringes. Nevertheless, X-ray diffraction data are indispensible, since the measured susceptibility cannot be ascribed to a specific material if its crystal structure is unknown. First of all, this is due to the frequently occurring polymorphism. In particular, a powder under study can actually be a mixture of several polymorph modifications of one compound. Second, it often happens that solvent molecules enter the crystal structure and thus the experimental NLO susceptibility has to be attributed to a solvate rather than pure compound.

Theoretical methods for the evaluation of NLO susceptibilities are typically based on the oriented gas model [48, 49] [see Eqn (6)], which assumes that the susceptibility of a crystal can be represented as a sum of molecular hyperpolarisabilities. The calculation of single components d_{ijk} of the crystal susceptibility tensor requires the knowledge of the hyperpolarisabilities of constituent molecules, local field factors (the approximate formula $f_i f_j f_k = 3$ can be employed in the case where no experimental data to estimate these factors are available) [389] and orientation of the consituent molecules in the unit cell.

The basic difference between the existing methods consists of the degree of neglect of the intermolecular interactions. The utilisation of Eqn (6) based on the values of β of an isolated molecule means the complete neglect of the intermolecular interactions. Zyss and Oudar [49] derived formulas for the calculation of d_{ijk} for the most common space groups under the assumption of the two-dimensional character of the hyperpolarisability, which is suitable for all nearly planar molecules. These formulas have relatively simple forms for monoclinic space groups but become increasingly complicated for higher symmetries. Furthermore, the original paper contains several misprints. This approach was further refined and implemented in the software code NLOP.[50, 390] This code operates with the full molecular hyper-

polarisability tensors and thus it makes possible to calculate the optical properties of any molecular crystal without restrictions to molecular geometry and space group. Furthermore, the probability of errors due to manual calculations with formulas from Ref. 49 is minimised [*e.g.*, see Ref. 391, where d_{xyz} of 2,5-di(benzylidene)cyclopentanone was overestimated twice due to a misprint in the original formula]. According to the calculations for model molecules **221** – **224**, for which the experimental values of d_{ijk} are also available, the theoretical approach agrees with the experiment at a semiquantitative level provided that the crystal structures reveal no specific strong intermolecular interactions (Table 35).[50,390] No doubt, this is sufficient for a preliminary evaluation of the potential of a compound under study and its appropriateness for a more thorough analysis.



Recently, the oriented gas model was improved by the introduction of a supermolecule concept, which means that the hyperpolarisabilities of molecular associates rather than isolated molecules are taken as input for the calculation of d_{ijk}. This makes it possible to include the dependence of the NLO properties of a molecule on its intermolecular environment into consideration to a certain accuracy level defined by the size and shape of the associate.

In particular, dimers of *p*-NA,[396] 2-methyl-4-nitroaniline (MNA, **225**)[397] and urea (**226**)[398] were considered. The structure of the H-bonded *p*-NA dimer was obtained by the geometry optimisation at the HF/6-31 + G** level; those of the MNA dimer (formed by weak stacking interactions) and the H-bonded urea dimer were taken from the experimental X-ray crystallographic data.[399,400] The hyperpolarisabilities β_z of the dimers calculated within the supermolecule approximation and by the additive scheme were 27.6×10^{-30} esu and 15.4×10^{-30} esu for **1** (CPHF/6-31 + G**), 10.5×10^{-30} esu and 15.3×10^{-30} esu for **225** (CPHF/6-31G with the frozen core) and 0.26×10^{-30} esu and 0.38×10^{-30} esu for **226** (CPHF/DZV), respectively.

As has been noted in the previous Section, in the case of molecular associates formed by the stacking interactions between π-systems, the additive scheme for the calculation of hyperpolarisabilities is violated. In particular, the values of β for a stacking dimer of *p*-NA at a distance between the benzene rings of 3.5 Å are 20.5×10^{-30} esu and 24.6×10^{-30} esu, as calculated within the supermolecule approximation and by the additive scheme, respectively.[327] Therefore, it becomes apparent that the additive scheme can be violated in different ways, depending on the dimer structure: the chain-like structure is more favourable than the columnar structure. However, in the case of urea, the supermolecule value of β for the H-bonded (chain-like) dimer is 1.5 times smaller than the additive one. Several authors[177,401,402] considered larger molecular clusters of MNA and urea. For a cluster of urea composed of 7 molecules (generated on the basis of crystallographic data),[401] the additive NLO susceptibility was smaller than the supermolecule value only by 15%. In the case of molecular associates of MNA (generated on the basis of crystallographic data), the additive susceptibility was 5 times smaller than the supermolecule value along the crystallographic axis *a* (which approximately conforms to the direction of the molecular dipole moment) but 30% – 50% larger than the supermolecule value in the perpendicular directions. On average, the additive scheme underestimated the NLO susceptibility by a factor of two as compared to the supermolecule model.

As has been mentioned above (see Section II), the desired level of accuracy should be considered as the basic appropriateness criterion in the selection of the theoretical method to be applied. The theoretical evaluation of the NLO properties at a semiquantitative level is well sufficient for the majority of tasks related to the systematic search for promising NLO compounds. In such a case, either the mere additive scheme or the supermolecule model based on a small molecular associate, depending on the presence of short intermolecular contacts in the molecular structure, will provide adequate results.

2. Methods for the design of NLO crystals

As has been mentioned above, only non-centrosymmetric crystals are capable of generating the second harmonic. Therefore, the major problem within the design of NLO crystals consists of the search for compounds that crystallise in non-centrosymmetric space groups. The use of chiral molecules is one of the most evident ways to meet this requirement. However, a non-centrosymmetric space group is the only necessary condition for the manifestation of the NLO activity, whereas the sifficient condition implies an optimum arrangement of molecules in a crystal in such a way that individual contributions of molecular hyperpolarisabilities are mutually enhanced.[49] Unfortunately, many chiral crystal packings are actually pseudo-centrosymmetric (with two crystallographically independent molecules in a unit cell) (see, for example, Refs 307, 403 – 405). The efficient design of NLO crystals is thus hampered by two major factors. First, there are currently no general approaches to the prediction of crystal structures.[406 – 408] Second, the vast majority of organic compounds tend to crystallise in centrosymmetric space groups.[409,410] The latter fact is traditionally explained by the influence of dipole – dipole interactions favouring the antiparallel orientation of the molecular dipole moments.[16] Nevertheless, the role of dipole – dipole interactions in the formation of crystal structures remains a subject of debate. Some authors[411,412] argue that the contribution of these interactions is small, while other authors[413,414] consider it significant. Interestingly, both the viewpoints are substantiated by statistical analyses of crystal structures retrieved from the Cambridge Structural Database (CSD).[415] Adopting the latter viewpoint, it becomes apparent that it is necessary to introduce specific intermolecular interactions which would prevent antiparallel orientation of dipoles in order to obtain a non-centrosymmetric crystal. Even assuming that the

Table 35. Calculated and experimental NLO susceptibilities [$10^9 d_{ij}$ (esu)] in crystals of selected D/A-substituted benzene derivatives.

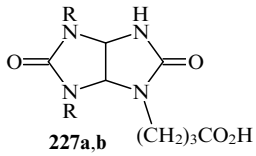
Molecule	d_{21}	d_{22}	d_{23}	d_{25}	Ref.	Molecule	d_{31}	d_{32}	d_{33}	Ref.
221						**223**				
calculation	67.4	16.5	3.1	16.0	50	calculation	0.73	4.83	6.93	50
experiment	119 ± 36	12.4 ± 2.4	3.6 ± 4.8	3.6 ± 4.8	392	experiment	9.6 ± 1.8	11.0 ± 3.0	19.2 ± 2.4	394
222						**224**				
calculation	119.2	12.9	1.0	4.5	50	calculation	34.2	4.5	2.2	50
experiment	114 ± 26	40 ± 10	–	–	393	experiment	31 ± 7	–	6.2 ± 1.4	395

dipole–dipole interactions are insignificant and the inversion symmetry of the majority of crystals is a net result of diverse factors, the involvement of specific forces overcoming these factors is a prerequisite for the formation of a non-centrosymmetric crystal. It would be appropriate to mention here that the NLO active molecules, which are in the focus of the present discussion, are typically characterised by large dipole moments, often exceeding 10 D,§ and thus the effects related to the dipole–dipole interactions are more pronounced for them than for a 'statistaical average' case.

Several approaches to the problem of construction of non-centrosymmetric crystals exploiting specific intermolecular interactions counteracting the forces that favour the centrosymmetric structures have been suggested. These include the utilisation of molecules containing fragments prone to H-bonding; the use of salts composed of charged ions for which the electrostatic interactions become significant; co-crystallisation with an inert component giving rise, for instance, to a 'dilution' of the structure and consequent attenuation of the dipole–dipole interactions between molecules of the NLO-active component. Various combinations of these approaches are also possible. But another question then arises: what kind of crystal packing should be anticipated, taking into account that rather strong specific intermolecular interactions are involved? Presently, this question cannot be unequivocally answered. A comprehensive survey of this problem would be a subject of a separate review. With this regard, below we attempt to critically assess this important problem only with a few representative examples.

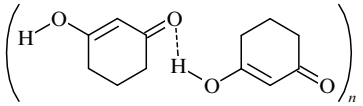
The importance of H-bonds as a key factor in the design of crystal structures is well documented.[410, 416–422] The following regularities of H-bonding in the crystal structures were formulated: (1) the most active proton donors and acceptors have to be involved in H-bonding; (2) H-bonds are preferably formed between the most efficient donor and acceptor.

As for crystalline NLO-active compounds, the principal role played by H-bonds in the formation of non-centrosymmetric structures has been addressed in numerous studies.[306, 307, 423–429] However, in all these cases, the conclusions were derived after the completion of X-ray crystallographic study and subsequent analysys of the crystal packings. It is also of note that weak intermolecular forces, such as van der Waals or C–H···X interactions, are always present in the crystal structures in addition to stronger ones. In the studies cited above, the strong specific interactions were responsible only for the formation of a basic motif of the crystal packing, whereas the mutual arrangement of these motifs was governed by weaker forces. Even if a certain basic motif is retained to a high confidence level over a wide series of compounds upon the variation of substituents, the prediction of fine effects of weaker interactions on the supramolecular organisation in the crystal is hardly possible. For instance, a comparative analysis of the crystal structures of more than 40 conjugated molecules with NH_2/NO_2-substituents retrieved from CSD showed that, in all cases, an aggregation of molecules along a specific direction to form H-bonded polar chains can be suggested, whereas the mutual orientations of such chains cannot be easily controlled.[430] Lyssenko *et al.*[431] reported the crystal structures of compounds **227a** and **b** differing from each other only in alkyl groups. Both the structures are built up of identical non-centrosymmetric H-bonded layers. Nevertheless, the neighbouring layers are stacked in parallel and thus are related by a translation in the structure of **227a**, whereas they are antiparallel and related by an inversion centre in the structure of **227b**. No specific interactions stabilising this particular chiral packing in the case of **227** were revealed.[431]

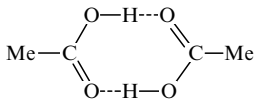


227a,**b** R = Me (**a**), Et (**b**).

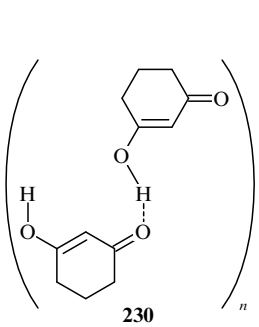
The problem of interpretation of quantum-chemical calculations on H-bonded associates occurring in crystal structures was specifically addressed by Turi and Dannenberg.[432–435] Their aim was to verify the predictive power of calculations by systematically checking whether the energetically most favourable associate, as predicted by means of quantum chemistry, actually occurs in the real crystal structure of the compound. They considered the following H-bonded associates of cyclohexane-1,3-dione and acetic acid



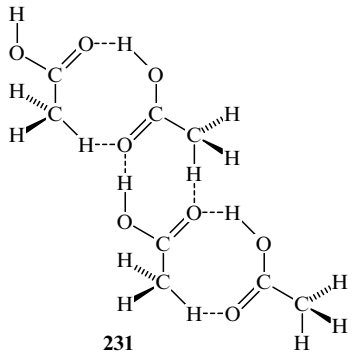
228



229



230



231

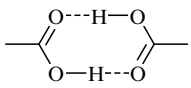
The crystal structure of the associate **228** is composed of molecules in the enol form adopting the *anti*-conformation. At the same time, according to the quantum-chemical calculations (HF/6-31G** and AM1), the stability of an isolated molecule decreases in the series ketone form > enol form/*syn*-conformation > enol form/*anti*-conformation. The relative gain in energy upon the formation of H-bonded associates with respect to the monomers in the ketone form can be analysed based on the results of AM1 calculations compiled in Table 36.

Table 36. Total energies (kcal mol^{-1}) for associates **228**, **230** composed of *N* molecules.

N	Molecule		*N*	Molecule	
	228	**230**		**228**	**230**
2	1.5	0.1	6	−3.1	−3.0
3	−0.7	−1.4	7	−3.5	−3.3
4	−1.9	−2.2	∞	−5.7	−4.9
5	−2.6	−2.7			

It is seen that at least three cyclohexane-1,3-dione molecules should associate to an H-bonded chain of either *syn*- or *anti*-conformers to become energetically more favourable than the same number of non-interacting isolated molecules in the ketone form. Furthermore, the chain of *anti*-conformers **228**, which actually occurs in the crystal, becomes the most energetically favourable structure only after association of no less than six molecules. H-bonded molecular associates of acetic acid (**229**, **231**) was yet another subject of studies by Turi and Dannenberg.[434, 435] The simulation of acetic acid dimers was unsuccessful in explaining its crystal structure. No H-bonded dimer with the expected structure

§ Unfortunately, to the best of our knowledge, no statistical studies regarding the distribution of centrosymmetric and non-centrosymmetric space groups for highly polar compounds have been reported so far.



232

is realised in the crystal because one of the C=O···H–O H-bonds is replaced by the C=O···H–CH_2 bond, which gives rise to the H-bonded chain **231** as the main motif of the crystal packing. A calculation of a three-dimensional cluster that included several chains and 36 molecules in total was required to demonstrate that such a structure is indeed energetically more favourable than that composed of H-bonded dimers. This result clearly illustrates the importance of cooperative effects in the formation of associates and implies that the energy additivity can be violated upon the attachment of a next molecule to the existing cluster.

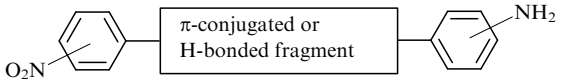
Similar conclusions were derived based on the analysis of crystal packings of nitroanilines, urea and *p*-benzoquinone.[436–438] It is of note that the quantum-chemical simulations described above were accomplished only for compounds with known crystal structures. For instance, the following statement is valid for carboxylic acids (distinctive features of their crystal structures were comprehensively analysed for the first time by Leiserowitz[439]): it is impossible to judge on the association pattern of molecules even in one dimension, not mentioning the full three-dimensional crystal structure, based exclusively on the molecular structure.[410,440]

Nevertheless, in specific cases, the theoretical approach based on the atom–atom potential method makes it possible to establish the relative energies of centrosymmetric and non-centrosymmetric dimers. The formation of a non-centrosymmetric crystal structure can be anticipated if the latter proves preferable.[81,82]

Unfortunately, in overall, the predictive power of contemporary methods for the theoretical crystal packing simulation is rather low. According to recent results devoted to testing of modern specialised software tools for the crystal structure prediction,[441–444] the correct structure is typically present among 5–10 energetically most favourable structures suggested by the codes, but in many cases it is not the most favourable structure.

Certain regularities in the formation of crystal structures can be revealed using a statistical analysis of the structural information stored in CSD for specific classes of compounds. Within the framework of the search for compounds that are crystallised in non-centrosymmetric space groups, Etter and Huang[445] accomplished such statistical analyses for nitroanilines, co-crystallisation products in the system phenol–pyridine[446] and benzoic acids.[447]

For NH_2/NO_2-substituted molecules of the type

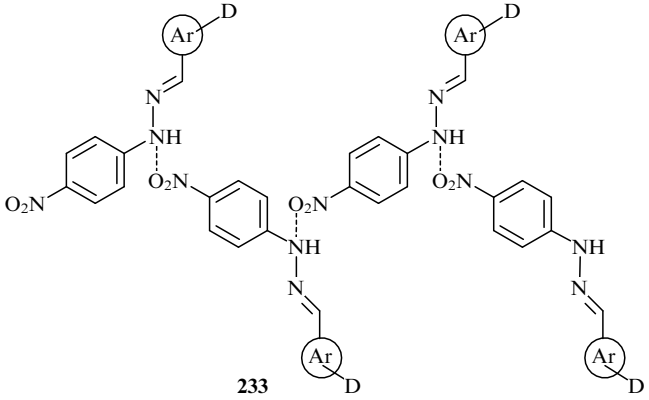


non-centrosymmetric packings are observed in 46% of all cases. Meanwhile, according to CSD, the probability of the crystallisation of an achiral compound in a non-centrosymmetric space group is only 11%.[445] NH_2/NO_2-substituted compounds typically reveal H-bonded non-centrosymmetric chains as the basic structural motif. Etter and co-workers[446] reported results of the NLO susceptibility measurements using the powder method for 22 co-crystallisation products in the system phenol–pyridine. The second harmonic generation was observed for four samples, which amounts to 18% of all cases, *i.e.*, slighlty exceeds the statistical average value. According to analysis of the crystal packings of benzoic acid,[447] centrosymmetric structures occur in 98% of all cases provided that the H-bonded dimer **232** acts as the basic structural block. On the other hand, if infinite H-bonded chains are observed, non-centrosymmetric packings occur with a probability of 52%. The probability of the formation of such chains is substantially higher for *ortho*-substituted acids due to, first, probable intramolecular H-bonding and, second, steric effects favouring the exit of the COOH group out of the ring plane.

The formation of centrosymmetric dimers can be prevented[448,449] by esterification of acids, *e.g.*, by the synthesis of 3-(4-nitrophenyl)-2-phenylacrylates. The compounds, in which *p*-MeO–C_6H_4 and Me groups substitute for the proton, crystallise in non-centrosymmetric space groups. Furthermore, the crystal packing occurring in the case of the Me-derivative appears to be close to the optimum one.

Studies on hydrazones were reported.[450,451] According to measurements of the NLO susceptibilities of powders, 20 out of 28 synthesised compound crystallised in non-centrosymmetric space groups.

Several compounds from this series were examined using X-ray crystallography. It was shown that in the vast majority of cases, λ-shaped non-centrosymmetric H-bonded chain **233** is formed as the basic structural motif, although the reasons responsible for the emergence of this particular structure were not identified.



233

Partly, this issue was clarified in studies of D–π–A–D′-imines[306,307] (see Section IV). As in the case of hydrazones, the crystal structures of imines were found to be built up of λ-shaped chains. Based on a detailed analysis of the crystal packing of imines, the authors[306,307] solidly argumented the formation of non-centrosymmetric groups. An isolated single H-bonded chain contains voids that tend to be filled with molecules constituting neighbouring chains thus giving rise to their non-parallel mutual arrangement, which excludes the formation of an antiparallel centrosymmetric packing.

X-Ray crystallographic data on other hydrazone derivatives[452–456] support the conclusions derived in other studies (Refs 450 and 451). It is worth mentioning that this series of crystal structures obeys the aforementioned main rule of H-bonding. Indeed, if an Ar–D group contains no auxiliary active H-bonding sites, the intermolecular N–H···O(NO) bonds are formed in all cases. On the other hand, the pattern of hydrogen bonds is altered upon introduction of donor OR groups; this can result in the formation of both non-centrosymmetric and centrosymmetric space groups.

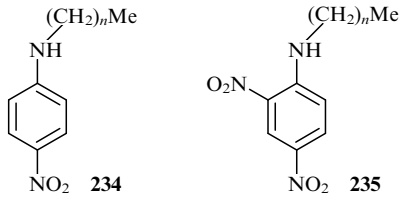
Crystal structures of salts composed of the organic cation, 2-amino-5-nitropyridinium ($2A5NP^+$), and an anion (An^-) of either organic or inorganic nature were investigated.[457–467] According to the results obtained, the probability of occurrence of a non-centrosymmetric space group correlates with the shortest $H_2N\cdots NH_2$ distance (Table 37). If this distance is longer than 4 Å, then a non-centrosymmetric packing is realised, whereas in the distance range of 3.8–4.0 Å, both centrosymmetric and non-centrosymmetric structures are possible. The authors suggestedly explain this correlation by an attenuation of the effects of dipole–dipole interactions with an increase in the $H_2N\cdots NH_2$ distance. In our opinion, this explanation is insufficient since it ignores the fact that it is the strong hydrogen bonds present in all structures that form the basic structural motifs therein. Additionally, it is currently impossible to predict *a priori* the $H_2N\cdots NH_2$ distance

Table 37. Correlation between the shortest $H_2N\cdots NH_2$ distance (r) and probability of the occurrence of a non-centrosymmetric space group in the crystal structures of $2A5NP^+ \cdot An^-$.

An^-	r /Å	Space group	An^-	r /Å	Space group
HSO_4^-	3.454	*Pbca*	Cl^-	4.702	$P2_1$
$InCl_6^{3-}$	3.465	$P2_1/a$	Br^-	4.807	$P2_1$
BF_4^-	3.528	$P2_1/n$	$H_2PO_4^-$	6.747	$Pna2_1$
$H_2PO_3^-$	3.809	$C2/c$	$H_2AsO_4^-$	6.941	$Pna2_1$
I^-	3.955	$P2_1/a$	$Cr_2O_7^{2-}$	3.896	$P2_1nb$
Br^-	4.029	$P2_1/a$	$CHCl_2COO_2^-$	3.949	$P2_12_12_1$
$CCl_3CO_2^-$	3.956	$P2_1/n$	$[(HO)_3PCH_2CO_2H)]^-$	7.070	$P2_12_12_1$

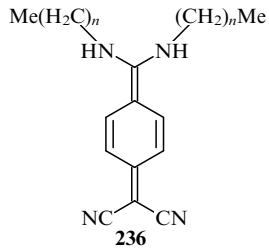
for a specific compound and, respectively, to conclude on the most probable packing type.

Gangopadhyay *et al.*[468–471] analysed compounds **234**–**237** for which non-centrosymmetric packing occurs only for a certain length of the alkyl fragments. The authors distinguished three major contributions to the lattice energy: H-bonds, dipole–dipole and dispersion interactions.

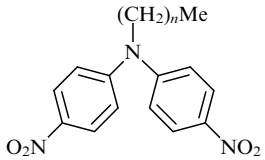


234

235



236



237

In the case of dinitro derivatives, only dipole–dipole and dispersion interactions contribute to the lattice energy due to the formation of intramolecular H-bonds. According to calculations with the atom–atom potential method, the dispersion contribution increases and dipole–dipole contribution decreases with an elongation of the alkyl group. The authors established that a balance between these interactions is settled in the case of the formation of a non-centrosymmetric structure. The dipole–dipole interactions evidently induce a centrosymmetric molecular packing. But what kind of structure is induced by the dispersion interactions? If one assumes that the dispersion interactions induce a non-centrosymmetric structure, it becomes puzzling, why that compounds resume to crystallise in centrosymmetric space groups upon further increase in the alkyl chain length after the balance point. As has been mentioned above, the effects of the dispersion forces on the packing of molecules in a crystal are difficult to predict, which is probably the main reason for the poor efficiency of modern approaches to the crystal structure prediction.

Yet another approach to the design of NLO crystals employs the polymorphism phenomenon [472, 473] and implies the search for the optimum conditions for the growth of a particular modification that crystallises in a non-centrosymmetric space group. Kuleshova and Antipin [474, 475] analysed some of the most common centrosymmetric–non-centrosymmetric polymorph pairs ($P2_1/c-P2_12_12_1$; $P2_1/c-P2_1$; $P2_1/c-Pc$; $P2_1/c-Pna2_1$) based on the structural information retrieved from CSD and derived several general conclusions. Typically, if one of the two polymorphs crystallises in a chiral space group, the crystal structures of both modifications include chiral structural fragments (*e.g.*, layers or chains). In such a case, the polymorphism relates to different mutual arrangements of these fragments induced, as has been discussed above, by weaker intermolecular interactions. These polymorphs are often accompanying and can be prepared under identical experimental conditions (solvent, temperature, concentration). This detailed analysis is definitely useful but it nevertheless does not answer the most important question: how can a non-centrosymmetric modification be purposefully prepared? Unfortunately, two (or more) polymorphs of a compound very often appear to be centrosymmetric.[476, 477]

Probably, one of the best substantiated approaches to the design of non-centrosymmetric crystals elaborated by Leiserowitz and Lahav [478, 479] employs 'tailor-made' additives that selectively inhibit the growth of undesired polymorph modifications. Such an approach is based on the assumption that nuclei of all possible modifications are present in the solution but only the most stable nucleus survives to give rise to the resultant crystal. If a small amount of an additive capable of interacting with the most rapidly growing crystal faces of a certain polymorph and thus inhibiting its growth is introduced to the mother liquor, this will greatly favour the formation of other modifications.

VI. Conclusion

The optimum route to the design of NLO materials should be based on the knowledge and effective utilisation of the contemporary experimental and theoretical methods for the elucidation of structure and properties of NLO-active compounds.

It is evident that the combinatorial approach to the search for new materials by synthesis and experimental testing (for instance, by the powder method) can hardly be accepted as the optimum one. In this case, the step of the evaluation of molecular hyperpolarisabilities (which is actually of no practical importance) is skipped, but it is extremely costly in terms of time and chemicals expenses. Furthermore, the powder method yields only the effective value of the NLO susceptibility and gives no information on factors affecting this value, which makes further purposeful optimisation impossible.

In our opinion, it would be logical and convenient to subdivide the problem of the design of highly efficient NLO materials into two successive steps: molecular design and crystal design.

Taking into account the recent advancement of experimental techniques for the determination of the NLO properties of molecules in solution, the major factor limiting the accuracy of the experimental results relates to the fact that the measurements are performed not for the isolated target molecule, but rather for a product of its interactions with solvent molecules, which is characterised by an unknown structure. The measured hyperpolarisability of a molecule can change severalfold, depending on the solvent. The gas-phase experiments provide a higher accuracy but the majority of polar organic compounds promising for NLO applications do not vaporise due to the decomposition. There are a lot of issues related to different ways of data representation [see formulas (3) and (4)] and the use of different reference values for standard samples. This complicates any comparative analysis of the experimental results obtained by different research groups. However, the data obtained by one research group within the same cycle of measurements can well be compared and analysed at a semiquantitative level. Furthermore, the independently meaured characteristics of a certain compound can often be referenced to the respective parameters of a previously studied molecule measured under identical conditions. Therefore, in the present review, we systematically compared and analysed the NLO properties of a broad assortment of molecules reliably determined either theoretically or experimentally, taking the above constrains into acount. The reported experimental and theoretical values for the same

molecule are typically in accordance with each other to at least a semiquantitative level. According to the literature data, DFT calculations based on hybrid functionals, such as B3LYP or B97, is the theoretical method of choice for the systematic exploration of the NLO properties of molecules.

The molecular design of NLO materials should differentiate between zwitter-ionic and neutral molecules (*i.e.*, molecules with a negligible contribution of the zwitter-ionic form into the ground state). In a schematic diagram showing hyperpolarisability as a function of intermixing between the neutral (ψ_{VB}) and zwitter-ionic (ψ_{CT}) forms (Fig. 10), zwitter-ionic and neutral molecules are located in the right-hand (*i.e.*, in the range of negative β) and left-hand parts, respectively. The hyperpolarisability of a neutral molecule is governed by the following key parameters: the strength of D/A groups, the energy barrier to the electron delocalisation over the π-system (aromaticity), the length of the conjugation system and the degree of its electron-deficiency(excessiveness). These parameters jointly determine the overall degree of the electron delocalisation over a D–π–A molecule. The majority of NLO molecules in the neutral form fall into the region to the left from the maximum. This gives a key to the construction of molecules with the optimum structure.

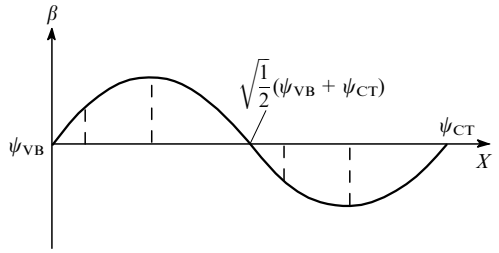


Figure 10. Hyperpolarisability as a function of key parameters (X); X is an increase in the strength of D/A groups, an elongation of the conjugation chain, a decrease in the degree of aromaticity of the π-system and an increase in the degree of electron-deficiency(excessiveness) of the π-system from the acceptor(donor) side.

In contrast, zwitter-ionic molecules containing aromatic D/A groups typically fall into the region to the left from the negative maximum, and thus a decrease in the degree of conjugation between the D/A groups, which additionally stabilises the zwitter-ionic form, gives rise to an enhancement of the NLO properties.

The results discussed in the present review indicate that the algoritm of the search for a molecular structure providing an ultimate hyperpolarisability is generally established.

Nevertheless, any NLO material should meet a number of additional requirements, including optical transparency (the lack of resonance absorption at the second harmonic frequency), thermal and chemical stability, stability towards laser irradiation, accessibility of large (up to 1 cm^3) optical-quality single crystals, *etc*. Two former properties can already be estimated at the molecular level (see Section IV). Unfortunately, it turns out that, as a rule, the modifications of molecules resulting in an enhanced hyperpolarisabilities simultaneously give rise to narrower ranges of the optical transparency and lower stabilities. Therefore, the greatest research efforts are currently put forth to locate the proper compromise between the desired spectral and thermal properties, on the one hand and sufficiently high hyperpolarisabilities, on the other.

The most important task within the design of crystals manifesting NLO properties consists of the elaboration of methods for growing of non-centrosymmetric crystals with the optimum molecular packings. Since X-ray crystallography is still the only source of unambiguous information on crystal structures, the current approach to the design of NLO active crystals is based on the 'trial-and-error' method. The contemporary theoretical methods for the crystal structure simulation are capable of providing the required information only to a limited extent.

The extended array of structural information stored in CSD makes it possible to analyse the regularities of molecular packings along series of closely related compounds and thus make probabilistic predictions. A complex approach combining the CSD-based data mining with available software capabilities of crystal structure simulations and quantum-chemical calculations on molecular associates can be of much help to reduce the probability of errors and increase the number of fruitful trials within the 'trial-and-error' approach.

Summarising all the above results and discussion we propose the following stepwise algoritm for the optimum design and construction of NLO materials.

1. Preliminary selection of molecules and evaluation of their hyperpolarisabilities on the basis of quantum-chemical calculations. The preliminary selection should take into account the literature data on the relationship between the structure of molecules and their spectral and thermal properties. An allowance should be made for the possibility of their crystallisation in non-centrosymmetric space groups. It is also advisable to perform in this step crystal packing simulations and a statistical analysis of the structural data on related compounds from CSD.

2. The synthesis of the selected compound and growing of its single crystals suitable for the X-ray crystallographic characterisation. The crystal structure determination and analysis aimed at the exploration of possibilities to obtain a non-centrosymmetric structure. The crystal structure simulation also can prove useful in this step for a more detailed interpretation of the X-ray crystallographic results. The achievable accuracy of crystallographic data gives indirect information on the accessibility of large optical-quality crystals of the compound.

3. The evaluation of components d_{ijk} of the NLO susceptibility tensor within the oriented gas model or supermolecule approximation. This can be done, for instance, using the software code NLOP. The results obtained can be supplemented with experimental measurements of NLO susceptibility on powders, which additionally enables the determination of the synchronism directions and evaluation of the radiation stability of the material.

4. Growing of large optical-quality single crystals of those compounds that successfully passed all the previous steps for the detemination of their NLO susceptibility along different crystallographic directions, including the synchronism direction, using the Maker fringe method. Based on the results obtained the final conlcusion concerning the potential of the material for NLO applications can be derived.

This review was written with a partial financial support from the Russian Foundation for Basic Research (Project Nos 02-07-90322 and 03-03-32716), the Federal Programme for the Support of Leading Scientific Schools (NSh-1060.2003.3) and the NASA Alliance for Nonlinear Optics (NAG5 6532).

References

1. S A Akhmanov, R V Khokhlov *Problemy Nelineinoi Optiki* (The Problems of Nonlinear Optics) (Moscow: VINITI, 1964)
2. N Blombergen *Nonlinear Optics* (New York: Benjamin, 1965)
3. L G Koreneva, V F Zolin, B L Davydov *Nelineinaya Optika Molekulyarnykh Kristallov* (Nonlinear Optics of Molecular Crystals) (Moscow: Nauka, 1985)
4. D S Chemla, J Zyss (Eds) *Nonlinear Optical Properties of Organic Molecules and Crystals* (Orlando, FL: Academic Press, 1987)
5. J Zyss (Ed.) *Molecular Nonlinear Optics: Materials, Physics and Devices* (New York: Academic Press, 1994)
6. B J Coe *Chem. – Eur. J.* **5** 2464 (1999)
7. J A Delaire, K Nakatani *Chem. Rev.* **100** 1817 (2000)
8. F Würthner, R Wortmann, K Meerholz *Chem. Phys. Chem.* **3** 17 (2002)

9. K Clays, K Wostyn, A Persoons *Adv. Funct. Mater.* **12** 557 (2002)
10. F Kajzar, K-S Lee, A K-Y Jen *Adv. Polym. Sci.* **161** 1 (2003)
11. B L Davydov, L D Derkacheva, V V Dunina, M E Zhabotinskii, V F Zolin, L G Koreneva, M A Samokhina *Pis'ma Zh. Eksp. Teor. Fiz.* **12** (1) 24 (1970) [a]
12. B L Davydov, L D Derkacheva, V V Dunina, M E Zhabotinskii, V F Zolin, L G Koreneva, M A Samokhina *Opt. Spektrosk.* **30** 503 (1971) [b]
13. B L Davydov, V V Dunina, V F Zolin, L G Koreneva *Opt. Spektrosk.* **34** 267 (1973) [b]
14. J R Gott *J. Phys. B: At. Mol. Phys.* **4** 116 (1971)
15. J Jerphagnon *IEEE J. Quantum Electron.* **7** 42 (1971)
16. H S Nalwa, S Miyata (Eds) *Nonlinear Optics of Organic Molecules and Polymers* (Boca Raton, FL: CRC Press, 1997)
17. J J Wolff, R Wortmann *Adv. Phys. Org. Chem.* **32** 121 (1999)
18. L Dalton *Adv. Polym. Sci.* **158** 1 (2002)
19. I Ledoux, J Zyss *Comptes Rendus Physique* **3** 407 (2002)
20. K Clays *J. Nonlinear Opt. Phys. Mater.* **12** 475 (2003)
21. M G Papadopoulos (Ed.) *Nonlinear Optical Responses of Molecules, Solids and Liquids: Methods and Applications* (Trivandrum, India: Research Signpost, 2003)
22. G de la Torre, P Vaquez, F Agullo-Lopez, T Torres *Chem. Rev.* **104** 3723 (2004)
23. H S Nalwa (Ed.) *Handbook of Advanced Electronic and Photonic Materials and Devices. Nonlinear Optical Materials* Vol. 9 (San Diego, CA: Academic Press, 2000)
24. D Pugh *Chem. Model.* **2** 294 (2002)
25. F L Gu, Y Aoki, A Imamura, D M Bishop, B Kirtman *Mol. Phys.* **101** 1487 (2003)
26. S Ohnishi, F L Gu, K Naka, A Imamura, B Kirtman, Y Aoki *J. Phys. Chem. A* **108** 8478 (2004)
27. J-I Iwata, K Yabana, G F Bertsch *J. Comput. Methods Sci. Eng.* **4** 461 (2004)
28. Y Kawabe, H Ikeda, T Sakai, R Kawasaki *J. Mater. Chem.* **2** 1025 (1992)
29. F Meyers, J L Bredas *Int. J. Quantum Chem.* **42** 1595 (1992)
30. C B Gorman, G H J Van Doremaele, S R Marder, in *Molecular and Biomolecular Electronics; Advances in Chemistry Series* Vol. 240 (Ed. R R Birge) (Washington, DC: American Chemical Society, 1994) p. 179
31. T Verbiest, S Houbrechts, M Kauranen, K Clays, A Persoons *J. Mater. Chem.* **7** 2175 (1997)
32. Y Luo, K Ruud, P Norman, D Jonsson, H Ågren *J. Phys. Chem. B* **102** 1710 (1998)
33. W B Davis, M R Wasielewski, M A Ratner *Int. J. Quantum Chem.* **72** 463 (1999)
34. R E Martin, F Diederich *Angew. Chem., Int. Ed.* **38** 1350 (1999)
35. V Alain, S Redoglia, M Blanchard-Desce, S Lebus, K Lukaszuk, R Wortmann, U Gubler, C Bosshard, P Günter *Chem. Phys.* **245** 51 (1999)
36. D Jacquemin, D Beljonne, B Champagne, V Geskin, J-L Brédas, J-M André *J. Chem. Phys.* **115** 6766 (2001)
37. B L Davydov, S G Kotovshchikov, V A Nefedov *Kvantovaya Elektron.* **4** 214 (1977) [*Quant. Electron* **4** 129 (1977)]
38. R V Vizgert, B L Davydov, S G Kotovshchikov, M P Starodubtseva *Kvantovaya Elektron.* **9** 380 (1982) [*Quant. Electron* **12** 214 (1982)]
39. D R Kanis, M A Ratner, T J Marks *Chem. Rev.* **94** 195 (1994)
40. S R Marder, C B Gorman, F Meyers, J W Perry, G Bourhill, J-L Brédas, B M Pierce *Science* **265** 632 (1994)
41. M Lequan, R M Lequan, K C Ching, M Barzoukas, A Fort, H Lahoucine, G Bravic, D Chasseau, J Gaultier *J. Mater. Chem.* **2** 719 (1992)
42. S R Marder, B Kippelen, A K-Y Jen, N Peyghambarian *Nature (London)* **388** 845 (1997)
43. I Asselberghs, K Clays, A Persoons, M D Ward, J McCleverty *J. Mater. Chem.* **14** 2831 (2004)
44. J Armstrong, N Bloembergen, J Ducuing, P S Pershan *Phys. Rev.* **127** 1918 (1962)
45. N Bloembergen, P S Pershan *Phys. Rev.* **128** 606 (1962)
46. M G Kuzyk, C W Dirk (Eds) *Characterization Techniques and Tabulations for Organic Nonlinear Optical Materials* (New York: Marcel Dekker, 1998)
47. A I Kitaigorodsky *Molecular Crystals and Molecules* (Orlando, FL: Academic Press, 1973)
48. J L Oudar, J Zyss *Phys. Rev. A: At., Mol., Opt. Phys.* **26** 2016 (1982)
49. J Zyss, J L Oudar *Phys. Rev. A: At., Mol., Opt. Phys.* **26** 2028 (1982)
50. T V Timofeeva, K Yu Suponitsky, B H Cardelino, R D Clark *Proc. SPIE* **2812** 201 (1999)
51. M P Cifuentes, M G Humphrey *J. Organomet. Chem.* **689** 3968 (2004)
52. B J Coe, in *Comprehensive Coordination Chemistry II* Vol. 9 (Eds J A McCleverty, T J Meyer) (Oxford: Elsevier, Pergamon Press, 2004) p. 621
53. B F Levine, G C Bethea *Appl. Phys. Lett.* **24** 445 (1974)
54. B F Levine, G C Bethea *J. Chem. Phys.* **60** 3856 (1974)
55. B F Levine, G C Bethea *J. Chem. Phys.* **63** 2666 (1974)
56. J P Hermann, D Ricard, J Ducuing *Appl. Phys. Lett.* **23** 178 (1973)
57. B F Levine, G C Bethea *J. Chem. Phys.* **65** 2429 (1976)
58. B F Levine, G C Bethea *J. Chem. Phys.* **69** 5240 (1978)
59. J L Oudar *Chem. Phys.* **67** 446 (1977)
60. R W Terhune, P D Maker, C M Savage *Phys. Rev. Lett.* **14** 681 (1965)
61. K Clays, A Persoons *Phys. Rev. Lett.* **66** 2980 (1991)
62. K Clays, A Persoons *Rev. Sci. Instrum.* **63** 3285 (1992)
63. K Clays, E Hendrickx, T Verbiest, A Persoons *Adv. Mater.* **10** 643 (1998)
64. E Hendrickx, K Clays, A Persoons, C Dehu, J L Bredas *J. Am. Chem. Soc.* **117** 3547 (1995)
65. P Kaatz, E Donley, D P Shelton *J. Chem. Phys.* **108** 849 (1998)
66. F L Huyskens, P L Huyskens, A P Persoons *J. Mol. Struct.* **448** 161 (1998)
67. F L Huyskens, P L Huyskens, A P Persoons *J. Chem. Phys.* **108** 8161 (1998)
68. D P Shelton, J E Rice *Chem. Rev.* **94** 3 (1994)
69. H A Kurtz, D S Dudis, in *Reviews in Computational Chemistry* Vol. 12 (Eds K B Lipkowitz, D B Boyd) (New York: Wiley-VCH, 1998) p. 241
70. S P Karna, A T Yeates (Eds) *Nonlinear Optical Materials. Theory and Modelling* (Washington, DC: American Chemical Society, 1996)
71. J Zyss *J. Chem. Phys.* **70** 3333 (1979)
72. J Zyss *J. Chem. Phys.* **70** 3341 (1979)
73. J Zyss *J. Chem. Phys.* **71** 909 (1979)
74. J L Oudar, D S Chemla *J. Chem. Phys.* **66** 2664 (1977)
75. H A Kurtz, J P J Stewart, K M Dieter *J. Comput. Chem.* **11** 82 (1990)
76. N Matsuzawa, D A Dixon *J. Phys. Chem.* **96** 6232 (1992)
77. N Matsuzawa, D A Dixon *Int. J. Quantum Chem.* **44** 497 (1992)
78. L-T Cheng, W Tam, S H Stevenson, G R Meredith, G Rikken, S R Marder *J. Phys. Chem.* **95** 10631 (1991)
79. L-T Cheng, W Tam, S R Marder, A E Stiegman, G Rikken, C W Spangler *J. Phys. Chem.* **95** 10643 (1991)
80. B H Cardelino, C E Moore, R E Stickel *J. Phys. Chem.* **95** 8645 (1991)
81. M Yu Antipin, T A Barr, B H Cardelino, R D Clark, C E Moore, T Myers, B Penn, M Romero, M Sanghadasa, T V Timofeeva *J. Phys. Chem. B* **101** 2770 (1997)
82. M Yu Antipin, T V Timofeeva, R D Clark, V N Nesterov, M Sanghadasa, T A Barr, B Penn, L Romero, M Romero *J. Phys. Chem. A* **102** 7222 (1998)
83. M Yu Antipin, R D Clark, V N Nesterov, M Sanghadasa, T V Timofeeva, K A Lyssenko *Mol. Cryst. Liq. Cryst.* **313** 85 (1998)
84. B J Orr, G F Ward *Mol. Phys.* **20** 513 (1971)
85. S J Lalama, A F Garito *Phys. Rev. A: At., Mol., Opt. Phys.* **20** 1179 (1979)
86. J A Morrell, A C Albrecht *Chem. Phys. Lett.* **64** 46 (1979)
87. A Dulcic, C Sauteret *J. Chem. Phys.* **69** 3453 (1978)
88. V J Docherty, D Pugh, J O Morley *J. Chem. Soc., Faraday Trans. 2* **81** 1179 (1985)
89. S Allen, J O Morley, D Pugh, V J Docherty *Proc. SPIE* **682** 20 (1986)

90. J O Morley, P Pavlides, D Pugh *Int. J. Quantum Chem.* **43** 7 (1992)
91. D Li, T J Marks, M A Ratner *Chem. Phys. Lett.* **131** 370 (1986)
92. D Li, T J Marks, M A Ratner *J. Phys. Chem.* **96** 4325 (1992)
93. D R Kanis, T J Marks, M A Ratner *Mol. Cryst. Liq. Cryst. Sci. Technol., Sect. B* **6** 317 (1994)
94. D R Kanis, T J Marks, M A Ratner *Int. J. Quantum Chem.* **43** 61 (1992)
95. J Ridley, M C Zerner *Theor. Chim. Acta* **32** 111 (1973)
96. A D Bacon, M C Zerner *Theor. Chim. Acta* **53** 21 (1979)
97. W P Anderson, W D Edwards, M C Zerner *Inorg. Chem.* **25** 2728 (1986)
98. M Kotzian, N Rösch, H Schröder, M C Zerner *J. Am. Chem. Soc.* **111** 7687 (1989)
99. H Sekino, R J Bartlett *J. Chem. Phys.* **85** 976 (1986)
100. S P Karna, M Dupuis *Chem. Phys. Lett.* **171** 201 (1990)
101. S P Karna, M Dupuis *J. Comput. Chem.* **12** 487 (1991)
102. H Sekino, R J Bartlett *J. Chem. Phys.* **98** 3022 (1993)
103. J E Rice, R D Amos, S Colwell, N C Handy, J Sanz *J. Chem. Phys.* **93** 8828 (1990)
104. J E Rice, N C Handy *J. Chem. Phys.* **94** 4959 (1991)
105. N C Handy, J E Rice *Int. J. Quantum Chem.* **43** 91 (1992)
106. K Sasagane, F Aiga, R Itoh *J. Chem. Phys.* **99** 3738 (1993)
107. F Aiga, K Sasagane, R Itoh *J. Chem. Phys.* **99** 3779 (1993)
108. F Aiga, R Itoh *Chem. Phys. Lett.* **251** 372 (1996)
109. T Kobayashi, K Sasagane, F Aiga, K Yamaguchi *J. Chem. Phys.* **110** 11720 (1999)
110. B L Hammond, J E Rice *J. Chem. Phys.* **97** 1138 (1992)
111. C Hättig, O Christiansen, H Koch, P Jørgensen *Chem. Phys. Lett.* **269** 428 (1997)
112. J Gauss, O Christiansen, J F Stanton *Chem. Phys. Lett.* **296** 117 (1998)
113. J Dudley, J Ward *J. Chem. Phys.* **82** 4673 (1985)
114. M Jaszunski, P Jørgensen, H Jørgen *Chem. Phys. Lett.* **191** 293 (1992)
115. D M Bishop, B Kirtman *J. Chem. Phys.* **95** 2646 (1991)
116. O Christiansen, J Gauss, J F Stanton *Chem. Phys. Lett.* **305** 147 (1999)
117. H Reis, M G Papadopoulos, A Avramopoulos *J. Phys. Chem. A* **107** 3907 (2003)
118. A Rizzo, S Coriani, B Fernandez, O Christiansen *Phys. Chem. Chem. Phys.* **4** 2884 (2002)
119. J F Ward, C K Miller *Phys. Rev. A: At., Mol., Opt. Phys.* **19** 826 (1979)
120. M Stähelin, C R Moylan, D M Burland, A Willetts, J E Rice, D P Shelton, E A Donley *J. Chem. Phys.* **98** 5595 (1993)
121. D M Bishop, F L Gu, S M Cybulski *J. Chem. Phys.* **109** 8407 (1998)
122. D A Roberts *IEEE J. Quantum Electron.* **28** 2057 (1992)
123. M Torrent-Sucarrat, M Sola, M Duran, J M Luis, B Kirtman *J. Chem. Phys.* **118** 711 (2003)
124. D M Bishop *Rev. Mod. Phys.* **62** 343 (1990)
125. K Ruud, P O Astrand, P R Taylor *J. Comput. Methods Sci. Eng.* **3** 7 (2003)
126. B Champagne, J M Luis, M Duran, J L Andres, B Kirtman *J. Chem. Phys.* **112** 1011 (2000)
127. B Beck, U-W Grummt *J. Phys. Chem. B* **102** 664 (1998)
128. W Koch, M C Holthausen *A Chemist's Guide to Density Functional Theory* (2nd Ed.) (Weinheim, New York: Wiley-VCH, 2002)
129. S J A van Gisbergen, J G Snijders, E-J Baerends *J. Chem. Phys.* **109** 10657 (1998)
130. A J Cohen, N C Handy, D J Tozer *Chem. Phys. Lett.* **303** 391 (1999)
131. B Champagne, E A Perpete, D Jacquemin, S J A van Gisbergen, E-J Baerends, C Soubra-Ghaoui, K A Robins, B Kirtman *J. Phys. Chem. A* **104** 4755 (2000)
132. M Grüning, O V Gritsenko, S J A van Gisbergen, E-J Baerends *J. Chem. Phys.* **116** 9591 (2002)
133. J B Foresman, A Frisch *Exploring Chemistry with Electronic Structure Methods* (2nd Ed.) (Pittsburg: Gaussian Inc., 1996)
134. J Guan, P Duffy, J T Carter, D P Chong, K C Casida, M E Casida, M Wrinn *J. Chem. Phys.* **98** 4753 (1993)
135. D A Dixon, N Matsuzawa *J. Phys. Chem.* **98** 3967 (1994)
136. H H Heinze, F D Sala, A Görling *J. Chem. Phys.* **116** 9624 (2002)
137. R-J Sa, K-C Wu, C-S Lin, P Liu, C-Y Mang *Chin. J. Chem.* **21** 377 (2003)
138. H Reis, M G Papadopoulos, I Boustani *Int. J. Quantum Chem.* **78** 131 (2000)
139. J J Wolff, D Längle, D Hillenbrand, R Wortmann, R Matschiner, C Glania, P Krämer *Adv. Mater.* **9** 138 (1997)
140. J J Wolff, F Siegler, R Matschiner, R Wortmann *Angew. Chem., Int. Ed.* **39** 1436 (2000)
141. S R Marder, D N Beratan, L-T Cheng *Science* **252** 103 (1991)
142. G Bourhill, J-L Bredas, L-T Cheng, S R Marder, F Meyers, J W Perry, B G Tiemann *J. Am. Chem. Soc.* **116** 2619 (1994)
143. S R Marder, C Gorman, B Tiemann, L-T Cheng *J. Am. Chem. Soc.* **115** 3006 (1993)
144. F Meyers, S R Marder, B M Pierce, J-L Bredas *J. Am. Chem. Soc.* **116** 10703 (1994)
145. B Kippelen, F Meyers, N Peyghambarian, S R Marder *J. Am. Chem. Soc.* **119** 4559 (1997)
146. C Gorman, S R Marder *Chem. Mater.* **7** 215 (1995)
147. H Lee, S-Y An, M Cho *J. Phys. Chem. B* **103** 4992 (1999)
148. W Zhu, Y Jiang *J. Mol. Struct.* **496** 67 (2000)
149. W Zhu, Y Jiang *Phys. Chem. Chem. Phys.* **1** 4169 (1999)
150. W Zhu, Y Jiang *Phys. Chem. Chem. Phys.* **2** 47 (2000)
151. D Lu, G Chen, J W Perry, W A Goddard III *J. Am. Chem. Soc.* **116** 10679 (1994)
152. S Hahn, D Kim, M Cho *J. Phys. Chem. B* **103** 8221 (1999)
153. Y-K Lee, S-J Jeon, M Cho *J. Am. Chem. Soc.* **120** 10921 (1998)
154. M Cho, H-S Kim, S-J Jeon *J. Chem. Phys.* **108** 7114 (1998)
155. M Cho *J. Phys. Chem. A* **103** 4712 (1999)
156. M Cho, S-Y An, H Lee, I Ledoux, J Zyss *J. Chem. Phys.* **116** 9165 (2002)
157. M Barzoukas, C Rusner, A Fort, M Blanchard-Desce *Chem. Phys. Lett.* **257** 531 (1996)
158. M Barzoukas, A Fort, M Blanchard-Desce *New J. Chem.* **21** 309 (1997)
159. M Blanchard-Desce, M Barzoukas *J. Opt. Soc. Am. B* **15** 302 (1998)
160. M Barzoukas, M Blanchard-Desce, in *Advances in Multi-Photon Processes and Spectroscopy* Vol. 13 (Ed. S H Lin) (Singapore: World Scientific, 2001) p. 261
161. D Laage, W H Thompson, M Blanchard-Desce, J T Hynes *J. Phys. Chem. A* **107** 6032 (2003)
162. S M Bachrach, in *Reviews in Computational Chemistry* Vol. 5 (Eds K B Lipkowitz, D B Boyd) (New York: Wiley-VCH, 1994) p. 171
163. X L Gao, J K Feng, C C Sun *Int. J. Quantum Chem.* **42** 1747 (1992)
164. J O Morley *J. Chem. Soc., Faraday Trans.* **87** 3009 (1991)
165. J O Morley, V J Docherty, D Pugh *J. Chem. Soc., Perkin Trans. 2* 1351 (1987)
166. J O Morley *Int. J. Quantum Chem.* **46** 19 (1993)
167. I D L Albert, D Pugh, J O Morley *J. Chem. Soc., Faraday Trans.* **90** 2617 (1994)
168. I D L Albert, J O Morley, D Pugh *J. Phys. Chem. A* **101** 1763 (1997)
169. B Champagne, D Jacquemin, J-M Andre *Proc. SPIE* **2527** 71 (1995)
170. B Champagne, D Jacquemin, J-M Andre, B Kirtman *J. Phys. Chem. A* **101** 3158 (1997)
171. D Jacquemin, X Assfeld, E A Perpete *J. Mol. Struct. (THEOCHEM)* **710** 13 (2004)
172. D Jacquemin, B Champagne, J-M Andre *Synth. Met.* **101** 490 (1999)
173. D Jacquemin, B Champagne, J-M Andre *Synth. Met.* **80** 205 (1996)
174. D Jacquemin, B Champagne, B Kirtman *J. Chem. Phys.* **107** 5076 (1997)
175. D Jacquemin, B Champagne, J-M Andre *Int. J. Quantum Chem.* **65** 679 (1997)
176. B Champagne *Chem. Phys. Lett.* **261** 57 (1996)
177. F Castet, B Champagne *J. Phys. Chem. A* **105** 1366 (2001)
178. C A van Walree, O Franssen, A W Marsman, M C Flipse, L W Jenneskens *J. Chem. Soc., Perkin Trans. 2* 799 (1997)

179. T Tsunekawa, T Gotoh, H Mataki, T Kondoh, S Fukuda, M Iwamoto *Proc. SPIE* **1337** 272 (1990)
180. T Tsunekawa, T Gotoh, M Iwamoto *Chem. Phys. Lett.* **166** 353 (1990)
181. T Tsunekawa, K Yamaguchi *J. Phys. Chem.* **96** 10268 (1992)
182. T Tsunekawa, K Yamaguchi *Chem. Phys. Lett.* **190** 533 (1992)
183. D Jacquemin, E A Perpete, B Champagne *Phys. Chem. Chem. Phys.* **4** 432 (2002)
184. D Jacquemin, O Quinet, B Champagne, J-M Andre *J. Chem. Phys.* **120** 9401 (2004)
185. D Jacquemin *J. Phys. Chem. A* **108** 500 (2004)
186. D Jacquemin *J. Phys. Chem. A* **108** 9260 (2004)
187. M Blanchard-Desce, J-M Lehn, M Barzoukas, I Ledoux, J Zyss *Chem. Phys.* **181** 281 (1994)
188. K J Drost, A K-Y Jen, V P Rao *Chem. Tech.* 16 (1995)
189. B Illien, P Jehan, A Bortel, A Darchen, I Ledoux, J Zyss, P LeMagueres, L Ouahab *New J. Chem.* **22** 633 (1998)
190. J Garin, J Orduna, R Andreu *Recent Res. Dev. Org. Chem.* **5** 77 (2001)
191. A E Asato, R S H Liu, V P Rao, Y M Cai *Tetrahedron Lett.* **37** 419 (1996)
192. P G Lacroix, I Malfant, G Iftime, A C Razus, K Nakatani, J A Delaire *Chem. – Eur. J.* 2599 (2000)
193. S Zhang, G Zhou, Z Yang, A Qin, P Wang, C Ye *Synth. Met.* **137** 1545 (2003)
194. S Millefiori, A Alparone *J. Mol. Struct. (THEOCHEM)* **431** 59 (1998)
195. K Kamada, M Ueda, H Nagao, K Tawa, T Sugino, Y Shmizu, K Ohta *J. Phys. Chem. A* **104** 4723 (2000)
196. B Jasnik, B Schimmelpfennig, P Norman, P Macak, H Ågren, K Ohta *J. Mol. Struct. (THEOCHEM)* **633** 237 (2003)
197. F Fringuelli, G Marino, A Taticchi, G Grandolini *J. Chem. Soc., Perkin Trans. 2* 332 (1974)
198. A T Balaban, D C Oniciu, A R Katritzky *Chem. Rev.* **104** 2777 (2004)
199. V Keshari, W M K Wijekoon, P N Prasad, S Karna *J. Phys. Chem.* **99** 9045 (1995)
200. A R Katritzky, V Feygelman, G Musumarra, P Barczynski, M Szafran *J. Prakt. Chem.* 870 (1990)
201. V P Rao, A K-Y Jen, K Y Wong, K Drost, R M Mininni *Proc. SPIE* **1775** 32 (1992)
202. A K-Y Jen,V P Rao, K Y Wong, K Drost *J. Chem. Soc., Chem. Commun.* 90 (1993)
203. V P Rao, A K-Y Jen, K Y Wong, K Drost *J. Chem. Soc., Chem. Commun.* 1118 (1993)
204. V P Rao, A K-Y Jen, K Y Wong, K Drost *Tetrahedron Lett.* **34** 1747 (1993)
205. A K-Y Jen, Y Cai, P V Bedworth, S R Marder *Adv. Mater.* **9** 132 (1997)
206. C W Dirk, H E Katz, M L Schilling, L A King *Chem. Mater.* **2** 700 (1990)
207. R D Miller, V Y Lee, C R Moylan *Chem. Mater.* **6** 1023 (1994)
208. S-S P Chou, G-T Hsu, H-C Lin *Tetrahedron Lett.* **40** 2157 (1999)
209. S-S P Chou, Y-H Yeh *Tetrahedron Lett.* **42** 1309 (2001)
210. I D L Albert, T J Marks, M A Ratner *J. Am. Chem. Soc.* **119** 6575 (1997)
211. V P Rao, A K-Y Jen, J Chandrasekhar, I N N Namboothiri, A Rathna *J. Am. Chem. Soc.* **118** 12443 (1996)
212. E M Breitung, C-F Shu, R J McMahon *J. Am. Chem. Soc.* **122** 1154 (2000)
213. A R Katritzky, P Barczynski, G Musumarra, D Pisano, M Szafran *J. Am. Chem. Soc.* **111** 7 (1989)
214. A R Katritzky, V Feygelman, G Musumarra, P Barczynski, M Szafran *J. Prakt. Chem.* 853 (1990)
215. T L Gilchrist *Heterocyclic Chemistry* (New York: Wiley, 1985)
216. C R Moylan, B J McNelis, L C Nathan, M A Marques, E L Hermstad, B A Brichler *J. Org. Chem.* **69** 8239 (2004)
217. A F Pozharskii *Teoreticheskie Osnovy Khimii Geterotsiklov* (Theoretical Foundations of the Chemistry of Heterocycles) (Moscow: Khimiya, 1985)
218. K Jug, S Chiodo, F Janetzko *Chem. Phys.* **287** 161 (2003)
219. B J Coe, J A Harris, I Asselberghs, K Clays, G Olbrechts, A Persoons, J T Hupp, R Johnson, S Coles, M Hursthouse, K Nakatani *Adv. Funct. Mater.* **12** 110 (2002)
220. B J Coe, J A Harris, I Asselberghs, K Wostyn, K Clays, A Persoons, B S Brunschwig, S Coles, T Gelbrich, M E Light, M Hursthouse, K Nakatani *Adv. Funct. Mater.* **13** 347 (2003)
221. K Clays, B J Coe *Chem. Mater.* **15** 642 (2003)
222. L Cristian, I Sasaki, P G Lacroix, B Donnadieu, I Asselberghs, K Clays, A C Razus *Chem. Mater.* **16** 3543 (2004)
223. S DiBella, I Fragala, M A Ratner, T J Marks *Chem. Mater.* **7** 400 (1995)
224. C A Daul, I Ciofini, V Weber *Int. J. Quantum Chem.* **91** 297 (2003)
225. S Maiorana, A Papagni, E Licandro, R Annunziata, P Paravidino, D Perdicchia, C Giannini, M Bencini, K Clays, A Persoons *Tetrahedron* **59** 6481 (2003)
226. B Champagne, J-M Andre, E Botek, E Licandro, S Maiorana, A Bossi, K Clays, A Persoons *ChemPhysChem.* **5** 1438 (2004)
227. R Andreu, J Garin, J Orduna, R Alcala, B Villacampa *Org. Lett.* **5** 3143 (2003)
228. R Andreu, M A Cerdan, J Garin, J Orduna *Arkivoc IV* 32 (2004)
229. J Diaz, A Dobarro, B Villacampa, D Velasco *Chem. Mater.* **13** 2528 (2001)
230. J Diaz, B Villacampa, F Lopez-Calahorra, D Velasco *Chem. Mater.* **14** 2240 (2002)
231. L Xiang, Y-G Liu, A-G Jiang, D-Y Huang *Chem. Phys. Lett.* **338** 167 (2001)
232. L Han, M-Z Hue, L Xiang, H-B Qian, Y-G Liu *Opt. Mater.* **27** 235 (2004)
233. K V Katti, K Raghuraman, N Pillarsetty, S R Karra, R J Gulotty, M A Chartier, C A Langhoff *Chem. Mater.* **14** 2436 (2002)
234. P Calaminici, K Jug, A M Köster, C Arbez-Gindre, G Screttas *J. Comput. Chem. 23* 291 (2002)
235. R Spreiter, C Bosshard, G Knöpfle, P Günter, R R Tykwinski, M Schreiber, F Diederich *J. Phys. Chem. B* **102** 29 (1998)
236. C Lambert, G Noll, M Zabel, F Hampel, E Schmälzlin, C Bräuchle, K Meerholz *Chem. – Eur. J.* **9** 4232 (2003)
237. I D L Albert, J O Morley, D Pugh *J. Phys. Chem.* **99** 8024 (1995)
238. H Pan, X Gao, Y Zhang, P N Prasad, B Reinhardt, R Kannan *Chem. Mater.* **7** 816 (1995)
239. B F Levine, C G Bethea, E Wasserman, L Leenders *J. Chem. Phys.* **68** 5042 (1978)
240. P G Lacroix, J-C Daran, P Cassoux *New J. Chem.* **22** 1085 (1998)
241. J G Dawber, S Etemad, M A Beckett *J. Chem. Soc., Faraday Trans.* **86** 3725 (1990)
242. J O Morley, R M Morley, R Docherty, M H Charlton *J. Am. Chem. Soc.* **119** 10192 (1997)
243. J Catalan, P Perez, J Elguero, W Meutermans *Chem. Ber.* **126** 2445 (1993)
244. J Catalan, E Mena, W Meutermans, J Elguero *J. Phys. Chem.* **96** 3615 (1992)
245. A Fort, C Runser, M Barzoukas, C Combellas, C Suba, A Thiebault *Proc. SPIE* **2285** 2 (1994)
246. A Boeglin, A Fort, L Mager, C Combellas, A Thiebault, V Rodriguez *Chem. Phys.* **282** 353 (2002)
247. I D L Albert, T J Marks, M A Ratner *J. Phys. Chem.* **100** 9714 (1996)
248. J O Morley *J. Chem. Soc., Faraday Trans.* **90** 1853 (1994)
249. J Abe, Y Shirai *J. Am. Chem. Soc.* **118** 4705 (1996)
250. J Abe, Y Shirai, N Nemoto, F Miyata, Y Nagase *J. Phys. Chem. B* **101** 576 (1997)
251. J Abe, Y Shirai, N Nemoto, F Miyata, Y Nagase *J. Phys. Chem. B* **101** 1910 (1997)
252. I D L Albert, T J Marks, M A Ratner *J. Am. Chem. Soc.* **119** 3155 (1997)
253. I D L Albert, T J Marks, M A Ratner *J. Am. Chem. Soc.* **120** 11174 (1998)
254. R Zaleśny, W Bartkowiak, S Styrcz, J Leszczynski *J. Phys. Chem. A* **106** 4032 (2002)
255. B A S Mendis, K M N de Silva *J. Mol. Struct. (THEOCHEM)* **678** 31 (2004)
256. W Bartkowiak, J Lipinski *J. Phys. Chem. A* **102** 5236 (1998)
257. P Gangopadhyay, M Ravi, T P Radhakrishnan *Indian J. Chem., Sect. A* **39** 106 (2000)
258. R Allmann *Z. Kristallogr.* **128** 115 (1969)
259. P Milart, K Stadnicka *Eur. J. Org. Chem.* 2337 (2001)

260. K Stadnicka, P Milart, A Olech, P K Olszewski *J. Mol. Struct.* **604** 9 (2002)
261. M Barzoukas, A Fort, G Klein, A Boeglin, C Serbutoviez, L Oswald, J F Nicoud *Chem. Phys.* **153** 457 (1991)
262. M Barzoukas, A Fort, G Klein, A Boeglin, C Serbutoviez, L Oswald, J F Nicoud *Chem. Phys.* **164** 395 (1992)
263. C A van Walree, A W Maarsman, A W Marsman, M C Flipse, L W Jenneskens, W J J Smeets, A J Spek *J. Chem. Soc., Perkin Trans. 2* 809 (1997)
264. O Y Borbulevich, R D Clark, A Romero, L Tan, M Yu Antipin, V N Nesterov, B H Cardelino, C Moore, M Sanghadasa, T V Timofeeva *J. Mol. Struct.* **604** 73 (2002)
265. M Ravi, T P Radhakrishnan *J. Phys. Chem.* **99** 17624 (1995)
266. M Ravi, S Cohen, I Agranat, T P Radhakrishnan *Struct. Chem.* **7** 225 (1996)
267. M Ravi, D N Rao, S Cohen, I Agranat, T P Radhakrishnan *J. Mater. Chem.* **6** 1119 (1996)
268. M Ravi, D N Rao, S Cohen, I Agranat, T P Radhakrishnan *J. Mater. Chem.* **6** 1853 (1996)
269. M Ravi, P Gangopadhyay, D N Rao, S Cohen, I Agranat, T P Radhakrishnan *Chem. Mater.* **10** 2371 (1998)
270. J L Rao, K Bhanuprakash *J. Mol. Struct. (THEOCHEM)* **458** 269 (1999)
271. A J Kay, A D Woolhouse, G J Gainsford, T G Haskell, T H Barnes, I T McKinnie, C P Wyss *J. Mater. Chem.* **11** 996 (2001)
272. A J Kay, A D Woolhouse, G J Gainsford, T G Haskell, C P Wyss, S M Giffin, I T McKinnie, T H Barnes *J. Mater. Chem.* **11** 2271 (2001)
273. C J Wyss, G J Smith, A D Woolhouse, A J Kay, W J Wadsworth, I T McKinnie, T G Haskell *Opt. Mater.* **16** 341 (2001)
274. C R Moylan, R D Miller, R J Twieg, K M Betterton, V Y Lee, T J Matray, C Nguyen *Chem. Mater.* **5** 1499 (1993)
275. C R Moylan, C A Walsh *Nonlinear Opt.* **6** 113 (1993)
276. R D Miller, C R Moylan, O Reiser, C A Walsh *Chem. Mater.* **5** 625 (1993)
277. C R Moylan *J. Phys. Chem.* **98** 13513 (1994)
278. M Blanchard-Desce, V Alain, P V Bedworth, S R Marder, A Fort, C Runser, M Barzoukas, S Lebus, R Wortmann *Chem. – Eur. J.* **3** 1091 (1997)
279. J K Feng, X Y Sun, A M Ren, K Q Yu, C C Sun *J. Mol. Struct. (THEOCHEM)* **489** 247 (1999)
280. J X Jhang, P Dubois, R Jerome *J. Chem. Soc., Perkin Trans. 2* 1209 (1997)
281. D dos Santos, T Kogej, J L Bredas, C Boutton, E Hendrix, S Houbrechts, K Clays, A Persoons, J X Jhang, P Dubois, R Jerome *J. Mol. Struct.* **521** 221 (2000)
282. R D Miller, J Michl *Chem. Rev.* **89** 1359 (1989)
283. G Mignani, A Krämer, G Puccetti, I Ledoux, G Soula, J Zyss, R Meyrueix *Organometallics* **9** 2640 (1990)
284. P F van Hutten, G Hadziioannou, R Bursi, D Feil *J. Phys. Chem.* **100** 85 (1996)
285. R Sudharsanam, S Chandrrasekaran, P K Das *J. Mater. Chem.* **12** 2904 (2002)
286. K D Singer, H E Katz, J E Sohn, C W Dirk, L A King, H M Gordon *J. Opt. Soc. Am. B* **6** 1339 (1989)
287. C-F Shu, Y-C Shu, Z-H Gong, S-M Peng, G-H Lee, A K-Y Jen *Chem. Mater.* **10** 3284 (1998)
288. Y-C Shu, Z-H Gong, C-F Shu, E M Breitung, R J McMahon, G-H Lee, A K-Y Jen *Chem. Mater.* **11** 1628 (1999)
289. C Zhang, A S Ren, F Wang, J Zhu, L R Dalton, J N Woodford, C H Wang *Chem. Mater.* **11** 1966 (1999)
290. J Luo, J Hua, J Qin, J Cheng, Y Shen, Z Lu, P Wang, C Ye *Chem. Commun.* 171 (2001)
291. J Hua, J Luo, J Qin, Y Shen, Y Zhang, Z Lu *J. Mater. Chem.* **12** 863 (2002)
292. A-G Jiang, Y-G Liu, D-Y Huang *J. Mol. Struct. (THEOCHEM)* **499** 203 (2000)
293. G Barbarella, O Pudova, C Arbizzani, M Mastragostino, A Bongini *J. Org. Chem.* **63** 1742 (1998)
294. Z-Y Hu, A Fort, M Barzoukas, A K-Y Jen, S Barlow, S R Marder *J. Phys. Chem. B* **108** 8626 (2004)
295. R J Twieg, K M Betterton, D M Burland, V Y Lee, R D Miller, C R Moylan, W Volksen, C A Walsh *Proc. SPIE* **2025** 94 (1993)
296. R D Miller, K M Betterton, D M Burland, V Y Lee, C R Moylan, R J Twieg, C A Walsh, W Volksen *Proc. SPIE* **2042** 354 (1994)
297. C R Moylan, R J Twieg, V Y Lee, S A Swanson, K M Betterton, R D Miller *J. Am. Chem. Soc.* **115** 12599 (1993)
298. R J Twieg, D M Burland, J Hedrick, V Y Lee, R D Miller, C R Moylan, C M Seymour, W Volksen, C A Walsh *Proc. SPIE* **2143** 2 (1994)
299. C R Moylan, R J Twieg, V Y Lee, R D Miller, W Volksen, J I Thackara, C A Walsh *Proc. SPIE* **2285** 17 (1994)
300. M Matsui, M Suzuki, M Hayashi, K Funabiki, Y Ishigure, Y Doke, H Shiozaki *Bull. Chem. Soc. Jpn.* **76** 607 (2003)
301. C Cai, I Liakatas, M-S Wong, M Bosch, C Bosshard, P Günter, S Concilio, N Tirelli, U W Suter *Org. Lett.* **1** 1847 (1999)
302. B K Spraul, S Suresh, T Sassa, M A Herranz, L Echegoyen, T Wada, D Perahia, D W Smith Jr *Tetrahedron Lett.* **45** 3253 (2004)
303. X Wu, J Wu, Y Liu, A K-Y Jen *Chem. Commun.* 2391 (1999)
304. J Hua, W Zhang, Z Li, J Qin, Y Shen, Y Zhang, Z Lu *Chem. Lett.* 232 (2002)
305. A Papagni, S Maiorana, P Del Buttero, D Perdicchia, F Cariati, E Cariati, W Marcolli *Eur. J. Org. Chem.* 1380 (2002)
306. V V Nesterov, M Yu Antipin, V N Nesterov, B G Penn, D O Frazier, T V Timofeeva *Cryst. Growth Des.* **4** 521 (2004)
307. V V Nesterov, M Yu Antipin, V N Nesterov, C E Moore, B H Cardelino, T V Timofeeva *J. Phys. Chem. B* **108** 8531 (2004)
308. T V Timofeeva, G H Kuhn, V V Nesterov, V N Nesterov, D O Frazier, B G Penn, M Yu Antipin *Cryst. Growth Des.* **3** 383 (2003)
309. V N Nesterov, N G Montoya, M Yu Antipin, M Sanghadasa, R D Clark, T V Timofeeva *Acta Crystallogr., Sect. C* **58** o72 (2002)
310. L A Chetkina, I M Gel'fand, S L Ginzburg, M G Neigauz, B P Bespalov, A V Dzyabchenko *Kristallografiya* **28** 470 (1983) [c]
311. L A Chetkina, G N Kurov, L L Dmitrieva, A N Sobolev *Kristallografiya* **36** 499 (1991) [c]
312. M Tomonari, N Ookubo *J. Mol. Struct. (THEOCHEM)* **451** 179 (1998)
313. H S Nalwa, T Watanabe, S Miyata *Adv. Mater.* **7** 754 (1995)
314. R Wortmann, S Lebus-Henn, H Reis, M G Papadopoulos *J. Mol. Struct. (THEOCHEM)* **633** 217 (2003)
315. C R Moylan, S Ermer, S M Lovejoy, I-H McComb, D S Leung, R Wortmann, P Krämer, R J Twieg *J. Am. Chem. Soc.* **118** 12950 (1996)
316. Yo Liu, Yi Liu, D Zhang, H Hu, C Liu *J. Mol. Struct.* **570** 43 (2001)
317. Yo Liu, Yi Liu, X Zhao, C Liu *Int. J. Quantum Chem.* **82** 65 (2001)
318. S-S P Chou, C-Y Yu *Synth. Met.* **142** 259 (2004)
319. W Wu, C Ye, D Wang *Arkivoc II* 59 (2003)
320. M Yang, B Champagne *J. Phys. Chem. A* **107** 3942 (2003)
321. P Wang, P Zhu, W Wu, H Kang, C Ye *Phys. Chem. Chem. Phys.* **1** 3519 (1999)
322. R Sudharsanam, S Chandrasekaran, P Das *J. Mol. Struct.* **645** 51 (2003)
323. A Datta, S K Pati *J. Phys. Chem. A* **108** 320 (2004)
324. E Kelderman, L Derhaeg, G J T Heesink, W Verboom, J F J Engbersen, N F van Hulst, A Persoons, D N Reinhoudt *Angew. Chem., Int. Ed. Engl.* **31** 1075 (1992)
325. E Kelderman, G J T Heesink, L Derhaeg, T Verbiest, P T A Klaase, W Verboom, J F J Engbersen, N F van Hulst, K Clays, A Persoons, D N Reinhoudt *Adv. Mater.* **5** 925 (1993)
326. E Brouyere, A Persoons, J L Bredas *J. Phys. Chem. A* **101** 4142 (1997)
327. S Di Bella, M A Ratner, T J Marks *J. Am. Chem. Soc.* **114** 5842 (1992)
328. S Di Bella, G Lanza, I Fragala, S Yitzchaik, M A Ratner, T J Marks *J. Am. Chem. Soc.* **119** 3003 (1997)

329. M Nakano, S Yamada, M Takahata, K Yamaguchi *J. Phys. Chem. A* **107** 4157 (2003)
330. G Y Lu, W Song, M H Liu, F Liu, C M Jin *Chin. J. Chem.* **19** 612 (2001)
331. C M Jin, M Z Gui, G Y Lu, X Guo, H Zhang, X You *Chin. J. Chem.* **21** 105 (2003)
332. J Zyss, I Ledoux, S Volkov, V Chernyak, S Mukamel, G P Bartholomew, G C Bazan *J. Am. Chem. Soc.* **122** 11956 (2000)
333. G P Bartholomew, G C Bazan *J. Am. Chem. Soc.* **124** 5183 (2002)
334. G P Bartholomew, I Ledoux, S Mukamel, G C Bazan, J Zyss *J. Am. Chem. Soc.* **124** 13480 (2002)
335. I V Fedyanin, K A Lysenko, M Yu Antipin, in *III Natsional'naya Kristallokhimicheskaya Konferentsiya (Tezisy Dokladov), Chernogolovka, 2003* [The IIIrd National Crystal Chemical Conference (Abstracts of Reports), Chernogolovka, 2003] p. 249
336. K A Lyssenko, M Yu Antipin, D Yu Antonov *Chem. Phys. Chem.* **4** 817 (2003)
337. I V Fedyanin, K A Lyssenko, N V Vorontsova, V I Rozenberg, M Yu Antipin *Mendeleev Commun.* 15 (2003)
338. A Bahl, W Grahn, S Stadler, F Feiner, G Bourhill, C Bräuchle, A Reisner, P G Jones *Angew. Chem., Int. Ed. Engl.* **34** 1485 (1995)
339. J Zyss, I Ledoux *Chem. Rev.* **94** 77 (1994)
340. J Zyss *Nonlinear Opt.* **1** 3 (1991)
341. S Brasselet, J Zyss *J. Nonlinear Opt. Phys. Mater.* **7** 397 (1998)
342. R Boese, G R Desiraju, R K R Jetti, M T Kirchner, I Ledoux, V R Thalladi, J Zyss *Struct. Chem.* **13** 321 (2002)
343. J Zyss, I Ledoux, H-C Weiss, D Bläser, R Boese, P K Thallapally, V R Thalladi, G R Desiraju *Chem. Mater.* **15** 3063 (2003)
344. M Joffre, D Yaron, R J Silbey, J Zyss *J. Chem. Phys.* **97** 5607 (1992)
345. J-L Bredas, F Meyers, B Pierce, J Zyss *J. Am. Chem. Soc.* **114** 4928 (1992)
346. C Andraud, T Zabulon, A Collet, J Zyss *Chem. Phys.* **245** 243 (1999)
347. B R Cho, S J Lee, S H Lee, K W Son, Y H Kim, J-Y Doo, G J Lee, T I Kang, Y K Lee, M Cho, S-J Jeon *Chem. Mater.* **13** 1438 (2001)
348. B R Cho, Y H Kim, K W Son, C Khalil, Y Ho Kim, S-J Jeon *Bull. Korean Chem. Soc.* **23** 1253 (2002)
349. B R Cho, S B Park, S J Lee, K H Son, S H Lee, M-J Lee, J Yoo, M Cho, S-J Jeon *J. Am. Chem. Soc.* **123** 6421 (2001)
350. B R Cho, C Khalil, H J Oh, K H Son, S-J Jeon *Org. Lett.* **4** 1703 (2002)
351. M J Lee, M Piao, M-Y Jeong, S H Lee, K M Kang, S-J Jeon, T G Lim, B R Cho *J. Mater. Chem.* **13** 1030 (2003)
352. S Di Bella *New J. Chem.* **26** 495 (2002)
353. G Hennrich, I Asselberghs, K Clays, A Persoons *J. Org. Chem.* **69** 5077 (2004)
354. X-J Liu, J-K Feng, A-M Ren, X Zhou, G Zhang *Chin. J. Chem.* **21** 1015 (2003)
355. J Brunel, I Ledoux, J Zyss, M Blanchard-Desce *Chem. Commun.* 923 (2001)
356. J Brunel, A Jutand, I Ledoux, J Zyss, M Blanchard-Desce *Synth. Met.* **124** 195 (2001)
357. J Brunel, O Mongin, A Jutand, I Ledoux, J Zyss, M Blanchard-Desce *Chem. Mater.* **15** 4139 (2003)
358. J L Rao, K Bhanuprakash *Synth. Met.* **132** 315 (2003)
359. E M Maya, E M Garcia-Frutos, P Vazquez, T Torres, G Martin, G Rojo, F Agullo-Lopez, R H Gonzalez-Jonte, V R Ferro, J M Garcia de la Vega, I Ledoux, J Zyss *J. Phys. Chem. A* **107** 2110 (2003)
360. G Martin, G Rojo, F Agullo-Lopez, V R Ferro, J M Garcia de la Vega, M V Martinez-Diaz, T Torres, I Ledoux, J Zyss *J. Phys. Chem. B* **106** 13139 (2002)
361. A Sastre, T Torres, M A Diaz-Garcia, F Agullo-Lopez, C Dhenaut, S Brasselet, I Ledoux, J Zyss *J. Am. Chem. Soc.* **118** 2746 (1996)
362. B del Rey, U Keller, T Torres, G Rojo, F Agullo-Lopez, F Nonell, C Marti, S Brasselet, I Ledoux, J Zyss *J. Am. Chem. Soc.* **120** 12808 (1998)
363. R E Williams *Chem. Rev.* **92** 177 (1992)
364. J Plešek *Chem. Rev.* **92** 269 (1992)
365. R N Grimes *Carboranes* (New York: Academic Press, 1970)
366. R N Grimes *Coord. Chem. Rev.* **200 – 202** 773 (2000)
367. D M Murphy, D M P Mingos, J M Forward *J. Mater. Chem.* **3** 67 (1993)
368. D M Murphy, D M P Mingos, J L Haggitt, H R Powell, S A Westcott, T B Marder, N J Taylor, D R Kanis *J. Mater. Chem.* **3** 139 (1993)
369. J Abe, N Nemoto, Y Nagase, Y Shirai, T Iyoda *Inorg. Chem.* **38** 172 (1998)
370. B Grüner, Z Janoušek, B T King, J N Woodford, C H Wang, V Všetečka, J Michl *J. Am. Chem. Soc.* **121** 3122 (1999)
371. D G Allis, J T Spencer *J. Organomet. Chem.* **614 – 615** 309 (2000)
372. D G Allis, J T Spencer *Inorg. Chem.* **40** 3373 (2001)
373. K Yu Suponitsky, T V Timofeeva, M Yu Antipin, in *Imeboron XIth International Conference on Boron Chemistry (Abstracts of Reports), Moscow, 2002* p. 154
374. K Yu Suponitsky, T V Timofeeva *Cent. Eur. J. Chem.* **1** 1 (2003)
375. K Yu Suponitsky, T V Timofeeva *J. Comput. Methods Sci. Eng.* **4** 411 (2004)
376. R W F Bader, D A Legare *Can. J. Chem.* **70** 657 (1992)
377. I R Epstein, W N Lipscomb *Inorg. Chem.* **10** 1921 (1971)
378. P v R Schleyer, K Najafian *Inorg. Chem.* **37** 3454 (1998)
379. V I Bregadze *Chem. Rev.* **92** 209 (1992)
380. E L Mutterties, W H Knoth *Polyhedral Boranes* (New York: Marcel Dekker, 1968)
381. B Champagne, D M Bishop, in *Advances in Chemical Physics* Vol. 126 (Eds I Prigogine, S A Rice) (New York: Wiley, 2003) p. 41
382. S K Kurtz, in *Quantum Electronics: a Treatise* Vol. 1, Part A (Eds H Rabin, C L Tang) (New York: Academic Press, 1975) p. 209
383. P D Maker, R W Terhune, M Nisenoff, C M Savage *Phys. Rev. Lett.* **8** 21 (1962)
384. J Jerphagnon, S K Kurtz *J. Appl. Phys.* **41** 1667 (1970)
385. J Jerphagnon, S K Kurtz *Phys. Rev. B: Solid State* **1** 1739 (1970)
386. S K Kurtz, T T Perry *J. Appl. Phys.* **39** 3798 (1968)
387. A Graja *Phys. Status Solidi* **27** k93 (1968)
388. A A Filimonov, V S Suvorov, I S Rez *Zh. Eksp. Teor. Fiz.* **56** 1519 (1969) [d]
389. M Barzoukas, D Josse, P Femaux, J Zyss, J F Nicoud, J O Morley *J. Opt. Soc. Am. B* **4** 977 (1987)
390. K Yu Suponitsky, B H Cardelino, M Yu Antipin, T V Timofeeva, in *The XIXth Austin Symposium on Molecular Structure (Abstracts of Reports), Austin, USA, 2002* p. 62
391. A V Yakimanski, U Kolb, G N Matveeva, I G Voigt-Martin, A V Tenkovtsev *Acta Crystallogr., Sect. A* **53** 603 (1997)
392. P Kerkoc, M Zgonik, K Sutter, C Bosshard, P Günter *J. Opt. Soc. Am. B* **7** 313 (1990)
393. K Sutter, C Bosshard, P Günter *Ferroelectrics* **92** 395 (1989)
394. A Carenco, J Jerphagnon, A Perigaud *J. Chem. Phys.* **66** 3806 (1977)
395. K Sutter, C Bosshard, M Ehrensperger, P Günter, R J Twieg *J. Quantum Electron.* **24** 2362 (1988)
396. V Moliner, P Escribano, E Peris *New J. Chem.* **22** 387 (1998)
397. T Hamada *J. Phys. Chem.* **100** 8777 (1996)
398. J Perez, M Dupuis *J. Phys. Chem.* **95** 6525 (1991)
399. G F Lipscomb, A F Garito, R S Narang *J. Chem. Phys.* **75** 1509 (1981)
400. J E Worsham, H A Levy, S W Peterson *Acta Crystallogr.* **10** 319 (1957)
401. K Wu, J G Snijders, C Lin *J. Phys. Chem. B* **106** 8954 (2002)
402. M Guillaume, E Botek, B Champagne, F Castet, L Ducasse *Int. J. Quantum Chem.* **90** 1378 (2002)
403. M V Makarov, V P Dyadchenko, K Yu Suponitsky, D A Lemenovskii, M Yu Antipin *Izv. Akad. Nauk, Ser. Khim.* 1864 (2004) [e]

404. T V Timofeeva, V N Nesterov, F M Dolgushin, Y V Zubavichus, J T Goldshtein, D M Sammeth, R D Clark, B Penn, M Yu Antipin *Cryst. Eng.* **3** 263 (2001)
405. T V Timofeeva, V N Nesterov, R D Clark, B Penn, D Frazier, M Yu Antipin *J. Mol. Struct.* **647** 181 (2003)
406. A Gavezzotti *Acc. Chem. Res.* **27** 309 (1994)
407. J D Dunitz *Chem. Commun.* 545 (2003)
408. N Blagden, R J Davey *Cryst. Growth Des.* **3** 873 (2003)
409. C P Brock, J D Dunitz *Chem. Mater.* **6** 1118 (1994)
410. G Desiraju *The Weak Hydrogen Bond* (New York: Oxford University Press, 1999)
411. A Gavezzotti *J. Phys. Chem.* **94** 4319 (1990)
412. J K Whitesell, R E Davis, L L Saunders, R J Wilson, J P Feagins *J. Am. Chem. Soc.* **113** 3267 (1991)
413. F H Allen, C A Baalham, J P M Lommerse, P R Raithby *Acta Crystallogr., Sect. B* **54** 320 (1998)
414. S Lee, A B Mallik, D C Fredrickson *Cryst. Growth Des.* **4** 279 (2004)
415. F N Allen, O Kennard *Chem. Des. Auto. News* **8** 31 (1993)
416. M C Etter *Acc. Chem. Res.* **23** 120 (1990)
417. M C Etter *J. Phys. Chem.* **95** 4601 (1991)
418. E Fan, C Vicent, S J Geib, A D Hamilton *Chem. Mater.* **6** 1113 (1994)
419. J Bernstein, M C Etter, L Leiserowitz, in *Structure Correlation* Vol. 2 (Eds H-B Bürgi, J D Dunitz) (New York: VCH, 1994) P. 431
420. L N Kuleshova, M Yu Antipin *Usp. Khim.* **68** 3 (1999) [*Russ. Chem. Rev.* **68** 1 (1999)]
421. A Gavezzotti *J. Mol. Struct.* **615** 5 (2002)
422. A Angeloni, P C Crawford, A G Orpen, T J Podesta, B J Shore *Chem. – Eur. J.* **10** 3783 (2004)
423. C Serbutovies, J Nicoud, J Fischer, I Ledoux, J Zyss *Chem. Mater.* **6** 1358 (1994)
424. M Kato, K Kobayashi, M Okunaka, N Sugita, M Kiguchi, Y Taniguchi *J. Mol. Struct.* **471** 139 (1998)
425. A Goeta, C C Wilson, J C Autino, J Ellena, G Punte *Chem. Mater.* **12** 3342 (2000)
426. M Ohkita, T Suzuki, K Nakatani, T Tsuji *Chem. Lett.* 988 (2001)
427. M K Marchewka, J Baran, A Pietraszko, A Haznar, S Debrus, H Ratajczak *Solid State Sci.* **5** 509 (2003)
428. M K Marchewka, J Janczak, S Debrus, J Baran, H Ratajczak *Solid State Sci.* **5** 643 (2003)
429. M K Marchewka, S Debrus, H Ratajczak *Cryst. Growth Des.* **3** 587 (2003)
430. T W Panunto, Z Urbanczyk-Lipkowska, R Johnson, M C Etter *J. Am. Chem. Soc.* **109** 7786 (1987)
431. K A Lyssenko, D G Golovanov, A N Kravchenko, I E Chikunov, O V Lebedev, N N Makhova *Mendeleev Commun.* 105 (2004)
432. L Turi, J J Dannenberg *J. Phys. Chem.* **96** 5819 (1992)
433. L Turi, J J Dannenberg *Chem. Mater.* **6** 1313 (1994)
434. L Turi, J J Dannenberg *J. Phys. Chem.* **97** 12197 (1993)
435. L Turi, J J Dannenberg *J. Am. Chem. Soc.* **116** 8714 (1994)
436. L Turi, J J Dannenberg *J. Phys. Chem.* **100** 9638 (1996)
437. A Masunov, J J Dannenberg *J. Phys. Chem. B* **104** 806 (2000)
438. J J Dannenberg *J. Mol. Struct.* **615** 219 (2002)
439. L Leiserowitz *Acta Crystallogr., Sect. B* **32** 775 (1976)
440. T Beyer, S L Price *J. Phys. Chem. B* **104** 2647 (2000)
441. J P M Lommerse, W D S Motherwell, H L Ammon, J D Dunitz, A Gavezzotti, D W M Hofmann, F J J Leusen, W T M Mooij, S L Price, B Schweizer, M U Schmidt, B P van Eijck, P Verwer, D E Williams *Acta Crystallogr., Sect. B* **56** 697 (2000)
442. W D S Motherwell, H L Ammon, J D Dunitz, A Dzyabchenko, P Erk, A Gavezzotti, D W M Hofmann, F J J Leusen, J P M Lommerse, W T M Mooij, S L Price, H Scheraga, B Schweizer, M U Schmidt, B P van Eijck, P Verwer, D E Williams *Acta Crystallogr.* **58** 647 (2002)
443. J A Chisholm *Acta Crystallogr., Sect. A* **60** s62 (2004)
444. G M Day, S Motherwell *Acta Crystallogr., Sect. A* **60** s63 (2004)
445. M C Etter, K-S Huang *Chem. Mater.* **4** 824 (1992)
446. K-S Huang, D Britton, M C Etter, S R Byrn *J. Mater. Chem.* **7** 713 (1997)
447. G M Frankenbach, M C Etter *Chem. Mater.* **4** 272 (1992)
448. B Tinant, R Touillaux, J P Declercq, M van Meerssche, G Leroy, J Weiler *Bull. Soc. Chim. Belg.* **92** 865 (1983)
449. L N Kuleshova, V N Khrustalev, K Yu Suponitsky, M Yu Antipin, D V Gusev, E S Bobrikova *Kristallografiya* **47** 1031 (2002) [c]
450. C Serbutoviez, C Bosshard, G Knopfle, P Wyss, P Pretre, P Gunter, K Schenk, E Solari, G Chapuis *Chem. Mater.* **7** 1198 (1995)
451. M Wong, V Gramlich, C Bosshard, P Gunter *J. Mater. Chem.* **7** 2021 (1997)
452. I Liakatas, M Wong, V Gramlich, C Bosshard, P Gunter *Adv. Mater.* **10** 777 (1998)
453. L N Kuleshova, M Yu Antipin, V N Khrustalev, D V Gusev, G V Grintselev-Knyazev, E S Bobrikova *Kristallografiya* **48** 645 (2003) [c]
454. C Glidewell, J N Low, J M S Skakle, J L Wardell *Acta Crystallogr., Sect. C* **59** o98 (2003)
455. S Shan, D-J Xu, J-Y Wu, M Y Chiang *Acta Crystallogr. Sect. E* **59** o342 (2003)
456. C Glidewell, J N Low, J M S Skakle, J L Wardell *Acta Crystallogr., Sect. C* **60** o19 (2004)
457. R Masse, J Zyss *Mol. Eng.* **1** 141 (1991)
458. M Bagieu-Beucher, R Masse, D Tranqui *Z. Anorg. Allg. Chem.* **606** 59 (1991)
459. J Pécaut, J-P Lévy, R Masse *J. Mater. Chem.* **3** 999 (1993)
460. J Pécaut, Y LeFur, R Masse *Acta Crystallogr., Sect. B* **49** 535 (1993)
461. J Pécaut, R Masse *Acta Crystallogr., Sect. B* **49** 277 (1993)
462. J Pécaut, J-P Lévy *Z. Kristallogr.* **208** 235 (1993)
463. J Zyss, R Masse, M Bagieu-Beucher, J-P Lévy *Adv. Mater.* **5** 120 (1993)
464. R Masse, M Bagieu-Beucher, J Pécaut, J-P Lévy, J Zyss *Nonlinear Opt.* **5** 413 (1993)
465. J Pécaut, R Masse *J. Mater. Chem.* **4** 1851 (1994)
466. Y LeFur, M Bagieu-Beucher, R Masse, J-F Nicoud, J-P Lévy *Chem. Mater.* **8** 68 (1996)
467. N Horiuchi, F Lefaucheux, A Ibanez, D Josse, J Zyss *J. Opt. Soc. Am. B* **19** 1830 (2002)
468. P Gangopadhyay, S V Rao, D N Rao, T P Radhakrishnan *J. Mater. Chem.* **9** 1699 (1999)
469. P Gangopadhyay, S Sharma, A J Rao, D N Rao, S Cohen, I Agranat, T P Radhakrishnan *Chem. Mater.* **11** 466 (1999)
470. P Gangopadhyay, T P Radhakrishnan *Chem. Mater.* **12** 3362 (2000)
471. P Gangopadhyay, N K M N Srinivas, D N Rao, T P Radhakrishnan *Opt. Mater. (Amsterdam)* **21** 55 (2002)
472. J Bernstein *Polymorphism in Molecular Crystals* (New York: Oxford University Press, 2002)
473. A Gavezzotti *Cryst. Eng. Commun.* **4** 343 (2002)
474. L N Kuleshova, M Yu Antipin *Kristallografiya* **47** 303 (2002) [c]
475. L N Kuleshova, M Yu Antipin *Kristallografiya* **48** 293 (2003) [c]
476. K Yu Suponitsky, D V Gusev, L N Kuleshova, M Yu Antipin *Kristallografiya* **47** 667 (2002) [c]
477. L N Kuleshova, B B Averkiev, D V Gusev, K Yu Suponitsky, M Yu Antipin *Kristallografiya* **49** 886 (2004) [c]
478. I Weissbuch, R Popovitz-Biro, M Lahav, L Leiserowitz *Acta Crystallogr., Sect. B* **51** 115 (1995)
479. I Weissbuch, M Lahav, L Leiserowitz *Cryst. Growth Des.* **3** 125 (2003)

[a] — *J. Exp. Theor. Phys. Lett. (Engl. Transl.)*
[b] — *Opt. Spectroscop. (Engl. Transl.)*
[c] — *Crystallogr. Rep. (Engl. Transl.)*
[d] — *Exp. Theor. Phys. (Engl. Transl.)*
[e] — *Russ. Chem. Bull., Int. Ed. (Engl. Transl.)*